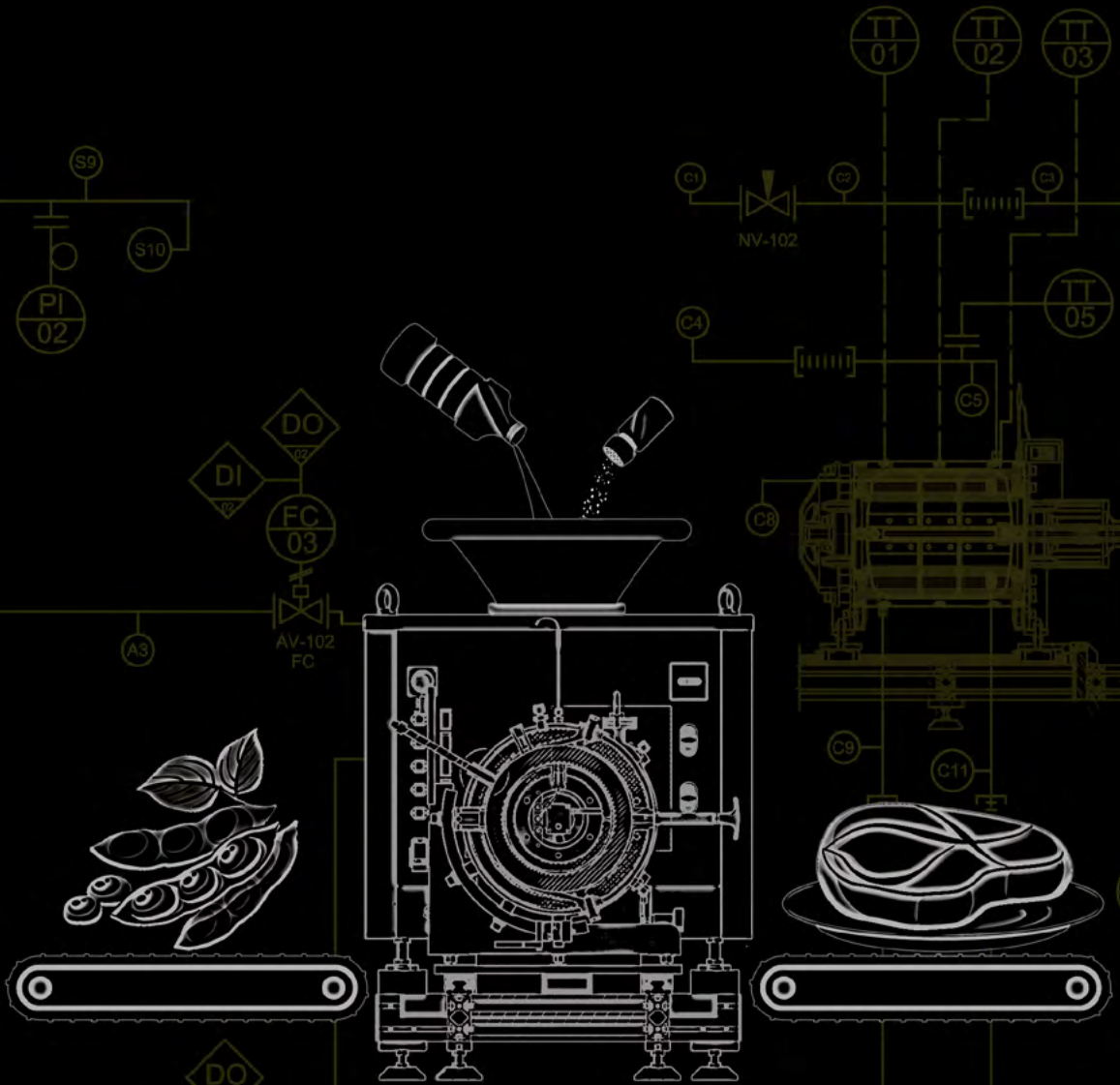# INTENSIFIED PROTEIN STRUCTURING FOR MORE

SUSTAINABLE FOODS

Development of the up-scaled Couette Cell for the production of meat replacers

Georgios A. Krintiras

Intensified Protein Structuring for more sustainable foods

Development of the up-scaled Couette Cell for the production of meat replacers

Proefschrift

ter verkrijging van de graad van doctor
aan de Technische Universiteit Delft,
op gezag van de Rector Magnificus prof. ir. K.C.A.M. Luyben,
voorzitter van het College voor Promoties,
in het openbaar te verdedigen op donderdag 03 maart om 12:30 uur

door

Georgios A. KRINTIRAS
Master of Science in Sustainable Energy Technology
Delft University of Technology, the Netherlands
geboren te Athens, Greece

This dissertation has been approved by the promotors:
Prof. dr. ir. A. I. Stankiewicz and Prof. dr. G. D. Stefanidis

Composition of the doctoral committee:

Rector Magnificus	Chairman
Prof. dr. ir. A. I. Stankiewicz	Delft University of Technology, promotor
Prof. dr. G. D. Stefanidis	KU Leuven, promotor

Independent members:

Prof. dr. J. H. van Esch	Delft University of Technology
Prof. dr. R. Kohlus	Universität Hohenheim, Germany
Dr. A. Krijgsman	Unilever, the Netherlands
Dr. F. Wild	Food Technology Consultant, Germany
Prof. dr. ir. H. J. Noorman	Delft University of Technology, reserve member

Other member:

Prof. dr. A. J. van der Goot	Wageningen UR, the Netherlands

Cover designed by CHRISTOS THEOLOGOUPHOTOGRAPHY

---

[1]Author e-mail address: gkrintiras@gmail.com

Dedicated to my beloved parents Andreas & Nerantzia,

my sister Aspa

and to my partner Anna-Maria
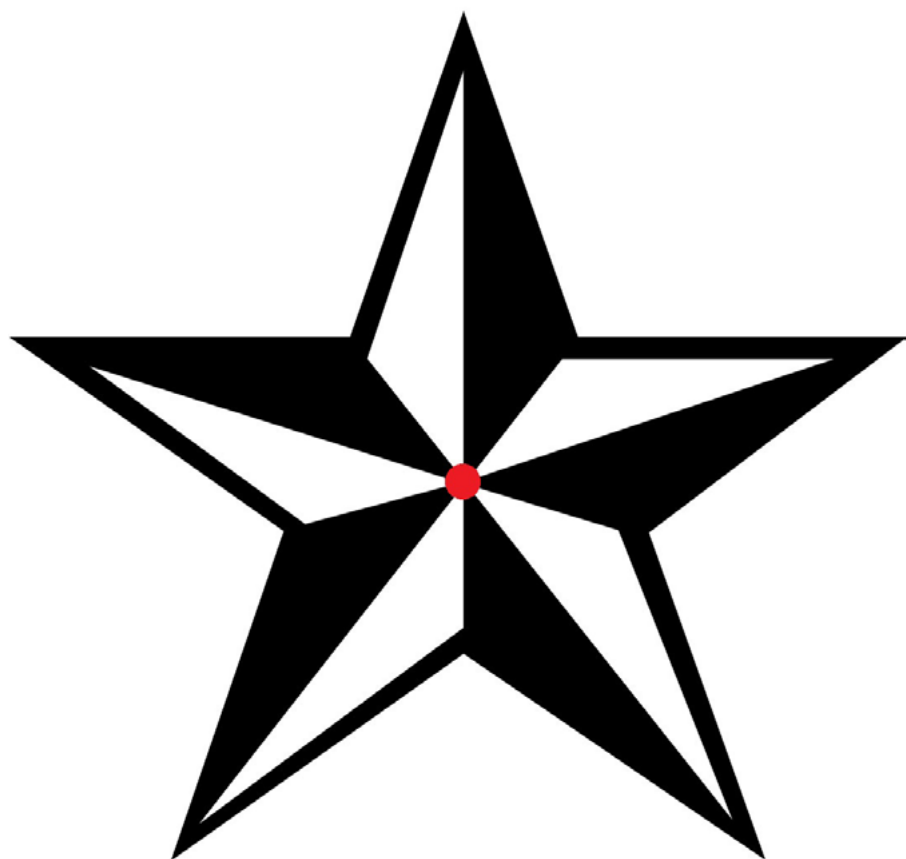
SUMMARY

To meet the increasing need for protein-rich food of an ever-growing population, plant-based proteins are being utilized in meat products as replacements for animal-based proteins. Legumes such as soy can serve as an alternative protein source, by featuring both high protein content (36%) and protein functionality (gelation). Nowadays various meat replacement products are commercially available and thus more and more customers are willing to switch their diet to a vegetable-based one. Currently, the most efficient technology for the production of meat replacers is extrusion cooking and new methods of protein structuring (Shear Cell and Couette Cell) have only recently been introduced. These two new technologies were developed based on the principle of applying simple shear flow and heat in the protein mixture. Initially, a device called the Shear Cell was developed featuring a cone-cone design that could structure soy-based mixtures in meat-like products. However, since the Shear Cell design is limited to lab use only, a new technology was developed and presented in this thesis.

The Couette Cell concept, which is based on the concentric cylinder principle, has been studied, since it allows for further upscaling at industrially relevant production volumes. The research starts with a proof of concept study by using the lab-scaled Couette Cell, which features a volume of 0.14 L and a *shearing zone* gap size of 5 mm, between the two cylinders (**Chapter 2**). Applying simple shear and heat at varying process conditions (temperature, time and rotation rate) to a soy-based mixture, has yielded anisotropic structures that resembled meat. In particular, fibrous structures were favoured at temperatures between 90 and 100 °C.

The fibrous products with the highest anisotropy indices were further examined and characterized with a set of complementary techniques (**Chapter 3**). With light microscopy we could observe structure formation over the visible surfaces of the specimens and by using a stain we could distinguish between the different ingredients. According to the texture analysis results, the anisotropy indices of the obtained meat replacer and raw meat (beef) are comparable. We introduced the use of neutron refraction method by utilizing spin-echo small angle neutron scattering (SESANS) to provide a *look inside* the bulk of the anisotropic meat replacer. It was therefore possible to quantify the number of fibre layers and the orientation distribution of the fibres present inside the specimens. The calculated fibre thickness was in line with the observations obtained with scanning electron microscopy (SEM).

Since the Couette Cell concept proved successful and enabled scalable operation, we developed a new up-scaled Couette Cell, which can treat 7 L per batch, 50 times more than the lab-scaled Couette Cell. The detailed design of the up-scaled Couette Cell is discussed in **Chapter 4**. The up-scaled device allows for production of fibrous meat replacers at industrially relevant scales and opens the possibility of commercial production in an emerging market. The device is comprised of two concentric cylinders with the inner cylinder rotating while both are

being heated by means of steam. The unique characteristic feature of the up-scaled Couette Cell is its 30 mm gap size, which is 6 times more than the lab-scaled counterpart.

Finally, a parametric study was used to find the optimum process conditions between the process time and rotation rate while maintaining a constant temperature (**Chapter 5**). This study yielded highly fibrous structures with a characteristic 30 mm thickness, which emulates meat accurately. The Couette Cell concept and the flexibility in its design allow production of meat replacers at proportions currently not available. Additionally, no barriers were found for further upscaling this concept by preferably designing a continuous process.

SAMENVATTING

Om de toenemende vraag naar proteïnerijk voedsel van een steeds groeiende bevolking tegemoet te komen, worden in vleesproducten plantaardige eiwitten gebruikt als vervangers voor dierlijke eiwitten. Peulvruchten zoals soja kunnen dienen als alternatieve bron van eiwitten, omdat ze zowel een hoog eiwitgehalte (36%) als een hoge proteïne functionaliteit (geleren) hebben. Tegenwoordig zijn verscheidene vlees vervangende producten commercieel beschikbaar, wat betekent dat steeds meer consumenten bereid zijn om hun dieet te veranderen naar een plantaardige variant. Momenteel is extrusie koken de efficiëntste technologie voor de productie van vleesvervangers. Nieuwe methodes voor het structureren van eiwitten zijn nog maar recentelijk geïntroduceerd. De twee nieuwe technologieën zijn gebaseerd op het toepassen van een lineair afschuifprofiel en warmte op het eiwitmengsel. Daartoe was eerst een apparaat ontwikkeld met een kegel-kegel ontwerp, Shear Cell genaamd, dat soja-gebaseerde mengsels in vleesachtige producten kan structureren. Echter, omdat het ontwerp van de Shear Cell gelimiteerd is tot gebruik in het laboratorium, is een nieuwe technologie ontwikkeld die gepresenteerd wordt in dit proefschrift.

Het concept van de Couette Cell, dat gebaseerd is op concentrische cilinders, is bestudeerd, aangezien het verdere opschaling tot industrieel relevante productievolumes toelaat. Het onderzoek start met een "proof of concept" met behulp van een Couette Cell op laboratoriumschaal met een volume van 0.14 L en een *afschuifzone* tussen de cilinders van 5 mm dik (**Hoofdstuk 2**). Het toepassen van een afschuifprofiel en warmte op een soja-gebaseerd mengsel bij verschillende proces condities (temperatuur, tijd en rotatiesnelheid) heeft anisotropische structuren opgeleverd die lijken op die van vlees. Vezelachtige structuren waren voornamelijk aanwezig bij temperaturen tussen 90 en 100 °C.

De vezelachtige producten met de hoogste anisotropie indices waren verder onderzocht en gekarakteriseerd met een set van complementaire technieken (**Hoofdstuk 3**). Met licht microscopie konden we structuurvorming observeren over de zichtbare oppervlakken van de monsters. Daarnaast konden we met een kleurmiddel de verschillende ingrediënten onderscheiden. Volgens de resultaten van de textuuranalyse zijn de anisotropie indices van de verkregen vleesvervanger vergelijkbaar met die van rauw vlees (rundvlees). Om *binnen in* de bulk van de anisotrope vleesvervanger te kijken hebben wij de neutron refractie methode geïntroduceerd door spin-echo small angel neutron scattering (SESANS) te gebruiken. Daardoor was het mogelijk om het aantal vezellagen en de distributie van oriëntaties van de vezels aanwezig in de monsters te kwantificeren. De berekende vezeldikte kwam overeen met de observaties gedaan met de scanning electron microscoop (SEM).

Omdat de Couette Cell zo succesvol bleek en schaalbaar is, hebben wij een Couette Cell ontwikkeld op grotere schaal, die 7 L per batch kan behandelen. Dat is 50 keer meer dan de Couette Cell op laboratoriumschaal. Het gedetailleerde ontwerp van de grote Couette Cell is

behandeld in **Hoofdstuk 4**. Het grote apparaat is geschikt voor de vervaardiging van vezelachtige vleesvervangers op industrieel relevante schaal en opent de mogelijkheid tot commerciële productie in een opkomende markt. Het apparaat bestaat uit twee concentrische cilinders, waarvan de binnenste cilinder roteert, terwijl beide worden opgewarmd met stoom. Het unieke kenmerk van de grote Couette Cell is de dikte van de afschuifzone. Deze bedraagt 30 mm en is daarmee 6 keer zo groot als die in zijn versie op laboratoriumschaal.
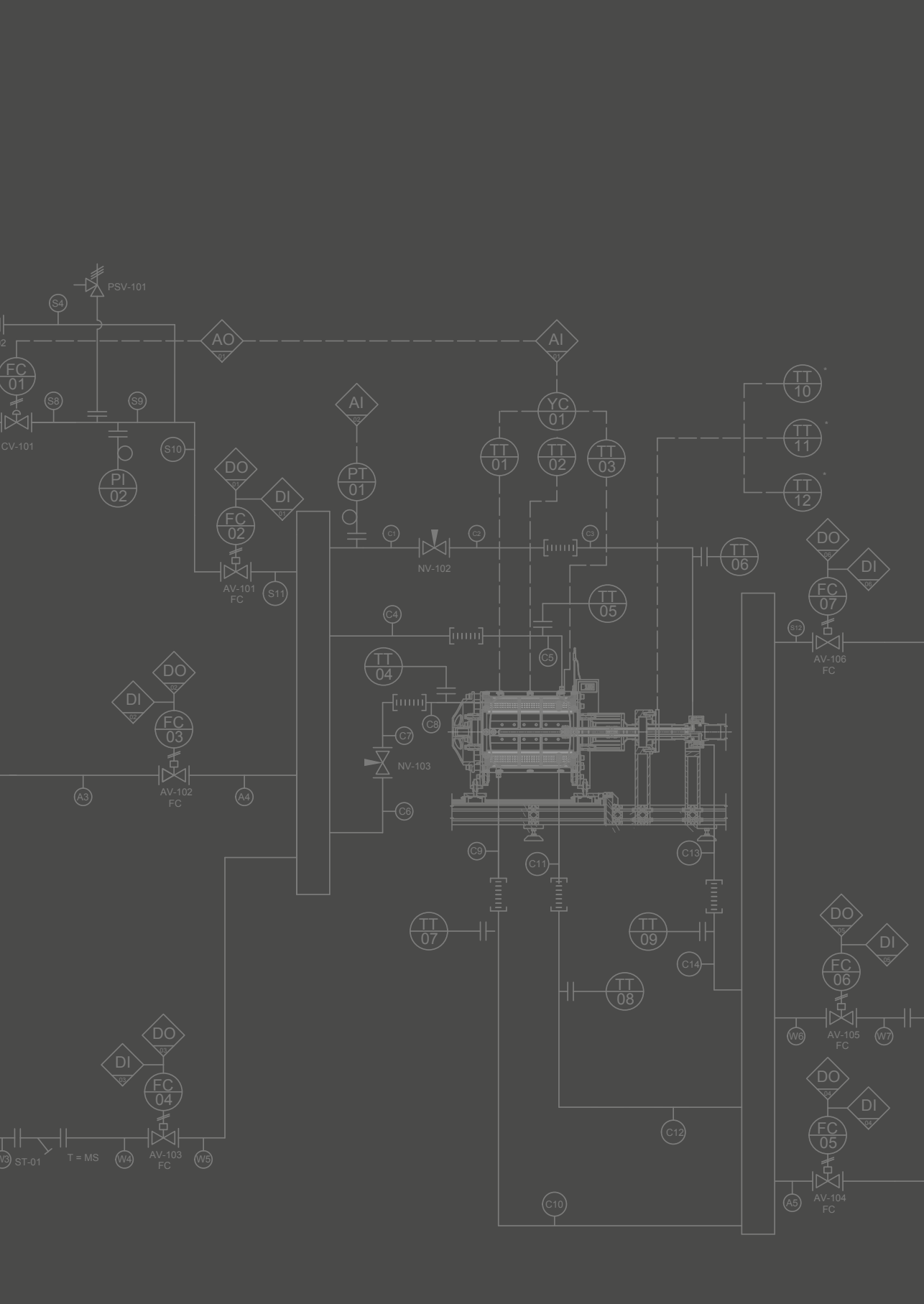
Tenslotte was een parametrische studie gebruikt om de optimale procescondities te vinden tussen de procestijd en rotatiesnelheid, terwijl een constante temperatuur werd aangehouden (**Hoofdstuk 5**). Dit onderzoek resulteerde in zeer vezelachtige structuren met een karakteristieke dikte van 30 mm, die vlees nauwkeurig nabootsen. Het concept van de Couette Cell en de flexibiliteit in het ontwerp ervan maken de productie van vleesvervangers mogelijk in hoeveelheden die momenteel niet beschikbaar zijn. Daarnaast zijn er geen grenzen gevonden voor het verdere opschalen van dit concept, bij voorkeur door het ontwerp van een continu proces.

Table of content

PSV-101

S4

AO

AI

FC
01

S8   S9

CV-101

S10

PI
02

DO

FC
02

DI

AV-101
FC

S11

AI

PT
01

YC
01

TT
01

TT
02

TT
03

TT
10

TT
11

TT
12

DO

FC
07

DI

S12

AV-106
FC

TT
06

NV-102
C1   C2   C3

C4

TT
05

C5

DO

DI

FC
03

TT
04

C8

C7

NV-103

A3   AV-102
FC   A4

C6

C9   C11   C13

C14

TT
07

TT
09

DO

FC
06

DI

AV-105
FC
W6   W7

TT
08

DO

DI

FC
04

DI

DO

FC
05

DI

W3 ST-01   T = MS   W4   AV-103   W5
FC

C12

AV-104
FC
A5

C10

Chapter **1**

INTRODUCTION

CT-02
Condensate

W12-16mm-PVC
W8
Water out

A6
Drain

1.1   The need for sustainable meat replacers

Meat has an integral part in the traditional food pyramid and should be consumed in moderate amounts (Williamson et al., 2005). However, in many countries meat consumption per capita is much higher than the recommended intake, which is a maximum of 80 g/day (McAfee et al., 2010) (28.8 kg/year). Industrial countries like the Netherlands or the United States, show much higher consumption rates, with an estimated average of 95.7 kg/capita by 2015 (Bruinsma, 2003). Excessive meat consumption has direct consequences on public health. Various studies have linked meat consumption with increased risk for cancer (Alavanja et al., 2001; Farvid et al., 2014), diabetes (Feskens et al., 2013), obesity (Wang and Beydoun, 2009) and cerebral infractions (Larsson et al., 2011) among others.

The excessive consumption of meat is also associated with numerous environmental, social and ethical problems. An important consequence of high overproduction of livestock, for instance, is the contamination of air, earth and water. When large numbers of animals are stacked together in a small space, their faeces accumulate rapidly which makes it difficult to handle efficiently (Haapapuro et al., 1997). Although, it is a common practice to spray animal manure on the fields as a fertilizer (Starmer, 2007), excessive fertilization may result in soil having a high concentration of hazardous components present in manure (Hooda et al., 2000b). In addition, pathogenic microorganisms can be vertically transported on the ground if proper impermeable land is not used (Mawdsley et al., 1995). Collectively, water contamination may be caused due to the runoff and discharge of nitrogen and phosphorus compounds, as well as pathogens and organic effluents (Hooda et al., 2000b).

Furthermore, a large part of the society criticizes the excessive use of meat in daily nutrition as unethical owing to the stressful living of animals, which are eventually slaughtered by billions every year (Starmer, 2007). In the United States alone, it is estimated that 7 bn. farm animals are killed yearly (Wolfson, 1996). As a consequence, more and more consumers nowadays are becoming aware of animal welfare (Horgan and Gavinelli, 2006) and many, especially in western countries, are switching to a vegetarian or vegan diet (Key et al., 2006).

Plant protein-based products (i.e. meat replacers) form a more sustainable source for food compared to meat. As it is seen on table 1.1, beef, pork, chicken and tofu (soy based product with a ~12% protein content) (U.S. Department of Agriculture, 2014) are compared based upon three different impact categories: climate change, water footprint and land use. In order to compare different protein sources, the units of the impact categories have been displayed on a per 60 g of protein basis, which is the daily protein intake of an average human (Trumbo et al., 2002). Data displayed in table 1.1 are applicable only to the Dutch agro industry. Since the agro industry in the Netherlands is considered as one of the most efficient and intensified in the world, the values for beef, pork and chicken in table 1.1 are rather conservative. To

illustrate this, the average water footprint for beef in the Netherlands is 1791 L/60 g protein with the world average being 4235 L/60 g protein (Aldaya et al., 2012).

Table 1.1: Impact categories on a daily protein intake basis.

Impact Category	Beef	Pork	Chicken	Tofu
Climate change [kg CO_2 eq./kg] (Head et al., 2011)	23.9	9.01	5.95	2.54
Water footprint [m³/ton] (Mekonnen and Hoekstra, 2010; Usman, 2011)	6513	4429	1787	851
Land use [m²·yr/kg] (Blonk et al., 2007; Head et al., 2011)	56.6	8.42	5.01	2.1

Regarding water consumption, the amount of water used per ton of product of soy beans is 6.6 times lower than the same amount of beef (Hoekstra and International Institute for Infrastructural Hydraulic and Environmental Engineering (IHE), 2003). On another example, water contamination with NO_{3-} due to poultry production is 21.9 mg/L; this value could be reduced to 6.2 mg/L if poultry production were to be substituted by a soybean production area (Hooda et al., 2000a).

In addition, plants, vegetables, legumes and particularly soy, can serve as healthier alternatives to meat since they offer the same amount of proteins with less fat and calories (Williams and Zabik, 1975). But consumers are interested in plant-based products that can replicate meat in terms of mouthfeel, texture, taste, colour and smell. In a recent survey however, consumers stated that these aspects were not at all recognized in current meat replacers (Hoek et al., 2011). Lack of fibrousness makes those products less appealing to the general public (Hoek et al., 2013). Even when in many cases the substitutes are healthier, this still is not enough to convince the consumers (Hoek et al., 2004). Those texturization processes that are currently available, such as extrusion, spinning and simple shear flow, can provide highly structured meat replacers.

1.2   Current structuring technologies

The best technologies currently used for the production of meat replacers are mixing, fibre spinning and extrusion cooking. The most common techniques to obtain meat replacers is by mixing, forming and shearing plant-based ingredients. There are many commercial examples of such techniques originating from Asian culture and cusine, for example, the vegetarian burgers (mixing), seitan (mock duck)(shearing), tofu (precipitation/cheece making) or tempeh (fermentation). Mixing is a simple and affordable technique; however, although it can easily

result in soft and doughy materials, it is impossible to obtain more complex textures like fibres. A typical example, see Figure 1.1(right), is vegan burgers which can emulate the characteristic texture of hamburgers. The process requires simple steps such as, washing all the ingredients; cooking the base grain, which can be made of rice or beans for example; cut the vegetables and finally mixing all of them to form the patties. In many cases, soy and gluten can be used. This combination conforms a soft material with a texture that recalls that of grounded beef; see Figure 1.1(left).

Figure 1.1: Left: Soy-based type ground beef, Right: Soy-based type hamburger. Reprinted with permission from De Vegetarische Slager, Copyright (2015).

Tempeh is a fermented soy bean meat replacer which is widely consumed in Asian countries. The process of making tempeh starts by fermenting soaked soy beans which have been dehulled and partially cooked (Steinkraus et al., 1960; Van Veen and Steinkraus, 1970). The final product is a relatively firm burger-type patty. Tofu on the other hand is made by coagulating soy milk (an emulsion of protein and oil) followed by moulding and pressing the produced curd (Cai and Chang, 1999). Salt, edible acid or enzymes are often used as coagulants for this product.

Another method, which forms seitan, consists of mixing and forming the plant proteins (i.e. gluten) (which are normally in powder form) with water and other ingredients. This particular meat substitute is achieved not only by mixing but also by stretching and compressing the ingredients. With these additional steps the product's texture changes, becoming a soft layered material that can be branded as mock duck.

The previously mentioned meat replacers primarily yield homogeneously structured products with the exception of seitan where shear is applied while forming the product. Wet-spinning is a method which allows the formation of fibres by pushing the protein mixture through a spinneret, which is a filter with a specific pore diameter. The outlet of the spinneret

is usually submerged in a cold fluid to allow solidification of the obtained fibres. There are different variations of the devices used in centrifugal spinning. In a study conducted by (Huang et al., 1995), a traditional wet-spinning system is used, with the filter and coagulation bath as main parts of the system. The pressure and temperature of the process play a determinant role in the characteristics of the final product. The obtained fibres can be improved by using an acid solution in the coagulation bath. In (Hildebolt, 1977) study, centrifugal spinning was employed, which combines the traditional wet-spinning principle with centrifugal forces to apply a higher shear force. The texturization procedure starts by introducing a mixture of dry proteins (at least 70%) with water in a confined chamber. High pressure steam is used to force the material enter through the inlet until it reaches the processing chamber. At this point, the protein slurry is forced to spin, inducing high shearing forces on the mixture. According to the study, the residence time inside the chamber does not have significant effect on the final product. The main advantage of the wet-spinning method is the possibility of obtaining fibrous materials without degrading the material or using expensive additives. The main drawbacks are the difficulty to upscale, the low strength of the produced fibres and the excessive water consumption and waste water production.

Finally, one of the oldest and most widely used techniques for the production of meat replacers nowadays is extrusion. Extrusion cooking is currently used in many common commercial products, for instance, cookies, pasta and breakfast cereals (Cheftel, 1986). Extrusion cooking (Bouvier and Campanella, 2014) is a form of texturization which employs a traditional screw extruder which treats the protein suspension under extreme temperature pressure and mixing conditions. Figure 1.2 shows a typical scheme of a twin-screw extruder and highlights the main process zones. This process is typically operated at high temperatures between 100 ºC and 160 ºC at short residence times ranging from 8 - 40 seconds (Crowe and Johnson, 2001). A cooling die is fitted at the end of the extruder where the material is deformed by means of shear resulting in an anisotropic product.
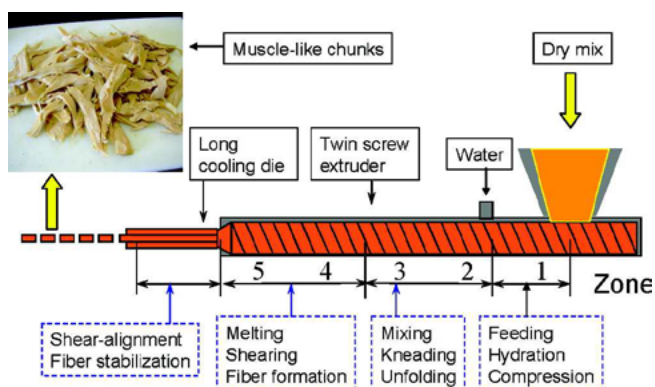

Figure 1.2: Scheme of a twin-screw extruder for high-moisture extrusion of proteinaceous materials into fibrous meat analogues. Reprinted with permission from (Liu and Hsieh, 2008). Copyright (2008), American Chemical Society.

Many studies have reported successful production of layered and fibrous structures (Huang et al., 1995; Lin et al., 2002; Liu and Hsieh, 2008; Osen et al., 2014; Thiébaud et al., 1996; Wild et al., 2014)   that can serve as meat replacers. Figure 1.3 shows as typical commercially available meat replacer produced with extrusion cooking of a Soy Protein Concentrate (SPC) and water mixture. A study by (Cheftel et al., 1992) reported production of anisotropic layered and coarse fibrous structures at high moisture levels by employing a twin screw extruder and by treating a mixture of Soy Protein Isolate (SPI) and gluten. The extrusion is a well-known and well-studied technology that has been optimized for the production of meat replacers, while at the same time allows for continuous processing at an industrial scale. However, the screw rotation and heating of the mixture result in a highly energy consuming process that is also energy inefficient due to the intensive heating at the barrel/screw region and rapid cooling at the die. Additionally, temperature and pressure gradients can lead to excessive drying and destruction of the formerly structured product.

Figure 1.3: Extruded soy-based type chicken bites. Reprinted with permission from De Vegetarische Slager, Copyright (2015).

1.3   Shear Cell structuring

A novel method for protein structuring was introduced by Wageningen University and Research Centre (WUR) with the development of a device called the Shear Cell (Peighambardoust et al., 2004). The Shear Cell design is based on the cone-plate rheometer. The device is comprised of a cone-cone assembly with the outer cone rotating while the inner remains stationary, as seen in Figure 1.4. The space between the outer and inner cones is a few millimetres, this space is called "*shearing zone*". This geometry does not allow for homogeneous shear stress over the whole material. Both cones can be heated by means of electric heaters and in more recent version of the device by means of water or oil depending on the desired temperature.
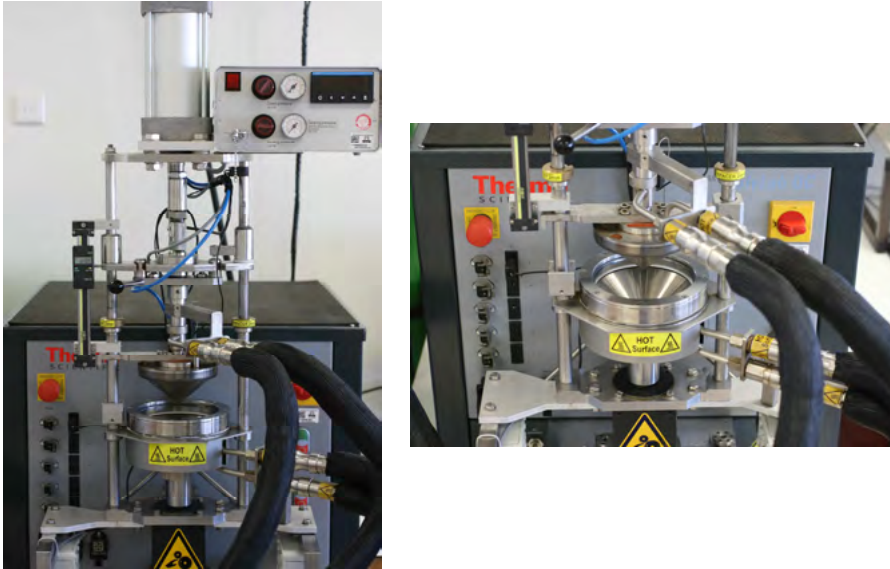
Figure 1.4: The Shear Cell device; on the left notice the top and bottom cones at the open position and; on the right notice the cone corrugations. Reprinted with permission from Wageningen University and Research (WUR), Copyright (2015).

The Shear Cell has been utilized to texturize a mixture based in Ca-Caseinate, a protein found in the milk (Manski et al., 2007). The experiments performed with this protein mixture revealed promising results by obtaining fibrous structures. The Shear Cell induces simple shear flow in the protein suspension which in turn aligns the proteins in layered and/or fibrous formations. Obtaining fibre structures was only possible when employing Transglutaminase, a binding enzyme. Recently, in a study by (Grabowska et al., 2014b) it was possible to structure plant-based protein mixtures containing a blend of Soy Protein Isolate (SPI) and vital Wheat Gluten (WG).

This method allows for lower energy consumption and controlled shear stress distribution while obtaining texturized products. Compared to extrusion cooking, the energy required to rotate the outer cone and power the heating elements or water/oil bath is lower. Compared to fibre spinning, there is no excessive water consumption and no wasted water streams during processing. On the other hand, the Shear Cell design does not allow for scaled up production. Due to its conical shape, increasing the product volume would require a significant increase in the whole device. Additionally, due to the radial changes over the surface of the cone, is leading to shear stress gradients and an inhomogeneous product from top to bottom.

1.4   Couette Cell structuring

Recently, a new method for plant-protein structuring was introduced by (Krintiras et al., 2015) called the lab-scaled Couette Cell. Initial studies were performed using the Couette Cell by (Peighambardoust et al., 2007) at Wageningen University and Research Centre (WUR) by treating wheat gluten-starch mixtures to determine the effect of simple shear processing. This device was further improved and modified at Delft University of Technology (TU Delft) by (Krintiras et al., 2015) to study the effect of simple shear flow on plant-protein based mixtures. The lab-scaled Couette Cell is comprised of two concentric cylinders with the inner cylinder rotating while the outer remains stationary. Both cylinders were heated by means of oil and they feature small corrugations to increase the surface contact between the cylinder wall and the mixture. During the study by (Krintiras et al., 2015) the lab-scaled Couette Cell was employed to treat a mixture of Soy Protein Isolate (SPI) and vital Wheat Gluten (WG) to form layered and fibrous structures. The experimental study generated positive results by obtaining layered and fibrous structures at mild process conditions. Hence, this study is a proof of principle that the lab-scaled Couette Cell can successfully process plant-based mixtures and that eventually this concept could be further developed to serve as a novel industrial process for the commercial production of fibrous meat replacers.

The lab-scaled Couette Cell served as an initial stage towards exploring optimum operating and process conditions for the formation of fibrous structures and the further development of an up-scaled device. It was found that filling the device and tightly packing it was crucial for the success of the process. Additionally, it was found that fibrous structures could be obtained at 95 °C process temperature with a rotational speed of 30 RPM and treating the mixture for 15 minutes.

Since the lab-scaled Couette Cell proved that simple shear flow could successfully induce structures in such a geometry an up-scaled Couette Cell was designed and developed towards an industrially relevant capacity (Krintiras et al., 2016). The up-scaled Couette Cell follows the same principle as the lab-scaled Couette Cell only the capacity has been increased by 50 times to ~7 litres as well as product thickness to 30 mm. The device is heated by means of steam and is positioned horizontally for easy handling and operation. The Couette Cell as a concept allows for linear upscaling and possible continuous operation. It is possible to create highly fibrous structures based on soy protein that can serve as meat replacers at a thickness of 30 mm which is not currently possible with other methods. The Couette Cell allows for simple shear deformation and low energy consumption during the process. Further developments and up-scaling of this technology can deliver industrial production of high quality meat replacers to the consumers, thus helping a swift towards a more sustainable food production and less consumption of meat.

1.5   Research objective

The general objective of this thesis is to develop a novel up-scaled device for the sustainable production of high quality plant protein based meat replacers. The device to be introduced should pave the way towards large-scale industrial production of meat replacers preferably in a continuous manner. Achieving this general objective is not trivial. So during this research additional (sub) objectives and areas of interest have been investigated. It was known that protein based mixtures when subjected to simple shear and heat would result anisotropic fibrous structures. Initially a model system with potential to be scaled up and be operated continuously had to be investigated. The experimental Couette Cell was considered for extensive parametric study and verification. Additionally, proper characterization of the products would provide comprehensive understanding of the structure formation. Further investigation of the flow and heat transfer phenomena within the Couette Cell was initiated. These preliminary studies helped design and develop the up-scaled Couette Cell. Finally, a parametric study was conducted to verify the structure formation with the up-scaled Couette Cell.

1.6   Outline of the thesis

Chapter 2

Chapter 2 presents the parametric study with the experimental Couette Cell which provides proof of concept for the production of structured meat replacers by applying simple shear flow and heat to a Soy Protein Isolate (SPI) – Wheat Gluten (WG) mixture. Highly anisotropic layer- or fibre-structured products were obtained at this stage. The optimal process conditions were found and their effect was found not to be critical. It is highlighted that simultaneous application of simple shear and heat is the key to obtaining structured meat replacers. The Couette Cell can be scaled-up which is appealing for commercial production of meat analogues.

Chapter 3

This chapter introduces the neutron refraction method by utilizing Spin-Echo Small Angle Neutron Scattering (SESANS) as a complementary technique for the characterization of meat replacers. With neutron refraction it was possible to quantify the number of fibre layers and their orientation distribution. Standard techniques were utilized such as light microscopy, scanning electron microscopy and texture analysis. A conclusive and all-around characterization study of an anisotropic SPI-gluten sample is therefore presented.

Chapter 4

In Chapter 4 the design and the features of the up-scaled Couette Cell are outlined. The main objective of this study is the introduction of a device that can be scalable and potentially operated continuously. We addressed this objective first by a proof of concept work with the experimental Couette Cell (chapter 2) which successfully yielded structured meat replacers. So the main design features of the experimental Couette Cell were retained. The dimensions of both inner and outer cylinders were increased as well as the thickness of the *shearing zone*. The overall capacity of the up-scaled Couette Cell is increased to ~ 7 litres and is operated in a batch mode.

Chapter 5

In Chapter 5 a parametric study with the up-scaled Couette Cell in which the production of structured meat replacers is presented. Similarly to the study in Chapter 2, by applying simple shear flow and heat to a Soy Protein Isolate (SPI) – Wheat Gluten (WG) mixture. Highly anisotropic layer- or fibre-structured products were obtained. The optimal process conditions were found and their effect was found not to be critical. It is highlighted that the up-scaled Couette Cell allowed the production of 30 mm thick samples which are currently not available in the market. The Couette Cell has additionally proven to be a scalable concept which in the future can be easily linearly scaled-up and possibly be operated in a continuous mode.

Chapter 6

The last chapter summarizes the findings of the thesis and gives recommendations for future research on food structuring with the Couette Cells. It also lists the design principles that were found. Additionally it concludes with highlighting the future possibilities for food structuring.

References

Alavanja, M.C.R., Field, R.W., Sinha, R., Brus, C.P., Shavers, V.L., Fisher, E.L., Curtain, J., Lynch, C.F., (2001). Lung cancer risk and red meat consumption among Iowa women. Lung Cancer 34(1), 37-46.

Aldaya, M.M., Chapagain, A.K., Hoekstra, A.Y., Mekonnen, M.M., (2012). *The water footprint assessment manual: Setting the global standard.* Routledge.

Blonk, H., Alvarado, C., Schryver, A.D., (2007). Milieuanalyse vleesproducten. PRé Consultants B.V. and Blonk Milieu Advies.

Bouvier, J.-M., Campanella, O., (2014). *Extrusion processing technology : food and non-food biomaterials.* John Wiley & Sons Inc., Chichester, West Sussex, UK.

Bruinsma, J., (2003). *World agriculture: towards 2015/2030. An FAO perspective.* Earthscan Publications Ltd.

Cai, T., Chang, K.-C., (1999). Processing Effect on Soybean Storage Proteins and Their Relationship with Tofu Quality. Journal of Agricultural and Food Chemistry 47(2), 720-727.

Cheftel, J.C., (1986). Nutritional effects of extrusion-cooking. Food Chemistry 20(4), 263-283.

Cheftel, J.C., Kitagawa, M., Quéguiner, C., (1992). New protein texturization processes by extrusion cooking at high moisture levels. Food Reviews International 8(2), 235-275.

Crowe, T., Johnson, L., (2001). Twin-screw extrusion texturization of extruded-expelled soybean flour. Journal of the American Oil Chemists' Society 78(8), 781-786.

Farvid, M.S., Cho, E., Chen, W.Y., Eliassen, A.H., Willett, W.C., (2014). *Dietary protein sources in early adulthood and breast cancer incidence: prospective cohort study.*

Feskens, E.M., Sluik, D., van Woudenbergh, G., (2013). Meat Consumption, Diabetes, and Its Complications. Current Diabetes Reports 13(2), 298-306.

Grabowska, K.J., Tekidou, S., Boom, R.M., van der Goot, A.-J., (2014). Shear structuring as a new method to make anisotropic structures from soy–gluten blends. Food Research International 64, 743-751.

Haapapuro, E.R., Barnard, N.D., Simon, M., (1997). Review—Animal Waste Used as Livestock Feed: Dangers to Human Health. Preventive Medicine 26(5), 599-602.

Head, M., Sevenster, M., Croezen, H., (2011). Life Cycle Impacts of Protein- rich Foods for Superwijzer. CE Delft.

Hildebolt, W.M., (1977). Protein texturization by centrifugal spinning. Google Patents.

Hoek, A.C., Elzerman, J.E., Hageman, R., Kok, F.J., Luning, P.A., Graaf, C.d., (2013). Are meat substitutes liked better over time? A repeated in-home use test with meat substitutes or meat in meals. Food Quality and Preference 28(1), 253-263.

Hoek, A.C., Luning, P.A., Stafleu, A., de Graaf, C., (2004). Food-related lifestyle and health attitudes of Dutch vegetarians, non-vegetarian consumers of meat substitutes, and meat consumers. Appetite 42(3), 265-272.

Hoek, A.C., Luning, P.A., Weijzen, P., Engels, W., Kok, F.J., de Graaf, C., (2011). Replacement of meat by meat substitutes. A survey on person- and product-related factors in consumer acceptance. Appetite 56(3), 662 - 673.

Hoekstra, A.Y., International Institute for Infrastructural Hydraulic and Environmental Engineering (IHE), (2003). *Virtual water trade*. IHE, Delft.

Hooda, P., Edwards, A., Anderson, H., Miller, A., (2000a). A review of water quality concerns in livestock farming areas. Science of the Total Environment 250(1), 143-167.

Hooda, P.S., Edwards, A.C., Anderson, H.A., Miller, A., (2000b). A review of water quality concerns in livestock farming areas. Science of the Total Environment 250(1-3), 143-167.

Horgan, R., Gavinelli, A., (2006). The expanding role of animal welfare within EU legislation and beyond. Livestock Science 103(3), 303-307.

Huang, H.C., Hammond, E.G., Reitmeier, C.A., Myers, D.J., (1995). Properties of fibers produced from soy protein isolate by extrusion and wet-spinning. Journal of the American Oil Chemists' Society 72(12), 1453-1460.

Key, T.J., Appleby, P.N., Rosell, M.S., (2006). Health effects of vegetarian and vegan diets. Proceedings of the Nutrition Society 65(01), 35-41.

Krintiras, G.A., Gadea Diaz, J., van der Goot, A.J., Stankiewicz, A.I., Stefanidis, G.D., (2016). On the use of the Couette Cell technology for large scale production of textured soy-based meat replacers. Journal of Food Engineering 169, 205-213.

Krintiras, G.A., Göbel, J., van der Goot, A.J., Stefanidis, G.D., (2015). Production of structured soy-based meat analogues using simple shear and heat in a Couette Cell. Journal of Food Engineering 160(0), 34-41.

Larsson, S.C., Virtamo, J., Wolk, A., (2011). Red meat consumption and risk of stroke in Swedish men. The American Journal of Clinical Nutrition 94(2), 417-421.

Lin, S., Huff, H.E., Hsieh, F., (2002). Extrusion Process Parameters, Sensory Characteristics, and Structural Properties of a High Moisture Soy Protein Meat Analog. Journal of Food Science 67(3), 1066-1072.

Liu, K., Hsieh, F.-H., (2008). Protein–Protein Interactions during High-Moisture Extrusion for Fibrous Meat Analogues and Comparison of Protein Solubility Methods Using Different Solvent Systems. Journal of Agricultural and Food Chemistry 56(8), 2681-2687.

Manski, J.M., van der Goot, A.J., Boom, R.M., (2007). Formation of fibrous materials from dense calcium caseinate dispersions. Biomacromolecules 8(4), 1271-1279.

Mawdsley, J.L., Bardgett, R.D., Merry, R.J., Pain, B.F., Theodorou, M.K., (1995). Pathogens in Livestock Waste, Their Potential for Movement through Soil and Environmental-Pollution. Applied Soil Ecology 2(1), 1-15.

McAfee, A.J., McSorley, E.M., Cuskelly, G.J., Moss, B.W., Wallace, J.M.W., Bonham, M.P., Fearon, A.M., (2010). Red meat consumption: An overview of the risks and benefits. Meat Science 84(1), 1-13.

Mekonnen, M., Hoekstra, A., (2010). The green, blue and grey water footprint of farm animals and animal products.

Osen, R., Toelstede, S., Wild, F., Eisner, P., Schweiggert-Weisz, U., (2014). High moisture extrusion cooking of pea protein isolates: Raw material characteristics, extruder responses, and texture properties. Journal of Food Engineering 127(0), 67-74.

Peighambardoust, S., Van der Goot, A., Hamer, R., Boom, R., (2004). A new method to study simple shear processing of wheat gluten-starch mixtures. Cereal Chemistry 81(6), 714-721.

Peighambardoust, S.H., Brenk, S.v., Goot, A.J.v.d., Hamer, R.J., Boom, R.M., (2007). Dough processing in a Coutte-type device with varying eccentricity: effect on glutenin macro-polymer properties and dough microstructure. Journal of Cereal Science 45(1), 34-48.

Starmer, E., (2007). Agricultural Business Initiative: Environmental and Health Problems in Livestock Production: Pollution in the Food System Issue Brief# 2 (Online). The Agribusiness Accountability Initiative.

Steinkraus, K.H., Hwa, Y.B., Van Buren, J.P., Provvidenti, M.I., Hand, D.B., (1960). Studies on tempeh - An Indonesian fermented soybean food. Journal of Food Science 25(6), 777-788.

Thiébaud, M., Dumay, E., Cheftel, J.C., (1996). Influence of Process Variables on the Characteristics of a High Moisture Fish Soy Protein Mix Texturized by Extrusion Cooking. LWT - Food Science and Technology 29(5–6), 526-535.

Trumbo, P., Schlicker, S., Yates, A.A., Poos, M., (2002). Dietary Reference Intakes for Energy, Carbohydrate, Fiber, Fat, Fatty Acids, Cholesterol, Protein and Amino Acids. Journal of the American Dietetic Association 102(11), 1621-1630.

U.S. Department of Agriculture, A.R.S., (2014). USDA National Nutrient Database for Standard Reference, *Release 27*. Nutrient Data Laboratory.

Usman, I., (2011). Assessing the Water Footprint of Tofu Produced from Organically Cultivated Crops. NOVIA University of Applied Sciences.

Van Veen, A.G., Steinkraus, K.H., (1970). Nutritive value and wholesomeness of fermented foods. Journal of Agricultural and Food Chemistry 18(4), 576-578.

Wang, Y., Beydoun, M.A., (2009). Meat consumption is associated with obesity and central obesity among US adults. International journal of obesity (2005) 33(6), 621-628.

Wild, F., Czerny, M., Janssen, A.M., Kole, A.P.W., Zunabovic, M., Domig, K.J., (2014). The evolution of a plant-based alternative to meat - From niche markets to widely accepted meat alternatives. Agro FOOD Industry Hi Tech 25(1), 45-49

Williams, C.W., Zabik, M.E., (1975). Quality Characteristics of Soy-Substituted Ground Beef, Pork and Turkey Meat Loaves. Journal of Food Science 40(3), 502-505.

Williamson, C.S., Foster, R.K., Stanner, S.A., Buttriss, J.L., (2005). Red meat in the diet Nutrition Bulletin Volume 30, Issue 4, *Nutrition Bulletin*, pp. 323-355.

Wolfson, D.J., (1996). Beyond the law: Agribusiness and the systemic abuse of animals raised for food or food production. Animal L. 2, 123.

Chapter **2**

PRODUCTION OF STRUCTURED SOY-BASED MEAT ANALOGUES USING SIMPLE SHEAR AND HEAT IN A COUETTE CELL

Condensate

CT-02

W12-16mm-PVC

Water out

W8

Drain

A6

Abstract

A Couette Cell device was employed to provide proof of concept for the production of structured meat analogues by application of simple shear flow and heat to a 31 wt% Soy Protein Isolate (SPI) - Wheat Gluten (WG) dispersion. Three relevant process parameters (temperature, time and rotation rate) were varied over a range of realistic values (90-110 ℃, 5-25 minutes and 5-50 RPM, respectively). Layer- or fibre-structured products with high stress and strain anisotropy indices have been demonstrated. Fibrousness is favoured at temperatures over 90 ℃ and under 100 ℃, whereas the role of process time and rotation rate is not critical. Simultaneous application of simple shear and heat is the key to obtaining structured plant protein-based products. The Couette Cell concept is scalable and can enable continuous operation. On this ground, it appears as a realistic option for production of meat analogues at commercial scale.

2.1   Introduction

With an increasing world population of nearly 7 billion people there is a growing demand for food supply. A plant protein-based diet can partially address the problem of food crisis and animal protein malnutrition in several developing countries. Further, in developed countries, increasing awareness of animal welfare and environmental protection has shifted the daily food consumption towards plant-based diet as well. Moreover, plant proteins provide desirable functional properties, such as solubility, viscosity, water and oil retention, foam formation, emulsification and gelation. In Western diets, significant reduction in meat consumption (up to 40%) is possible without risk of lack of micro-nutrients normally supplied through meat products. Therefore, an introduction of new alternative forms of food products and room for development of an attractive market around plant protein-based products in food industry is needed (Boye et al., 2010; Rodrigues et al., 2012). Meat analogues created from plant-based materials can form one class of these products, which will be accepted by consumers provided that they have pronounced fibrous structure and are competitive in price compared to meat. The latter prerequisites simple technology for making the products (Hoek et al., 2011).

Currently, extrusion (Lin et al., 2002; Thiébaud et al., 1996; Yao et al., 2004) and spinning (Huang et al., 1995; Rampon et al., 1999; Suchkov et al., 1988) are the main techniques available to make anisotropic structures. However, these techniques come with some disadvantages. Spinning produces large waste water streams. In addition, the necessity for low pH, high salt concentrations and chemical additives makes the process complex (Manski et al., 2007b). Extrusion, which is the current best technology for production of meat analogues, applies thermo-mechanical treatment using high temperatures and shear rates inside the barrel/screw region resulting in melting of the protein suspension and intensive mixing. Only at the die region, where the mixture is cooled down and simple shear flow is present, structure formation can occur (Riaz, 2000). This process was first demonstrated in 1797 by Josef Bramah, England, who was the first to apply the extrusion principle using a hand-operated piston press to extrude seamless lead pipes for use in guns and rifles (Blackmore, 1986). The use of extrusion for high moisture applications (40 - 80%) has been reviewed by Cheftel (Cheftel et al., 1992). Cheftel reported that application of a twin-screw extruder combined with a long cooling die to Soy Protein Concentrate (SPC), or mixtures of Soy Protein Isolate (SPI) and 5 - 10% vital wheat gluten (WG) enabled the formation of anisotropic structures with layers and coarse fibres oriented in the direction of the flow through the die. However, it was very difficult to extrude and structure pure SPI.

Recently, a new technique based on the concept of flow-induced structuring (Manski et al., 2007b; Manski et al., 2008; Peighambardoust et al., 2004) was introduced. For this purpose, a cone-cone device based on a cone-plate rheometer was developed which is referred to as Shear Cell. The top cone is stationary while the bottom cone rotates. Both cones can be heated and cooled with the use of an oil bath. Contrary to extrusion, the deformation inside the

device is well defined and constant upon processing. Due to a combination of simple shear and heat, proteins are aligned forming fibrous structures. (Manski et al., 2007b; Manski et al., 2008) reported that it is possible to fibrilize dairy proteins (calcium caseinate) in a Shear Cell. However, the shear rate in the Shear Cell is not constant over the entire protein sample volume due to the gradually increasing distance between the cones along the radius. Most importantly, the scalability of this configuration is limited, which limits its applications to lab-scale testing.

In this work, a Couette Cell is explored as an alternative scalable geometry. The Couette Cell design favours increased product thickness and capacity by simply increasing the cylinders' size and length. Additionally, the Couette Cell can be potentially operated in a continuous mode in the future. The device was originally developed to study the behaviour of dough under simple shear flow and was not optimized for operation at elevated temperatures (Peighambardoust et al., 2007). After several design upgrades of the original device to improve heat management and material handling, the Couette Cell has been used in this work to shear a blend of plant proteins. A limited parametric study, with respect to process temperature, process time and rotations per minute (RPM) of the inner cylinder, was performed to prove the process concept. The products were characterized by means of visual inspection, texture analysis/tensile stress and scanning electron microscopy (SEM). It is remarked that the purpose of the experimental study was not a full optimization of the operating conditions, but the first demonstration of the potential of a Couette Cell to make anisotropic plant protein-based structures under mild process conditions.

2.2 Materials and Methods

2.2.1 Materials

A blend of soy protein isolate (SPI) (SUPRO EX37 HG IP, Solae, USA) and vital wheat gluten (WG) (VITEN, Roquette, France) was used. In the event of SPI, the protein content was 90%, while gluten had a protein content of 81% based on a nitrogen-to-protein conversion factor of 6.25, measured with the Dumas method. Sodium chloride, referred to as salt hereafter, was also used, as it has been reported that it may enhance the formation of anisotropic structures (Grabowska et al., 2012).

2.2.2   Experimental set-up – Couette Cell

The Couette Cell is shown in Figure 2.1. It is based on the common concentric cylinder rheometer concept. The device is connected to a rheodrive unit (Haake PolyLab QC, Thermo Fisher Scientific, Karlsruhe, Germany), which is used to record temperature and torque while keeping the angular velocity of the rotating inner cylinder constant. The outer cylinder remains stationary. Both the inner and outer cylinders are heated by means of oil. The sample material is placed in the space between the two cylinders; this space is called *shearing zone*. The temperature in the *shearing zone* is measured in two positions in the middle of the total height.
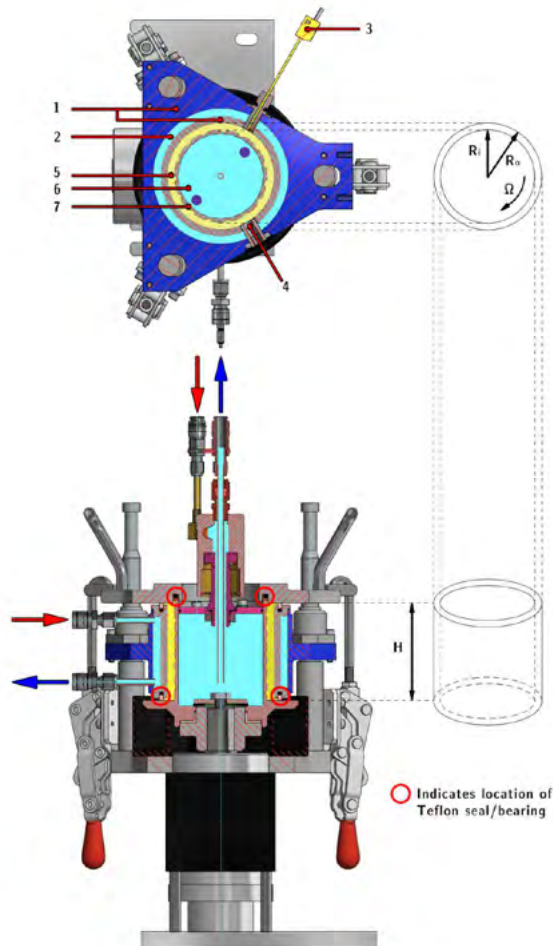

Figure 2.1: Horizontal (top) and vertical (bottom) cross sections of the Couette Cell. 1. Outer cylinder; 2. Heating chamber of outer cylinder; 3. PT100 temperature sensor; 4. Filling opening and location of J-type thermocouple; 5. Shearing zone; 6. Heating chamber of inner cylinder; 7. Inner cylinder. R_i (radius of inner cylinder) = 0.0425 m, R_o (radius of outer cylinder) = 0.0485 m and H (height of both cylinders) = 0.085 m.

Two oil baths are used; one "hot" oil bath to heat up the Couette Cell before and during an experiment and one "cold" oil bath, at 60 °C, to cool the Couette Cell down after shearing. A PT100 temperature sensor is placed in the wall of the outer cylinder with its tip located at the inner wall of the outer cylinder. The PT100 is connected to the hot oil bath to allow temperature reading and control of the Couette Cell. The temperature of the hot oil bath is controlled by the Lauda Wintherm software (Lauda DR. R. Wobser GmbH & Co. KG, Lauda-Königshofen, Germany) on a PC connected to the hot oil bath via an R232 connector. A J-type thermocouple is placed at a position closer to the inlet of the heat transfer fluid in the middle of the plug to seal the filling hole (see Figure 2.1 and 2.2). The J-type thermocouple was calibrated with a dry block calibrator (T-350P, PRESYS) and a high precision thermometer (F252, ASL). The incoming flow of the heat transfer fluid is split before it enters the Couette Cell, so the inner and outer cylinders are heated simultaneously (in parallel).
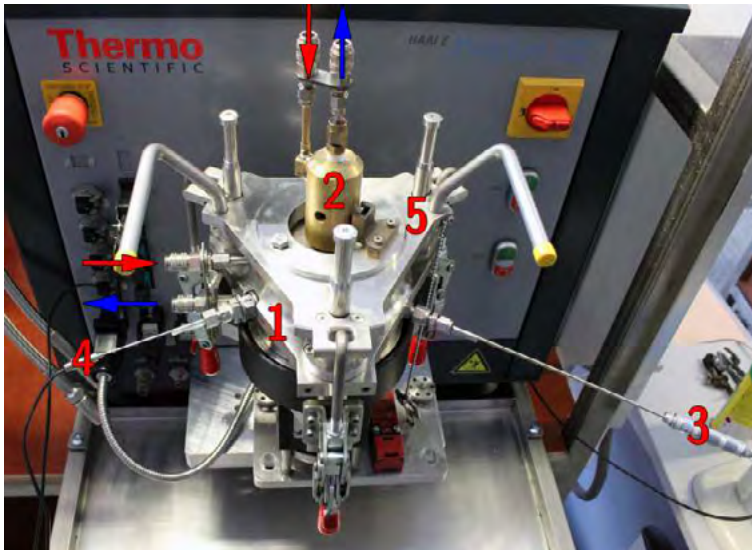

Figure 2.2: Top view of the Couette Cell with arrows showing the inlet and outlet of the heat transfer fluid. 1. Outer cylinder; 2. Rotary joint; 3. PT100 temperature sensor; 4. J-type thermocouple; 5. Lid.

An important aspect of the Couette flow is that the velocity gradient and shear stress are constant throughout the flow domain provided no slip at the walls. The absence of wall slip is one of the assumptions made concerning fluid flow in the Couette Cell. The other assumptions are laminar flow and incompressible Newtonian fluid implying constant viscosity. It can also be assumed that the concentric cylinder device can be approximated by two infinite bending parallel plates. On these assumptions, the velocity gradient and the shear stress across the Couette Cell are constant. Since the shear stress is constant, the processed material experiences the same conditions everywhere except near the top and the bottom of the Couette Cell.

The simplest approximation of the shear rate is given in Equation 2.1:

$$\dot{\gamma} = \frac{\upsilon_{R_i}}{h} \tag{2.1}$$

Where, $\dot{\gamma}$ [s^{-1}] is the shear rate, h [m] is the gap distance between the rotating and stationary cylinders and υ_{R_i} [m/s] is the circumferential velocity of the inner rotating cylinder calculated as

$$\upsilon_{R_i} = \Omega R_i = 2R_i \pi \frac{RPM}{60} \tag{2.2}$$

Where, R_i [m] is the radius of the inner cylinder and Ω [rad/s] is the rotational speed.

The shear rate in Equation 2.1 depends only on the geometry of the Couette Cell and not on the processed material. Therefore, it is only valid for Newtonian fluids (i.e., the shear viscosity is not dependent on the shear rate) and for narrow-gap concentric-cylinder viscometers (or Couette Cells) (Barnes et al., 1989). In page 92, of this thesis, equations 5.6 and 5.7 can be found which can more accurately predict the shear rate and velocity profiles in concentric cylinder devices.

2.2.3   Sample preparation filling procedure

For each experiment, 200 g of sample material was made according to the recipe in Table 2.1. The mixture created had a dry matter content of 31 wt%, with an SPI - gluten ratio of 3.3:1. First, 138.0 g of demi-water and 2.0 g of salt was measured. The salt was added to the demi-water in a flask, and was shaken to completely dissolve the salt. The demi-water - salt solution was added to 46.0 g SPI in a glass beaker and the mixture was manually mixed with a spatula for 1 min. The glass beaker was covered to prevent moisture from escaping. The mixture was left to rest for 30 minutes, as it was found during preliminary work that pre-humidification for 30 minutes enhances protein structuring. To prevent gluten particles from lumping together, 14.0 g of it was added last followed by mixing with the spatula for 1 minute. After this step, the SPI - gluten - demi-water - salt mixture, further referred to as mixture, was ready for processing in the Couette Cell. Figure 2.3 shows the final mixture created.

The protein mixture consists of deformable granules (Figure 2.3). A transparent (caulking) filling gun container using a funnel and a pounder was employed to fill the material in the Couette Cell. This step can effectively deaerate the mixture upon filling the Couette Cell.

The Couette Cell is filled from the side using a filling tube that is screwed onto the filling hole. When the space between the cylinders (*shearing zone*) was completely filled and the mixture was tightly packed, the filling tube was removed and the filling hole was sealed using a screw plug with a thermocouple attached. Then, the experiment was initiated as fast as possible. The fill-up time, defined as the time period between the end of the mixing process and the start of the experiment, was 3.5 minutes. The actual filling time of the Couette Cell with the caulk gun was 30 seconds.

Table 2.1: Ingredients for 200 g sample.

Ingredients	Weight [g]	w/w [%]
Soy Protein Isolate	46.0	23
Demi – water	138.0	69
Salt (sodium chloride)	2.0	1
Gluten	14.0	7
Total	200.0	100

No mixture preheating prior to the experiment was needed according to an estimation of the characteristic heat conduction timescale for the process $t_c = \dfrac{\varrho c_p (R_o - R_i)^2}{4k} \approx 73 \text{ s}$, using the following mass fraction average mixture properties (Aguilera and Lillford, 2008): density ϱ =1023.63 kg/m³; heat capacity $c_p = 3506.8$ J/kg·K and thermal conductivity $k = 0.4407$ W/m·K.

Figure 2.3: The SPI - gluten - demi-water - salt mixture before it is filled in the Couette Cell.

At the end of each experiment, the oil circulation from the hot oil bath was switched off and the cold oil bath was switched on to cool down the material inside the Couette Cell to ~90 °C.

Then, the lid and the outer cylinder were removed and the sample was cut vertically so a rectangular slab was formed. The sample weight was measured immediately after the sample was taken out of the Couette Cell. The average sample weight for all 58 experiments in this study was 141.5g $\pm$ 0.7 g. The weighed sample was packaged in a seal bag and put in the freezer (at –20 °C). Room temperature and relative humidity were recorded for each sample.

2.2.4   Process Conditions

In a first step, the temperature was varied at a constant rotation rate of 30 RPM and a constant process time of 15 minutes. Temperature varied from 90 °C to 110 °C with intervals of 5 °C. Next, the rotation rate varied from 0 to 50 RPM with a 5 RPM interval keeping the process time and temperature constant at 15 minutes and 95 °C, respectively. Finally, in the third step, process time was varied from 5 to 25 minutes with a 5 minute interval at a constant temperature of 95 °C and 30 RPM. Those ranges were chosen based on preliminary experimental investigations, which had indicated that good fibrous structures could be obtained under these operating conditions. Finally, the torque was measured by the rheodrive unit (Haake PolyLab QC, Thermo Fisher Scientific, Karlsruhe, Germany), which imparts rotation to the inner cylinder of Couette Cell at constant RPM values.

2.2.5   Texture Analysis

Tensile tests were performed on a Zwick Roell Z005 universal testing machine (Zwick Roell AG., Ulm, Germany) in order to determine the degree of stress and strain anisotropy in the samples obtained. Specifically, fibrous structures have different mechanical properties parallel and perpendicular to the direction of the fibres. The direction of fibres is in the direction of rotation, while the direction perpendicular to the fibres is that along the height of the Couette Cell. Defrosted samples were subjected to texture analysis.

At least three samples were created for each experimental point (set of process conditions) resulting in a total of 58 samples tested with texture analysis. The tensile tests were performed with a constant deformation rate of 0.5 mm s^{-1} at room temperature. Each experiment was repeated at least three times. Three specimens in the direction parallel to the formed fibres and three specimens in the direction perpendicular to the formed fibres were cut from each sample and were tested. The specimens were cut in a rectangular shape (85 x 5.5 mm) with a thickness of 5.5 mm. Thus, the cross sectional area relevant for calculating the normal stress was $3.025 \cdot 10^{-5}$ m^2.

Roller clamps with a rough surface were used to fixate the specimens in the tester. The roller clamps press the specimens against a piece of sandpaper glued onto a metal plate. The rollers were fitted with rubber rings of 3 mm thickness to prevent excessive compression of the specimens. The distance between the points of application of the rollers was 58.34 mm. This distance is used to calculate the tensile strain. The force, distance, tensile stress and strain were recorded using the Zwick's testXpert software.

The maximum values for tensile stress and strain were determined for each specimen. The maximum tensile strain was determined at the point of maximum tensile stress. The maximum tensile stress and strain per direction were averaged and the relevant Anisotropy Indices (AI) were calculated through Equations 2.3 and 2.4, respectively.

$$AI_\sigma = \frac{\sigma_\parallel}{\sigma_\perp} \tag{2.3}$$

where, AI_σ[-] is the stress anisotropy index, $\sigma_{\parallel}$ [Pa] is the normal stress for specimens cut parallel to the fibres and $\sigma_\perp$ [Pa] is the normal stress for specimens cut perpendicular to the fibres

$$AI_\varepsilon = \frac{\varepsilon_\parallel}{\varepsilon_\perp} \tag{2.4}$$

where, AI_ε[-] is the strain anisotropy index, $\varepsilon_{\parallel}$ [mm/mm] is the normal strain for specimens cut parallel to the fibres and $\varepsilon_\perp$ [mm/mm] is the normal strain for specimens cut perpendicular to the fibres.

The Anisotropy Index (AI) reveals the physical presence of anisotropic structures in our sample and the degree of fibrousness. Furthermore, it can quantify the textural and sensorial characteristics of the meat replacer, which are relevant for consumer acceptance and product success (Manski et al., 2008).

2.2.6   Scanning Electron Microscopy (SEM) Analysis

The microstructures of the samples were investigated with SEM (S-4800, Hitachi, Tokyo, Japan). The SEM at hand is a cold field emission scanning electron microscope, which features a maximum resolution of 1.0 nm at 15 kV. Inspection of the samples is possible with acceleration voltages of 0.5 - 30 kV without beam deceleration. The SEM bears a beam deceleration feature that can be used to inspect sensitive or charging samples. For these

inspections, a low voltage of 2 kV was utilized. The microscope allowed for specimen imaging without gold or other coating. In SEM, the samples were cut parallel to the fibres, at room temperature, in specimens of 5 x 5 x 5 mm. The specimens were dried for 24 hours in an oven set at 60 °C, to reduce the moisture content. Both the parallel and perpendicular surfaces to the fibres were inspected by SEM.

2.3   Results and discussion

Processing SPI-gluten mixtures in the Couette Cell resulted in formation of a range of different structures. By optically examining the sample right after the experiment, we could get a first impression of the structures obtained. Further examination was done with texture analysis and SEM imaging.

In the study by (Wolf et al., 2000), it is stated that phase separated biopolymer mixtures can be aligned using simple shear flow. The same structure formation mechanism is expected when utilizing simple shear flow in a Couette Cell. Soy and gluten are expected to form separate phases that align as well. In a previous study (Grabowska et al., 2014), SPI and gluten were sheared independently as well as in a mixture of both similar to this study. It was found that SPI alone could not yield any structures whereas gluten alone at 30 wt.% blend could form fibrous structures. Furthermore, the sheared SPI-gluten blend resulted in anisotropic structures and the possible formation mechanism was linked to the existence of two separate phases (SPI and gluten) and their careful balance. Similarly in the study by (Manski et al., 2007a), it is stated that highly viscous systems favour structure formation when simple shear is applied. High viscosity favours anisotropic structure formation since it allows for the transfer of shear stress on each individual phase. Additionally, by applying heat to the system these anisotropic structures will solidify.

Based on the outcomes of previous studies, and our current findings, we hypothesize that gluten forms a continuous, anisotropic phase enrobing elongated SPI-domains. The SPI domains consist of porous SPI particles (Figure 2.4) with low density and water dispersibility. It is suggested that the porous SPI particles absorb water upon hydration. During processing, the hydrated SPI will expand and become more flexible, due to the heat added to the system from the walls, and deform due to the rotation of the inner cylinder (simple shear flow) taking a shape similar to an elongated sphere. The proposed theory corresponds to the need to pre-humidify SPI for 30 min before applying heating and shear to allow sufficient hydration, as described in this study.

Figure 2.4: SEM image of SPI particles.

We have categorized the samples obtained as homogeneous, layered and fibrous. We believe that all three structures could form a starting point for the development of novel meat analogues. Nevertheless, we are especially interested in the formation of fibre-structured samples, which were obtained under specific process conditions. It is also noted that some samples were destroyed, deformed or broken during or after the experiments. Due to the high water vapour pressure when exceeding 100 °C, bubble formation occurred inside the sample; this resulted in expel of the sample when removing the lid. To prevent this, the sample was cooled to 90 °C in the experiments presented below.

Figure 2.5 shows pictures of a typical sample exhibiting fibre formation. The fibres in this sample, created at 95 °C, 30 RPM and 15 minutes, are clearly visible to the naked eye. Individual samples showing clear fibrous structures possess a high tensile stress anisotropy index (1.5-3.2). These results support the intuitive expectation that the tensile strength will be higher in the direction parallel to the fibres. When a specimen with a layered structure is tested, an anisotropy index, AI_σ and AI_ε, of 1 is measured.

Figure 2.6 shows the tensile stress and strain in the directions perpendicular and parallel to the direction of the fibres with varying temperature over the range 90-110 °C.

Figure 2.5: Samples displaying fibres. Left: View of the sample when frozen; the fibres are more visible; notice the sample cuts on the left. Right: Details of sample displaying fibrous structures. This sample was created at 95 °C, 30 RPM and 15 minutes of process time.

Figure 2.6 shows significant differences in the tensile stress and strain in the directions perpendicular and parallel to the fibres with the exception of temperatures higher than 100 °C. The line connecting the Anisotropy Index points is only to guide the eye. No distinct anisotropic structures were observed in the samples created at 90 °C despite the high AI values in Figure 2.6. Rather, samples created at 95 °C repeatedly exhibited fibre formation over the whole domain of the sample. Samples created at 100 °C were not consistent. Sometimes, pronounced fibres were formed, whereas, in other events, samples with layers or even isotropic structure with bubbles formed throughout the domain were obtained. Bubble formation appeared at 105 °C and 110 °C as well. At these temperatures, the samples were mostly deformed or did not exhibit clear anisotropic structures. Collectively, an operating temperature higher than 90 °C and lower than 100 °C results in consistent and pronounced production of fibrous structures in the soy-gluten mixture under study.
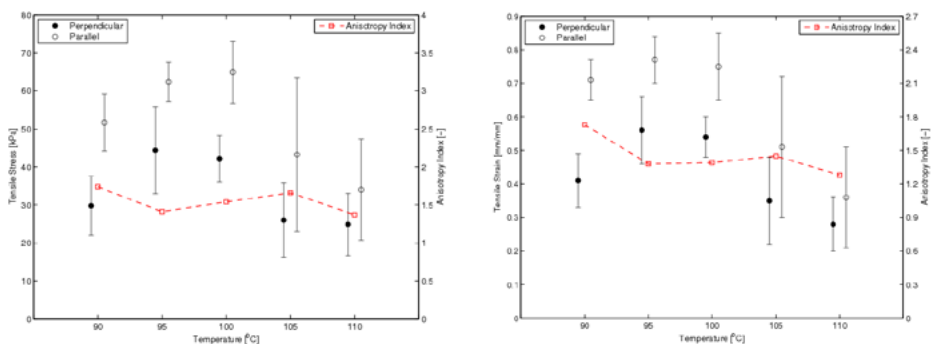

Figure 2.6: Tensile stress (left) and strain (right), with 95% confidence intervals, in the direction parallel and perpendicular to the formed fibres (direction of rotation) vs. temperature. The line connecting the Anisotropy Index points is only to guide the eye. Rotation rate = 30 RPM and Process time = 15 minutes.

In the study by (Krintiras et al., 2014) it was found that a similar sample (SPI-gluten mixture) processed at 95 °C and 30 RPM for 15 min with the Couette Cell had comparable anisotropy indices with raw beef. This implies that the samples produced with the Couette Cell can serve as potential meat analogues.

Samples created with 0 RPM were tested to investigate the influence of heat alone on the formation of anisotropic structures. The tensile stress and strain results for the samples that were not sheared (0 RPM) display no significant difference between the perpendicular and parallel directions, though small differences can be caused through the filling procedure (Figure 2.7). Shearing (0<RPM<50) weakens the perpendicular stress and strain resulting in $1.2<AI_\sigma<2$ and $1.1< AI_\epsilon <1.7$, respectively (Figure 2.7).
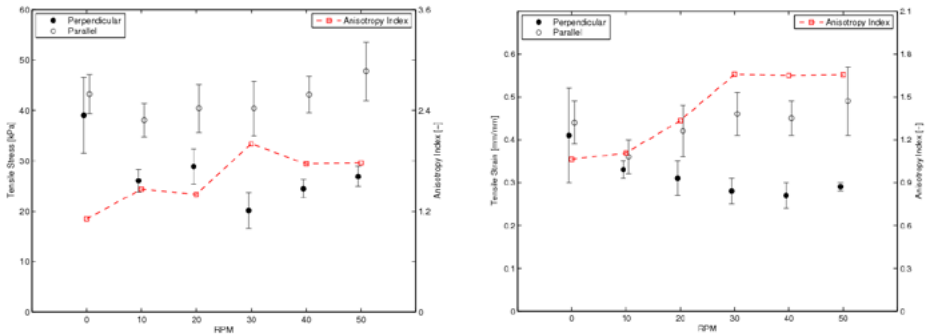

Figure 2.7: Tensile stress (left) and strain (right), with 95% confidence intervals, in the direction parallel and perpendicular to the formed fibres (direction of rotation) vs. rotation rate (RPM). The line connecting the Anisotropy Index points is only to guide the eye. Temperature = 95 °C and process time = 15 minutes.

Figure 2.8 shows the variation of tensile stress and strain in the perpendicular and parallel directions to the formed fibres for process times in the range 5-25 minutes. Temperature was 95 °C and the rotation rate equal to 30 RPM. Fibres are observed over the entire process time range. The role of process time does not seem to be critical. It was reported by (Manski et al., 2008) that prolonged shear time resulted in a damaged structure and this had been manifested in the torque curve trend as a sharp torque increase (Manski et al., 2008). In our experiments, the anisotropy indices for both stress and strain decrease after 15 minutes and this could be an indication of created structures being damaged. However, no damaging of the samples, created after 20 and 25 minutes of processing, was observed by visual inspection or via a trend change in the torque curves. The torque curve for a 25-minute treated sample is displayed in Figure 2.9; despite the curve fluctuations, the mean torque value remains approximately constant over time after ~3 minutes.
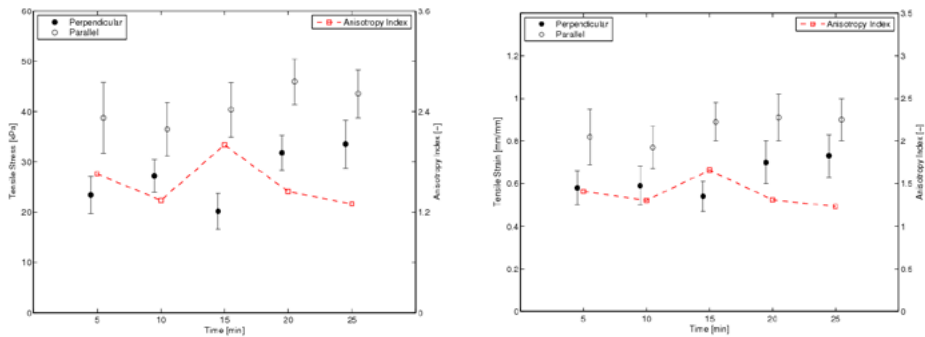
Figure 2.8: Effect of process time on tensile stress (left) and strain (right), with 95% confidence intervals, in the direction parallel and perpendicular to the formed fibres (direction of rotation). The line connecting the Anisotropy Index points is only to guide the eye. Rotation rate = 30 RPM and Temperature = 95 °C.
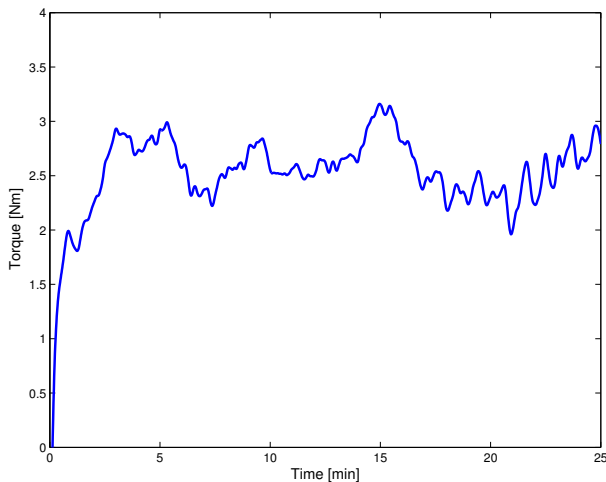

Figure 2.9: Torque curve for a sample created at 95 °C, 30 RPM and 25 minutes

A homogeneous sample was investigated by SEM in order to form a basis for comparison with the textured samples. The homogeneous sample was created at 95 °C, 0 RPM (stationary system) and 15-minute process time. The SEM image is shown in Figure 2.10. Figure 2.10 (left) shows a crack in the middle of the sample, which was probably caused during the drying process. Furthermore, a lot of circular cavities are visible. There was no sign of anisotropic structure in any place of the sample. Figure 2.10 (right) zooms in the area of red rectangle of Figure 2.10 (left). There is a fibre-like structure of 15 µm visible in Figure 2.10 (right). It is believed that this is a gluten fibre spontaneously created after addition of water to gluten (Belton, 1999; Wellner et al., 2005).
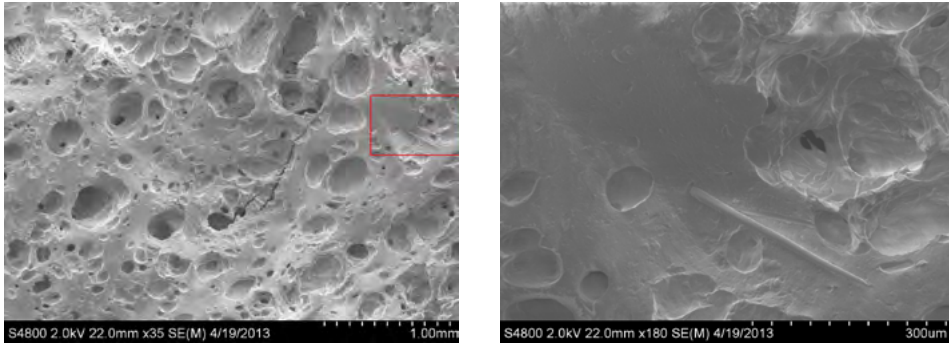
Figure 2.10: SEM images of a homogeneous sample. The right picture zooms in the red rectangle area of the left picture. Process conditions: Temperature = 95 °C; Rotation rate = 0 RPM; Process time = 15 minutes.

The textured samples have layer- or fibre-based structures (Figure 2.11). Figures 2.12 and 2.13 show SEM images of layered and fibrous samples, respectively. The layered sample in Figure 2.12 was created at 100 °C, 30 RPM and 15 min process time. The fibrous sample in Figure 2.13 was created at 95 °C, 30 RPM and 15 min process time. The structures in Figure 2.12 (left) and Figure 2.13 (left) range between 150 - 300 µm and 50 - 200 µm, respectively. Figure 2.13 suggests that the large fibrous structures are made of smaller ones and that the structures are interconnected with much smaller fibres (1-5 µm diameter). These fibres are probably gluten.

No clear distinction can be made between the fibrous and layered specimens from the surfaces oriented in the R-v plane. This is expected based on the schematic of Figure 2.11. Figure 2.12 (right) and 2.13 (right) show the surfaces of the specimens oriented in the H-R plane. Figure 2.12 (right) has been rotated ~35° counter-clockwise with the top left part showing the surface oriented in the H-v plane. Figure 2.12 (right) clearly shows a more layered-like structure compared to Figure 2.13(right).
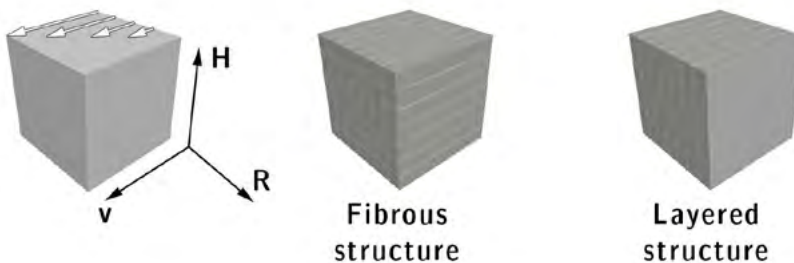

Figure 2.11: Schematic display of the orientation of layered and fibrous structures related to the direction of the flow in the Couette Cell. H is the height, R is the radius and v is the direction of velocity in the device.
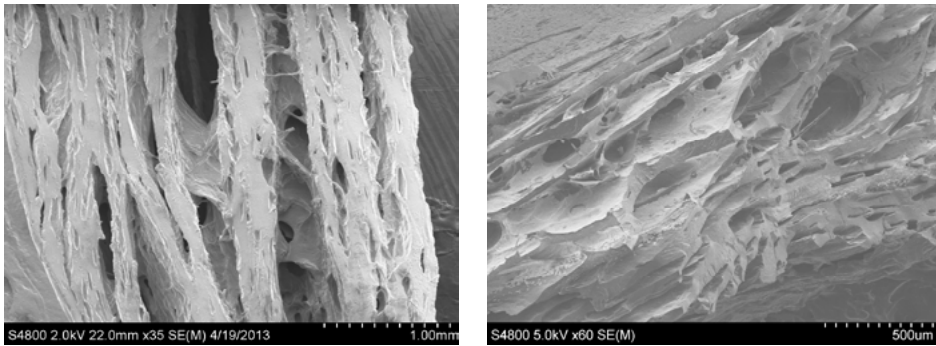
Figure 2.12: SEM images of a layered sample at different view planes; left: the displayed surface is oriented in the R-v plane (see Figure 2.11); right: the displayed surface is oriented in the H-R plane (see Figure 2.11). Process conditions: Temperature = 100 °C; Rotation rate = 30 RPM; Process time = 15 minutes.
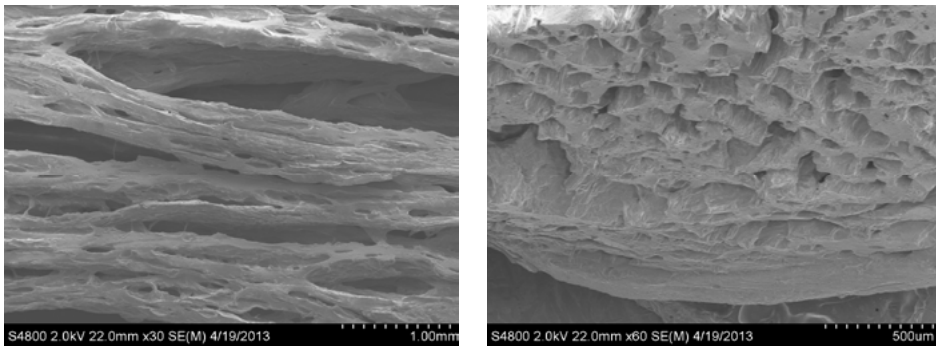

Figure 2.13: SEM images of a fibrous sample at different view planes; left: the displayed surface is oriented in the R-v plane (see Figure 2.11); right: the displayed surface is oriented in the H-R plane (see Figure 2.11). Process conditions: Temperature = 95 °C; Rotation rate = 30 RPM; Process time = 15 minutes.

2.4   Conclusions

We have shown that it is possible to structure SPI-gluten blends into fibrous anisotropic and layered materials using a Couette Cell under realistic process conditions (temperature: 90-110 °C, process time: 5-25 minutes, rotation rate: 5-50 RPM). The dependence of the process on the process time and rotation rate is not critical. Process temperatures over 90 °C and under 100 °C consistently resulted in fibrous structures. Fibrous and layered structures in the product from the Couette Cell were apparent by naked eye. Fibrousness became more pronounced after sample freezing. SEM imaging verified the existence of anisotropic structures at microscale. Measured tensile stress and strain in the direction parallel and perpendicular to the

fibres, using texture analysis, revealed stress and strain anisotropy indices in the range $1.2<AI_\sigma<2$ and $1.1< AI_\epsilon <1.7$, respectively.

The Couette Cell concept is introduced as a novel, dedicated technique for production of fibrous meat analogues via the application of simple shear and heat at mild conditions. Moreover, the concept allows for continuous and scalable processing. Scale-up in the axial direction is straightforward and does not require redesign of the process and equipment. Scale-up in the radial direction is more valuable as it would result in increased product thickness. However, this necessitates investigation of the effect of rotation rate, shear forces, energy input and heating time on the flow and heating patterns developed within the material as function of the distance between the two cylinders. We are currently building an up-scaled Couette Cell with a batch capacity of ~7 litres.

Acknowledgements

References

Aguilera, J.M., Lillford, P., (2008). *Food materials science : principles and practice*. Springer, New York.

Barnes, H.A., Hutton, J.F., Walters, K., (1989). *An Introduction to Rheology*. Elsevier Sci.

Belton, P.S., (1999). On the elasticity of wheat gluten. Journal of Cereal Science 29(2), 103-107.

Blackmore, H.L., (1986). *A Dictionary of London Gunmakers*.

Boye, J., Zare, F., Pletch, A., (2010). Pulse proteins: Processing, characterization, functional properties and applications in food and feed. Food Research International 43(2), 414-431.

Cheftel, J.C., Kitagawa, M., Quéguiner, C., (1992). New protein texturization processes by extrusion cooking at high moisture levels. Food Reviews International 8(2), 235-275.

Grabowska, K.J., Tekidou, S., Boom, R.M., Goot, A.J.v.d., (2014). Shear structuring as a new method to make anisotropic structures from soy-gluten blends. Food Research International.

Grabowska, K.J., van der Goot, A.J., Boom, R.M., (2012). Salt-modulated structure formation in a dense calcium caseinate system. Food Hydrocolloids 29(1), 42-47.

Hoek, A.C., Luning, P.A., Weijzen, P., Engels, W., Kok, F.J., de Graaf, C., (2011). Replacement of meat by meat substitutes. A survey on person- and product-related factors in consumer acceptance. Appetite 56(3), 662 - 673.

Huang, H.C., Hammond, E.G., Reitmeier, C.A., Myers, D.J., (1995). Properties of fibers produced from soy protein isolate by extrusion and wet-spinning. Journal of the American Oil Chemists' Society 72(12), 1453-1460.

Krintiras, G.A., Gobel, J., Bouwman, W.G., Jan van der Goot, A., Stefanidis, G.D., (2014). On characterization of anisotropic plant protein structures. Food & Function 5(12), 3233-3240.

Lin, S., Huff, H.E., Hsieh, F., (2002). Extrusion Process Parameters, Sensory Characteristics, and Structural Properties of a High Moisture Soy Protein Meat Analog. Journal of Food Science 67(3), 1066-1072.

Manski, J.M., van der Goot, A.J., Boom, R.M., (2007a). Advances in structure formation of anisotropic protein-rich foods through novel processing concepts. Trends in Food Science & Technology 18(11), 546 - 557.

Manski, J.M., van der Goot, A.J., Boom, R.M., (2007b). Formation of fibrous materials from dense calcium caseinate dispersions. Biomacromolecules 8(4), 1271-1279.

Manski, J.M., van der Zalm, E.E.J., van der Goot, A.J., Boom, R.M., (2008). Influence of process parameters on formation of fibrous materials from dense calcium caseinate dispersions and fat. Food Hydrocolloids 22(4), 587 - 600.

Peighambardoust, S., Van der Goot, A., Hamer, R., Boom, R., (2004). A new method to study simple shear processing of wheat gluten-starch mixtures. Cereal Chemistry 81(6), 714-721.

Peighambardoust, S.H., Brenk, S.v., Goot, A.J.v.d., Hamer, R.J., Boom, R.M., (2007). Dough processing in a Coutte-type device with varying eccentricity: effect on glutenin macro-polymer properties and dough microstructure. Journal of Cereal Science 45(1), 34-48.

Rampon, V., Robert, P., Nicolas, N., Dufour, E., (1999). Protein Structure and Network Orientation in Edible Films Prepared by Spinning Process. Journal of Food Science 64(2), 313-316.

2

Riaz, M.N., (2000). *Extruders in Food Applications*. Taylor & Francis.

Rodrigues, I.M., Coelho, J.F.J., Carvalho, M.G.V.S., (2012). Isolation and valorisation of vegetable proteins from oilseed plants: Methods, limitations and potential. Journal of Food Engineering 109(3), 337-346.

Suchkov, V.V., Grinberg, V.Y., Bikbov, T.M., Muschiolik, G., Schmandke, H., Tolstoguzov, V.B., (1988). Non-spinneret formation and functional properties of fibrous texturates based on a liquid two-phase system water-casein-soya protein isolate. Food / Nahrung 32(7), 669-678.

Thiébaud, M., Dumay, E., Cheftel, J.C., (1996). Influence of Process Variables on the Characteristics of a High Moisture Fish Soy Protein Mix Texturized by Extrusion Cooking. LWT - Food Science and Technology 29(5–6), 526-535.

Wellner, N., Mills, E.N.C., Brownsey, G., Wilson, R.H., Brown, N., Freeman, J., Halford, N.G., Shewry, P.R., Belton, P.S., (2005). Changes in protein secondary structure during gluten deformation studied by dynamic Fourier transform infrared spectroscopy. Biomacromolecules 6(1), 255-261.

Wolf, B., Scirocco, R., Frith, W.J., Norton, I.T., (2000). Shear-induced anisotropic microstructure in phase-separated biopolymer mixtures. Food Hydrocolloids 14(3), 217-225.

Yao, G., Liu, K.S., Hsieh, F., (2004). A New Method for Characterizing Fiber Formation in Meat Analogs during High-moisture Extrusion. Journal of Food Science 69(7), 303-307.
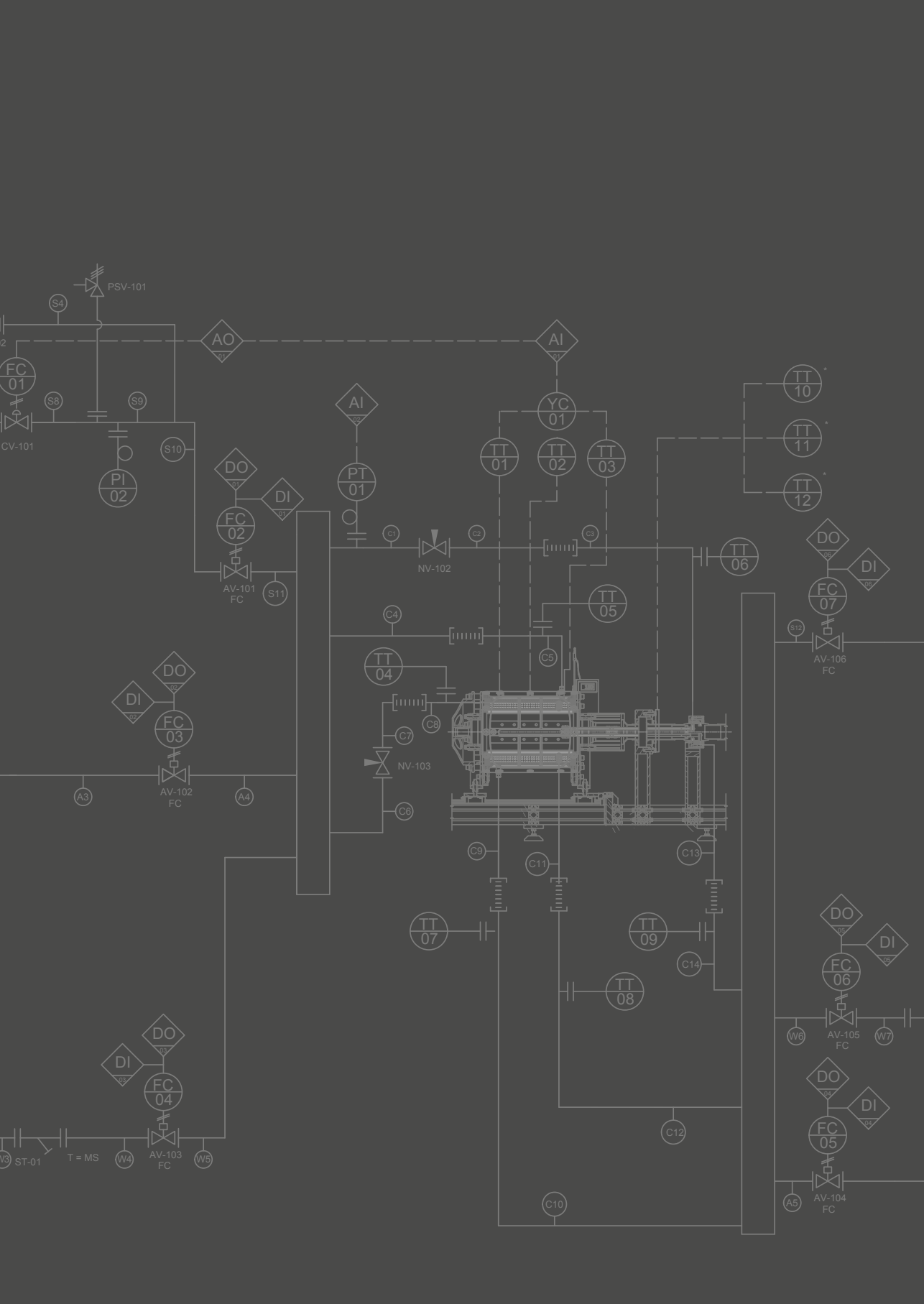
Chapter **3**

ON CHARACTERIZATION OF ANISOTROPIC PLANT PROTEIN STRUCTURES

Condensate

CT-02

W12-16mm-PVC

W8

Water out

Drain

A6

Abstract

In this paper, a set of complementary techniques was used to characterize surface and bulk structures of an anisotropic Soy Protein Isolate (SPI) – vital wheat gluten blend after it was subjected to heat and simple shear flow in a Couette Cell. The structured biopolymer blend can form a basis for a meat replacer. Light microscopy and scanning electron microscopy provided a detailed view of structure formation over the visible surfaces of the SPI-gluten blend. Protein orientation in the direction of the flow was evident and fibrous formation appeared to exist in the macro- and micro-scale. Further, according to texture analysis, the structured biopolymer obtained from the Couette Cell after processing at 95 °C and 30 RPM for 15 min has high tensile stress and strain anisotropy indices (~2 and ~1.8, respectively), comparable to those of raw meat (beef). The novel element in this work is the use of the neutron refraction method, utilizing spin-echo small angle neutron scattering (SESANS), to provide a look inside the anisotropic biopolymer blend complementing the characterization provided by the standard techniques above. With SESANS, it is possible to quantify the number of fibre layers and the orientation distribution of fibres. For a specimen thickness of 5 mm, the obtained number of fibre layers was 36 ± 4 and the standard deviation of the orientation distribution was 0.66 ± 0.04 radians. The calculated thickness of one layer of fibres was 138 µm in line with SEM inspection.

3.1   Introduction

Meat production has an enormous impact on the environment and natural resources. According to a 2006 study by the United Nations Food and Agriculture Organization (FOA) (Steinfield et al., 2006), 18% of the annual worldwide Greenhouse Gas (GHG) emissions are attributed to livestock (cattle, buffalo, sheep, goats, camels, horses, pigs, and poultry). This is higher than the contribution of transportation emissions (13%) on global scale (Pachauri, 2008). Similar claims can be made for land use and water footprint. Besides, the issue of animal welfare is another major concern. Clearly, there is need to reduce meat consumption. From consumer research, it becomes clear that they are prepared to switch to plant-based alternatives, provided that these resemble meat more accurately. Unfortunately, current meat replacers do not meet all consumer wishes or are too expensive (Hoek et al., 2011). Further development of meat replacers is also hindered by lack of analytical methods that allow inspection of structures inside the products.

Currently, extrusion and spinning are the main techniques available to produce anisotropic structured meat replacers (Cheftel et al., 1992; Gallant et al., 1984). Recently, two new techniques based on the concept of flow-induced structuring were introduced. A cone-cone device (Shear Cell) (Grabowska et al., 2014a) and a concentric cylinder device (Couette Cell) (Krintiras et al., 2014) were developed. A model system of Soy Protein Isolate (SPI) and vital wheat gluten blend has been used in both devices yielding anisotropic structures that can serve as meat replacers.

Several characterization techniques, such as light microscopy (LM), scanning electron microscopy (SEM) and texture analysis (TA) (Aguilera and Stanley, 1999; Gaonkar, 1995) are typically used to extract information regarding food structures we produce or consume. LM and SEM characterize food sample surfaces. TA can be used to quantify mechanical properties (stresses and strains) and the anisotropy of food samples. In this work, we introduce the neutron refraction method with the technique of Spin-Echo Small Angle Neutron Scattering (SESANS) (Plomp et al., 2007; Rekveldt et al., 2005) as a new characterization method of anisotropic biopolymer blends, such as soy protein isolate and vital wheat gluten. SESANS can be used to quantify the number and thickness of fibrous layers inside the material and should be seen as a complementary method to LM, SEM and TA.

In order for analysis of the bulk structure of a material, a *look inside* is required. To this end, regular light is sufficient in case of transparent materials, but for opaque materials, different techniques need to be used. Refraction is defined as the change in direction of a wave (or neutron) due to a change in the optical medium. When a neutron passes through a sample, containing structures of material that is different than the surrounding material, refraction can occur. When structures inside a sample are relatively large (much larger than the coherence

3

length of the neutron in the instrument (Plomp et al., 2007)), the effect of refraction is predominant over scattering.

A technique that can measure neutron refraction is called SESANS standing for Spin Echo Small Angle Neutron Scattering. Neutrons are refracted by the scattering length density variations, due to different concentrations of isotopes. Neutron refraction is useful for the study of biopolymer structures in that the isotopic scattering length b has a large negative value, -3.742 fm, for hydrogen (^{1}H), compared with 6.671 fm for deuterium (^{2}H), 6.651 fm for carbon (^{12}C), 9.400 fm for nitrogen (^{14}N) and 5.804 fm for oxygen (^{16}O) (Byron and Gilbert, 2000). Therefore, important (biological) elements with low atomic numbers like hydrogen, carbon and oxygen are well visible in neutron refraction. This renders neutron refraction a suitable method for study of proteins since these molecules are mostly made up of hydrogen, carbon, nitrogen and oxygen.

Refraction depends on the number of interfaces (density changes) the beam has to pass through and the shape of the interfaces. For example, when a fibre is placed perpendicular to the direction of a neutron beam, a neutron changes direction when passing the air - metal interface and again when leaving the wire through the metal - air interface. Consequently, the distance travelled within the wire does not influence refraction and the diameter of the wire does not influence the final deviation of the neutron from the incoming direction. Assuming that the fibres (in meat or soy) can be modelled as cylindrically shaped wires and that these fibres are composed of material (proteins) other than the material that surrounds them (e.g. air or heavy water), the principle of refraction can be used to obtain information on fibrous materials. Plomp et al.(Plomp et al., 2007) described the theory of neutron refraction by cylindrical metal wires, which can be used as a basis for the interpretation of SESANS measurements on fibrous materials.

3.2   Materials and recipe

A blend of soy protein isolate (SPI) (SUPRO EX37 HG IP, Solae, USA) and vital wheat gluten (WG) (VITEN, Roquette, France) was used. According to the manufacturer specification, SPI has a minimum protein content of 90% on a moisture-free basis, while gluten contains a minimum of 83% proteins on dry basis. Analysis for comparison was performed on beef (specifically the blade, which is part of the chuck; front part of the cow). Each SPI/gluten and raw meat sample was packaged in a seal bag and was stored in a freezer (at -20 °C). Samples were defrosted prior to further analysis.

All characterization methods were applied to samples prepared with the same recipe (Table 3.1) and procedure. The mixture created had a dry matter content of 31 wt%, with an

SPI-gluten ratio of 3.3:1. First, the demi-water-salt solution was made and added to SPI. The mixture was manually mixed with a spatula and then rested for 30 minutes. Finally, gluten was added followed by mixing with the spatula.

Table 3.1: Ingredients for recipe preparation.

Ingredients	w/w [%]
Soy Protein Isolate	23
Demi - water	69
Salt (sodium chloride)	1
Gluten	7
Total	100

3.3   Preparation of structured samples in a Couette Cell

The protein mixture consists of deformable granules. A transparent (caulking) filling gun container using a funnel and a pounder is employed to fill the Couette Cell with the material. The Couette Cell is filled from the side using a filling tube that is screwed onto the filling hole. When the space between the cylinders (*shearing zone*) was completely filled, the filling tube was removed and the filling hole was sealed using a screw plug with a thermocouple attached. Then, the experiment was started as fast as possible.

The Couette Cell (Krintiras et al., 2014; Peighambardoust et al., 2007) is a concentric cylinder device comprising an inner rotating cylinder (R_i = 0.0425 m) and an outer cylinder (R_o = 0.0485 m), which remains stationary. Both the inner and outer cylinders are heated by means of oil. The sample material is placed in the space between the two cylinders (gap size = 0.006 m); this space is called *shearing zone*. The height of both cylinders is H = 0.085 m.

During a previous study (Krintiras et al., 2014), several samples with the composition of Table 3.1 were processed in the Couette Cell at different process conditions (temperature, rotation speed (RPM) and process time). The products were characterized afterwards by means of TA and SEM. It was found that samples processed for 15 min at 95 °C and 30 RPM yielded products with high Anisotropic Indices (AI). These samples had distinct anisotropic structures present and, in particular, fibrous structures. A detailed overview of the device used and the experiments performed can be found in the experimental parametric study by (Krintiras et al., 2014).

3.4   Characterization methods

3.4.1   Light Microscopy

The microscope used is a Nikon Optiphot 200 (Nikon Corporation, Tokyo, Japan), which comes with CF Plan BD 5/10/20/50x objectives for bright and dark fields and the possibility to obtain images with a digital camera, mounted on the eyepiece tube, and a rotating diascopic polarizer. The light microscope has been used to observe structured samples. The observations took place at room temperature and provisions were taken to ensure that limited drying of the samples occurred. Specifically, samples have been kept in airtight compartments with glass windows. Samples were strained using toluidine blue stain moutant, which enabled visual differentiation between the two plant proteins (SPI, gluten) used in the study (Flint and Firth, 1988). A couple of droplets of toluidine were applied to the surface and the specimen, which was then left to rest for a couple of minutes. Toluidine stained the SPI protein with a dark purple-blue colour and the wheat gluten with a pale blue-green colour.

3.4.2   Scanning Electron Microscopy

The micro- and nanostructures of the samples were investigated with SEM (JSM-5400, Jeol, Tokyo, Japan). The specimens were coated with an ultra-thin layer of gold with an ion sputter coater (JFC-1100E, Jeol, Tokyo, Japan) in order for the surface of the specimens to become electrically conductive. The SEM at hand features high resolution and low voltage imaging with a maximum resolution of 4.0 nm and a variable acceleration voltage of 0.5 - 30 kV. Both secondary electron and backscattering electron detectors are available for imaging.

3.4.3   Texture Analysis-Mechanical Testing

Tensile tests were performed on a Zwick Roell Z005 universal testing machine (Zwick Roell AG., Ulm, Germany) to determine the degree of stress and strain anisotropy in the obtained samples. As shown in Figure 3.1, "parallel" is defined by the vector v (direction of velocity in the Couette Cell) and "perpendicular" by vector H (height of Couette Cell). Defrosted SPI/gluten samples and raw meat (beef) were subjected to texture analysis.
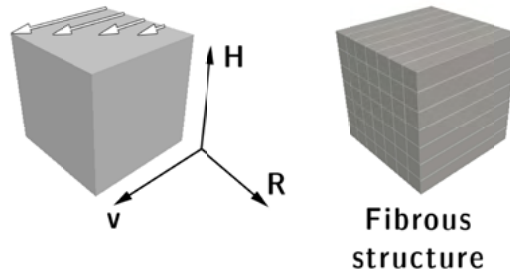
Figure 3.1: Schematic display of the orientation of fibrous structures related to the direction of flow in the Couette Cell. H is the height, R is the radius and v is the direction of velocity in the device.

The tensile tests were performed with a constant deformation rate of 0.5 mm s⁻¹ at room temperature. Three samples have been used and at least three test specimens per direction were cut from each sample at the locations indicated in Figure 3.2. The specimens were cut in rectangular shape (85 x 5.5 mm) with a thickness of 5.5 mm. Thus, the cross sectional area relevant for calculating the normal stress was $3.025 \cdot 10^{-5}$ m².
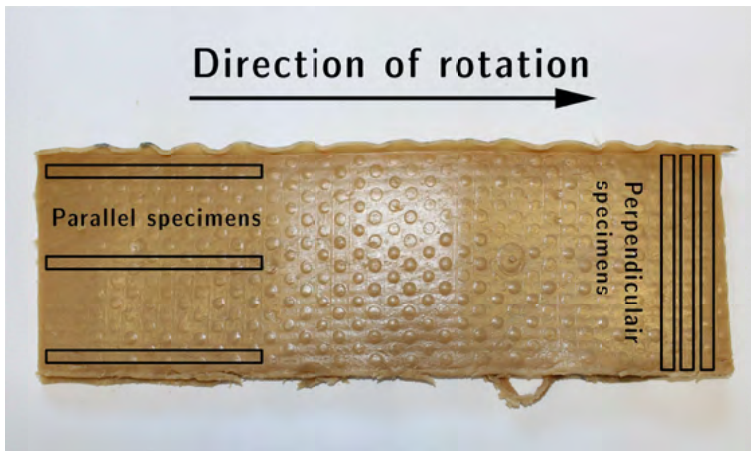
Figure 3.2: Locations on sample where cuts were made for texture analysis. The surface pattern is a result of the dimples on the surface of both the inner and outer cylinder made to avoid slip.

Roller clamps with a rough surface were used to fixate the specimens in the tester. The roller clamps press the specimens against a piece of sanding paper glued onto a metal plate. The rollers were fitted with rubber rings of 3 mm thickness to prevent excessive compression of the specimens. The distance between the points of application of the rollers was 58.34 mm. This distance was used to calculate the tensile strain. The force, distance, tensile stress and strain were recorded using Zwick's testXpert software.

The maximum values for tensile stress and strain were determined for each specimen. The maximum tensile strain is determined at the point of maximum tensile stress. The maximum tensile stress and strain per direction were averaged and the relevant anisotropy indices (AI) were calculated through Equations 3.1 and 3.2, respectively.

$$AI_\sigma = \frac{\sigma_\parallel}{\sigma_\perp} \tag{3.1}$$

where AI_σ[-] is the stress anisotropy index; $\sigma_{\parallel}$ [Pa] is the normal stress for specimens cut parallel to the fibres and $\sigma_\perp$ [Pa] is the normal stress for specimens cut perpendicular to the fibres

$$AI_\varepsilon = \frac{\varepsilon_\parallel}{\varepsilon_\perp} \tag{3.2}$$

where, AI_ε[-] is the strain anisotropy index; $\varepsilon_{\parallel}$ [mm/mm] is the normal strain for specimens cut parallel to the fibres and $\varepsilon_\perp$ [mm/mm] is the normal strain for specimens cut perpendicular to the fibres.

3.4.4   Neutron refraction detected by spin-echo

3.4.4.1   Sample preparation

One sample was tested in the SESANS instrument located at the Reactor Institute Delft (RID). The sample selected was the one with the most pronounced fibrous structure based on visual inspection. This sample had an anisotropy index of AI_σ=3.16.

The partly frozen sample was cut parallel to the flow plane, which is the plane defined by vector v and H in Figure 3.1, into slices with a thickness of 3.5 mm for the horizontally oriented specimen and 1.5 mm for the vertically oriented specimen. After cutting, the sample was rested to allow complete defrosting. The thickness difference is corrected during the fitting procedure of the experimental data. Two specimens were cut per slice with a circular die cutter. The specimens were placed into round transparent airtight containers, which were mounted on a specimen holder.

One specimen was placed in the specimen holder with the fibres orientated perpendicular to the sensitive direction of the instrument, i.e. with the fibres in the y-direction as shown in

Figure 3.3, and the other one was placed in the specimen holder with the fibres orientated parallel to the sensitive direction of the instrument. Both specimens were measured for 6 h.
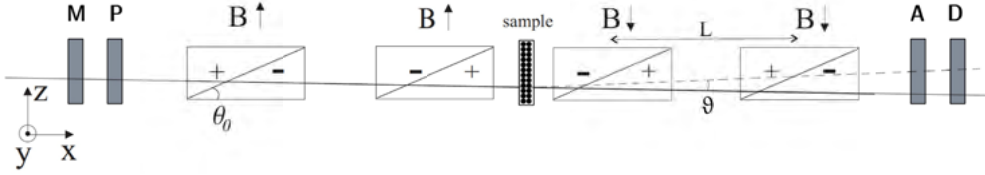

Figure 3.3: Schematic monochromatic SESANS arrangement with monochromator (M) polariser (P), flipper magnets (B), analyser (A) and detector (D), adapted from (Plomp et al., 2007).

3.4.4.2 Fitting Method

The result of a SESANS measurement is a set of data points that relate the polarization, $P(B,\lambda)$ to the magnetic induction, B in each of the flipper magnets and the wavelength λ. For the analysis in this study, λ is constant. The polarization for n layers of fibres is given by:

$$P(B,\lambda) = \left(\varkappa K_1(\varkappa)\right)^n \tag{3.3}$$

where $K_1(\varkappa)$ is the first-order modified Bessel function of the second kind and $\varkappa$ is a scanning parameter expressed in Equation 3.4.

$$\varkappa = 2\delta c L \cot\theta_0 B\lambda \tag{3.4}$$

where $c\,[T^{-1}m^{-2}]$ is the Larmor precession constant, $c = 4.632\cdot10^{14}\ T^{-1}m^{-2}$, $L[m]$ is the length between the centres of the two magnetized foil flippers in each magnetic arm and $\theta_0\,[rad]$ is the inclination angle in the SESANS device.

As described before, the way neutrons are refracted depends on the shape and the number of structures that cause the refraction. When introducing the refractive index η for thermal neutrons, Equation 3.5 is obtained.

$$\eta = 1 - \delta \tag{3.5}$$

where the deviation δ from 1 is given by:

$$\delta = \frac{\varrho \lambda^2 \bar{b}}{2\pi}$$

(3.6)

where $\varrho\,[m^{-3}]$ is the number of nuclei per unit volume; $\lambda\,[m]$ is the wavelength of a neutron; $\bar{b}\,[m]$ is the mean coherent scattering length, which is positive for most materials and the product $\varrho\bar{b}\,[m^{-2}]$ is the scattering length density (SLD). Since $\bar{b}$ is positive, n is less than 1; this means that a cylinder will act as a lens with a negative focal length in the direction perpendicular to the cylinder axis.

From Equations 3.3, 3.4 and 3.6, it can be deduced that polarization is not dependent on the diameter of the fibres, but, rather, on the material of the sample (SLD) and the number n of layers of fibres in the sample. The SLD and n have a similar effect on the calculated polarization.

Measurements in this study were done on a monochromatic SESANS instrument with a wavelength of $\lambda = 0.2 \cdot 10^{-9}$ m (2.0 Å). Since the number of layers in a sample and the composition of the fibres are unknown, Equation 3.3 must be fitted to the measurement data. The fitting parameters are the number of layers, n and the normalized Gaussian distribution of angles $\varphi(a)$ with a standard deviation σ.

To get an idea of how a polarization curve looks like, Equation 3.3 is evaluated for different layers of wires, n, with a composition based on calculated SLD, displayed in Figure 3.4. This Figure illustrates that a specimen without fibres, or with fibres, oriented parallel to the sensitive direction of the instrument - i.e. with the fibres in the z-direction as shown in Figure 3.3 - will not show depolarization. Multiple layers of fibres will increase the depolarization.

The exact composition of the fibres is unknown; it can be pure SPI, pure gluten or an SPI - gluten mixture with H_2O and salt in any ratio. An initial guess for the SLD can be made assuming that the fibres consist of SPI only.

The SLD of SPI can be calculated with the SLD calculator on the website of the National Institute of Standards and Technology (NIST) (NIST, 2013). The calculator on this website uses Equation 3.7 for calculating the SLD.

$$SLD = \frac{\sum_{i=1}^{n} b_c}{v_m}$$

(3.7)

where b_c [m] is the bound coherent scattering length of the ith of n atoms in a molecule with molecular volume v_m [m^3 / mol]. In the calculator, the empirical formula of the material is needed to determine the right values for b_c and v_m.
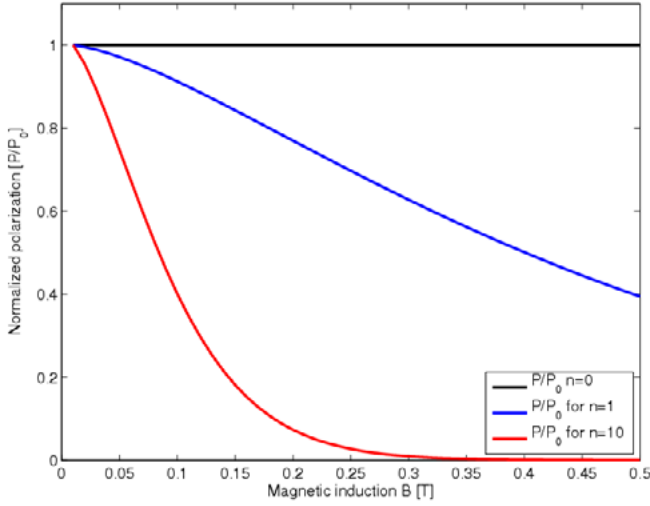

Figure 3.4: Equation 3.3 evaluated for different layers of wires, n.

We have determined the bulk empirical formula of SPI to be $C^{196}H^{380}N^{51}O^{102}S^1$. For the calculation of the SLD, the density of the fibrous material is needed as well. Not all the densities of the amino acids are known; however, looking at the densities that are known, it is assumed that the average density is in the order of 1.5 g/cm^3 (Singh et al., 2008).

Using the above empirical formula and density in the SLD calculator, we can get a calculated value for the SLD_{SPI} of $1.68 \cdot 10^{-6} \text{Å}^{-2}$ ($1.68 \cdot 10^{14}$ m-2). In addition, SLDair=0 and the $SLD_{D2O} = 6.38 \cdot 10^{14}$ m-2. From the SLD_{SPI}, SLD_{air} and SLD_{D2O}, we can define the lower and upper limits of SLD for our system with the lower one being the SPI/air interface of $1.68 \cdot 10^{14}$ m-2 and the upper one being the SPI/D$_2$O interface of $4.7 \cdot 10^{14}$ m-2.

The SLD of both the vertical and horizontal specimens is equal since they are cut out of the same sample. The vertical specimen has a thickness of 1.5 mm compared to 3.5 mm for the horizontal specimen. Since the number of layers is proportional to the thickness, the number of layers in the sample can be calculated.

With the calculated value of the SLD and the density, Equation 3.3 can be fitted to the measurement data. The fitting method used is the common minimization function in

MATLAB called fminsearch, which finds the local minimum of a function of several variables, starting at an initial estimate.

3.4.4.3 Effect of orientation of the fibres

The orientation of the specimen in the specimen holder is important because the SESANS device is only sensitive to refraction in the xz - plane. This means that when the vertical specimen (with fibres oriented in the z direction) is rotated with a small angle $a < 1°$ in the yz - plane, it will cause a small amount of refraction in the xz - plane. The depolarization caused by this refraction is calculated by scaling $\varkappa$ in Equation 3.4 with $\cos a$. The alignment of the horizontal specimen is less important given the fact that $\varkappa$ scales with a cosine. At $\chi = 90$ (vertical position), $\cos(a - \chi)$ has a maximum slope compared to $\chi = 0$ (horizontal position) where the slope of $\cos(a)$ is at a minimum. To verify how sensitive the method is to misalignment, Figure 3.5 shows how the polarization curve shifts from its original position, the line y=1, if a vertical specimen with 10 layers of fibres is rotated at various angles in the yz-plane.

At 1°, no significant depolarization is calculated, but at 5°, high depolarization should be visible. This shows that the results obtained by SESANS for the vertical specimens are very sensitive to alignment, implying that it is a useful method to measure the orientation distribution. In our case, both vertically and horizontally placed specimens showed different depolarization, which indicates a finite orientation distribution.

Now the deviation angle, a, is used as a fitting parameter in Equation 3.3, where $\varkappa$ is defined as

$$\varkappa = \cos(a - \chi) 2\delta c L \cot \theta_0 B\lambda \qquad (3.8)$$

This fit finds its optimum if we assume that the fibres in the specimen are not perfectly parallel to each other. In fact, there is actually a normalized Gaussian distribution of angles $\varphi(a)$ with a standard deviation σ.

$$\varphi(a) = \frac{e^{-\left(\frac{a^2}{2\sigma^2}\right)} + e^{-\left(\frac{(a-\pi)^2}{2\sigma^2}\right)}}{2\sigma\sqrt{2\pi}} \qquad (3.9)$$

In Equation 3.9, we take into account the contribution of the same anti-parallel orientation to the distribution in order to avoid discontinuities at $a = \pi / 2$.
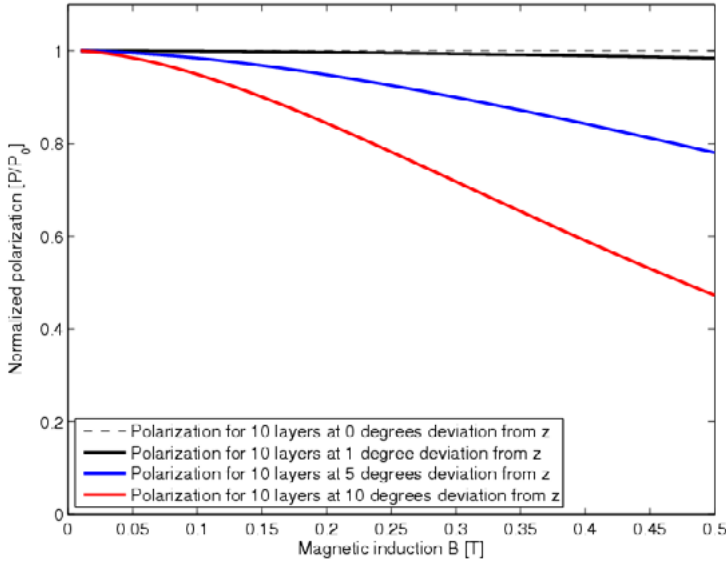
Figure 3.5: Theoretical polarization curves for specimens at various deviation angles assuming a specimen with 10 layers of wires and the calculated SLD.

3.5   Results

3.5.1   Light Microscopy

Figure 3.6 shows LM images of a structured sample at 5x and 10x magnification. We observe that the stained proteins follow a certain direction indicating anisotropic structure formation. A closer look at the picture reveals that lighter parts in the sample are enrobed with a stranded continuous network. Possibly, this corresponds with SPI being dispersed in a continuous gluten matrix (Grabowska et al., 2014a). The LM indicated evidence for existence of anisotropic structures.
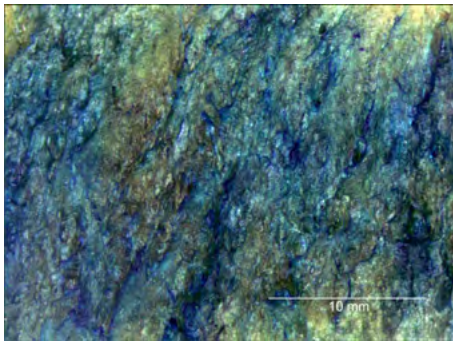
Image of a structured sample at 5x magnification   *Image of a structured sample at 10x magnification*
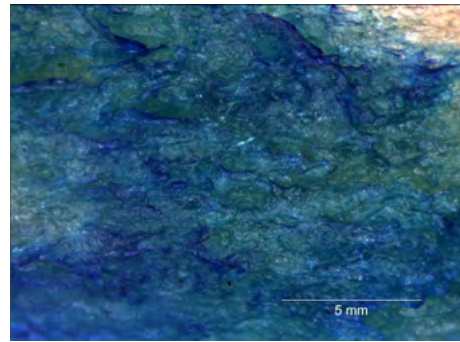
Figure 3.6: Images of structured sample using toluidine blue stain moutant (dark purple-blue colour for the SPI protein and pale blue-green colour for the wheat gluten)

3.5.2   Scanning Electron Microscopy

The textured samples can have fibre-based structures (see Figure 3.1). Figure 3.7 shows SEM images of fibrous samples. The structures in Figure 3.7(left) have widths in the range of 150 - 300 µm. Figure 3.7(left) suggests that the large fibrous structures are made up of smaller ones and that the structures are interconnected with much smaller fibres (1-5 µm diameter). The red box area in Figure 3.7(left) includes various fibres that form a single bigger fibrous bundle. These fibres are probably gluten. Figure 3.7(right) shows the surface of the specimen oriented in the H-R plane. Figure 3.7(right) has been rotated ~35° counter-clockwise with the top left part showing the surface oriented in the H-v plane. In Figure 3.7(right), the tips of the fibres can be seen; the shape is irregular, which can be attributed to various fibres connected to form a larger one. The red box area in Figure 3.7(left) highlights the presence of what is thought to be a single gluten fibril.
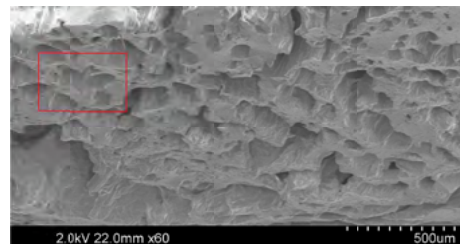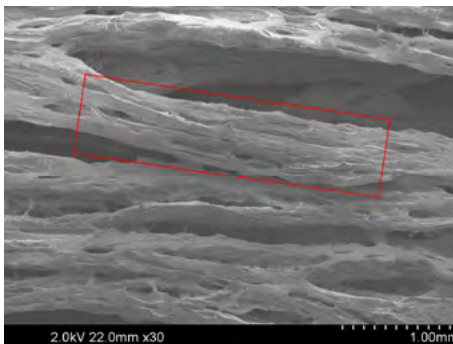

Figure 3.7: SEM images of a fibrous sample at different view planes; left: the displayed surface is oriented in the R-v plane (see Figure 3.1); right: the displayed surface is oriented in the H-R plane (see Figure 3.1).

3.5.3   Texture Analysis – Mechanical Testing

The materials selected in this study, (soy protein isolate and vital wheat gluten) have potential to form the basis for a meat replacer. It is therefore interesting to compare the samples obtained with raw meat. To this end, tensile tests were performed on raw beef. All the samples were first frozen for 3 h to make it easier to cut the specimens; then, the specimens were packed in plastic seal bags. The specimens were tested when they reached room temperature.

The results of the tensile tests for raw meat are presented in Figure 3.8 and compared to a typical fibrous structured sample. The results are presented in terms of the tensile stress and strain parallel and perpendicular to the fibres. In the event of beef, three specimens were tested parallel and perpendicular to the fibres. The anisotropy index is displayed as a blue graph in Figure 3.8. The anisotropy index is the ratio between the parallel and perpendicular direction (stress or strain); the connecting line between the dots is for visual convenience.

In Figure 3.8, it is shown that a typical fibrous structured sample obtained, after processing at 95 °C and 30 RPM for 15 min, has comparable stress and strain anisotropy indices (~2 and ~1.8, respectively) with raw meat (beef). All displayed error bars represent the margin of error at 95% confidence interval. This implies that the meat replacers obtained with the Couette Cell exhibit similar mechanical properties as raw meat. This makes it a promising process to develop the meat replacers.

Tensile stress results   *Tensile strain results*
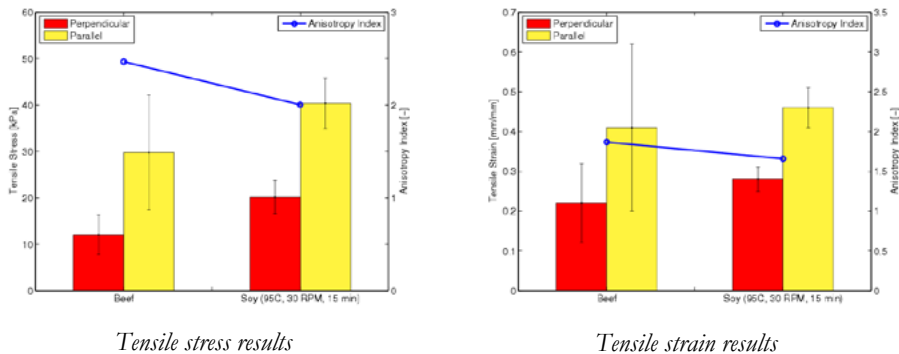
Figure 3.8: Tensile stress and strain measurements for raw meat (beef) and a typical fibrous structured sample obtained with the Couette Cell.

3.5.4 Neutron refraction

Figure 3.9 shows two neutron refraction measurements performed on a sample in which D_2O had replaced H_2O. These measurements were meant to check whether any depolarization would be visible for this type of material. Thicker specimens could contain more layers of fibres and therefore show more depolarization. The experimental data in Figure 3.9 have been fitted using a fixed realistic value for SLD being $4.3 \cdot 10^{14}$ m^{-2}. This SLD value corresponds to experimental data fitting with the lowest error for n and σ. It also indicates that there is air entrapped in the treated samples as can been seen in Figure 3.7. The obtained number of layers of fibres (n) is 36 $\pm$ 4 for the total specimen thickness of 5 mm and the standard deviation (σ) of the orientation distribution is 0.66 $\pm$ 0.04 radians. The thickness of one layer of fibres is 138 µm and this value is in good agreement with the SEM inspection reported in (Krintiras et al., 2014) and Figure 3.7. There is a distinct difference in the depolarization between the vertical and horizontal specimens, providing verification of anisotropic structuring.
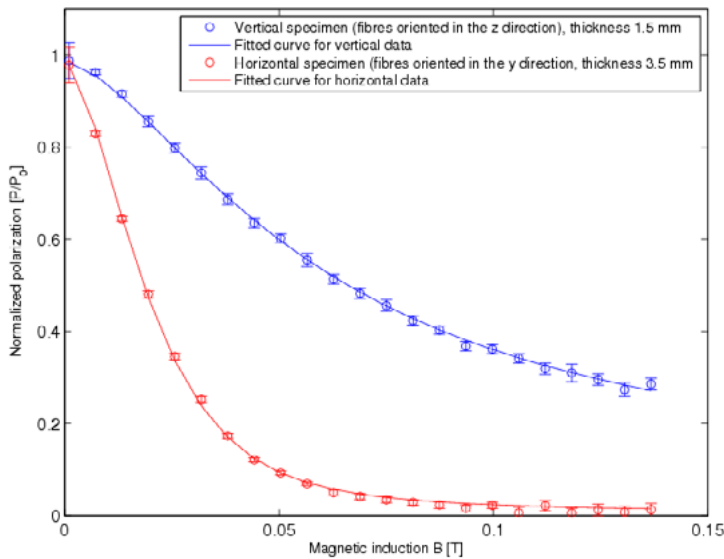
Figure 3.9: Fitted curve for SESANS measurement data for horizontal and vertical specimens.
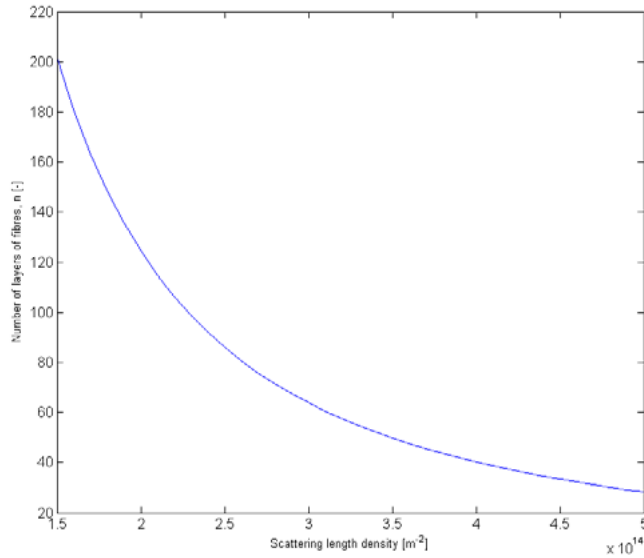
Figure 3.10: Number of layers of fibres for the sum of both vertical and horizontal measurement data as function of SLD.

Figure 3.10 shows how the number of layers of fibres n varies with SLD. This graph is the combined analysis of both vertical and horizontal data of the specimen. Assumptions about the water content of the specimen had to be made to calculate the SLD for meat replacers. As explained earlier, we can define the lower and upper limits of SLD for our system with the lower one being the SPI/air interface of $1.68 \cdot 10^{14}$ m^{-2} and the upper one being the SPI/D$_2$O interface of $4.7 \cdot 10^{14}$ m^{-2}. Therefore, in Figure 3.10, SLD is varied within these limits. Figure 3.10 shows the close relation between n and SLD and that these parameters are completely coupled when both are fitted. This implies that the fibre diameter can be between 30 and 150 µm if our assumptions about the water content were not correct.

3.6   Synopsis of complementary characterization techniques

Light microscopy together with SEM provided a detailed view of anisotropic SPI-gluten blend, illustrating the structure formed over the visible or created surfaces. Protein orientation in the direction of the flow was evident and fibrous formation appeared to exist in the macro- and micro-scale. Use of toluidine blue stain moutant enabled visual observation of the SPI and

gluten protein distribution using light microscopy. Texture Analysis provided quantitative comparison between raw meat (beef) and the obtained meat replacer. The meat replacer obtained from the Couette Cell after processing at 95 °C and 30 RPM for 15 min exhibited high stress and strain anisotropy indices (~2 and ~1.8, respectively), comparable to those of raw meat (beef).

By employing neutron refraction with the novel SESANS technique, a complementary investigation of the structure formation was enabled. We were able to quantify the number of fibre layers (36 ± 4) and the orientation distribution of fibres (0.66 ± 0.04 radians). The neutron refraction results were in line with SEM observations; specifically, same values were obtained for the sample fibre thickness (138 µm) both with SEM and neutron refraction. The structure formation of the treated sample shown in the light microscopy images follows approximately the same orientation distribution (± 40°) in the direction of the flow. Perfectly oriented fibres would result in higher anisotropy index values.

3.7   Conclusions

We have used a range of complementary techniques to characterize plant-based meat replacers, produced in a Couette Cell. The techniques used provided insight into the structures formed at the surface and bulk of the material. Light Microscopy (LM) was used to differentiate between proteins (SPI, gluten) and revealed anisotropic formations in the direction of the flow. Scanning Electron Microscopy (SEM) was used to observe the morphology of the treated biopolymer mixture of SPI-gluten (plant-based meat replacer) at micro-scale. Based on the SEM observations, the fibre thickness was found to be ± 150 µm. Texture Analysis (TA) was done to enable quantitative comparison between the mechanical properties (tensile stress and strain) of raw meat (beef) and the novel meat replacers produced in the Couette Cell. For the treated sample high tensile stress and strain anisotropy indices (~2 and ~1.8, respectively) were found, which are comparable to those of raw meat (beef). Most importantly, a novel technique called spin-echo small angle neutron scattering (SESANS) was used to quantify the number of fibre layers (± 36) in the bulk of the meat replacers (a *look inside* the material). From the number of fibre layers within the tested specimens, the thickness of fibre layers (± 138 µm) was calculated and was found to be in agreement with SEM observations.

As a final note, combinatorial use of several characterization techniques is necessary for better understanding of the nature of plant-based meat replacers as well as their functionality and structuring mechanisms. In this context, common techniques, such as LM, SEM and TA complemented by SESANS can give the full qualitative and quantitative three-dimensional picture of structures formed inside the material.

Acknowledgements

References

H. Steinfield, P. Gerber, T. Wassenaar, V. Castel, Food, A. O. of the United Nations, E. Livestock, D. (Firm) and C. De Haan, Livestock's long shadow: environmental issues and options, Food and agriculture organization of the United Nations, 2006.

R. K. Pachauri, 2008.

A. C. Hoek, P. A. Luning, P. Weijzen, W. Engels, F. J. Kok and C. de Graaf, Appetite, 2011, 56, 662 - 673.

J. C. Cheftel, M. Kitagawa and C. Quéguiner, Food Reviews International, 1992, 8, 235-275.

D. J. Gallant, B. Bouchet and J. Culioli, Food Microstruct, 1984, 3, 175-183.

K. J. Grabowska, S. Tekidou, R. M. Boom and A. J. v. d. Goot, Food Res Int, 2014.

G. A. Krintiras, J. Göbel, A. J. van der Goot and G. D. Stefanidis, Food and Bioprocess Technology, 2014, under review.

J. M. Aguilera and D. W. Stanley, Microstructural principles of food processing and engineering, Aspen Publishers, Gaithersburg, MD, 1999.

A. G. Gaonkar, Characterization of food : emerging methods, Elsevier, Amsterdam ; New York, 1995.

J. Plomp, J. G. Barker, V. O. de Haan, W. G. Bouwman and A. A. van Well, Nuclear Instruments and Methods in Physics Research Section A: Accelerators, Spectrometers, Detectors and Associated Equipment, 2007, 574, 324 - 329.

M. T. Rekveldt, J. Plomp, W. G. Bouwman, W. H. Kraan, S. Grigoriev and M. Blaauw, Rev Sci Instrum, 2005, 76.

O. Byron and R. J. Gilbert, Current Opinion in Biotechnology, 2000, 11, 72 - 80.

S. H. Peighambardoust, S. v. Brenk, A. J. v. d. Goot, R. J. Hamer and R. M. Boom, J Cereal Sci, 2007, 45, 34-48.

F. O. Flint and B. M. Firth, Analyst, 1988, 113, 365-366.

NIST, NIST Scattering Length Density Calculator.

R. P. Singh, R. P. Singh and D. R. Heldman, Introduction to Food Engineering, Elsevier Science, 2008.

PSV-101

S4

AO

AI

FC 01

S8 S9

CV-101

S10

PI 02

DO

FC 02

DI

AV-101 FC

S11

AI

PT 01

YC 01

TT 01 TT 02 TT 03

TT 10

TT 11

TT 12

DO DI

FC 07

S12

AV-106 FC

TT 06

C1 NV-102 C2 C3

TT 05

C4

C5

TT 04

C8

C7 NV-103

C6

DO

DI

FC 03

AV-102 FC

A3 A4

TT 07 C9 C11 C13 TT 09

C14

TT 08

DO

DI

FC 06

W6 AV-105 FC W7

DO

DI

FC 05

A5 AV-104 FC

C12

DO

DI

FC 04

W3 ST-01 T = MS W4 AV-103 FC W5

C10
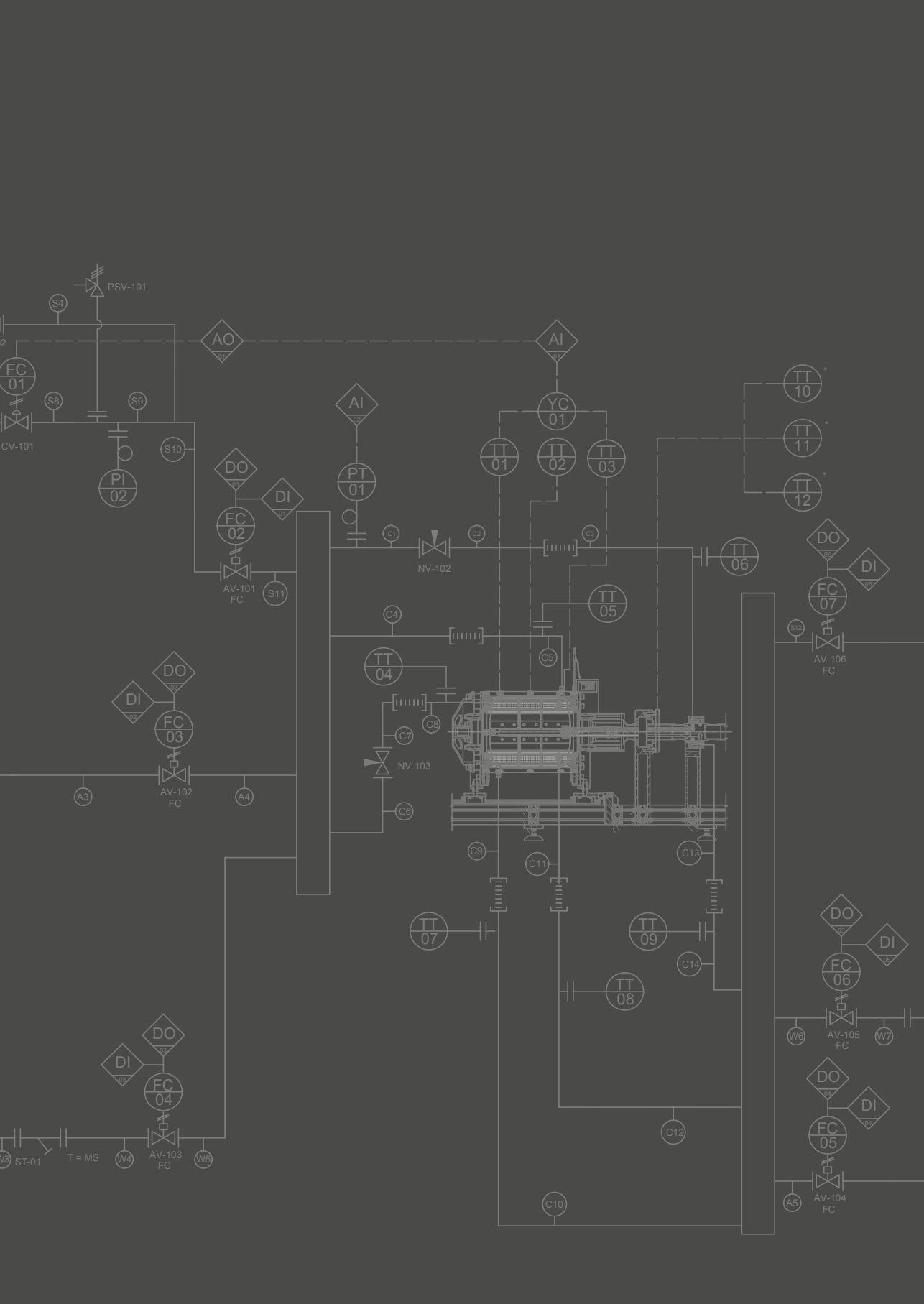
Chapter **4**

ON THE DESIGN OF THE UP-SCALED COUETTE CELL

Condensate

CT-02

W12-16mm-PVC

Water out

W8

Drain

A6

4.1   Introduction

Nowadays, for the production of meat replacers, mixing, forming and extrusion cooking can be used. In the case of meat-like structured products extrusion cooking is currently the most widely used process. Though the structures obtained are more layered-like with low moisture content. Extrusion cooking can be energy inefficient since it demands intensive mixing and heating in the barrel/screw region and subsequently cooling and structuring in the die region. As an alternative, we aimed towards the introduction of a technology that would be purpose-built for the production of highly fibrous meat replacers that emulate meat very accurately. As shown in previous research work this could only be achieved by applying simple shear flow and heat to a high moisture content plant protein-based mixture. As a result, we considered several conceptual designs and concepts that would follow these principles. The selected process for the production of fibrous meat replacers was chosen according to the following design requirements and assumptions:

- **Application of simple shear flow**

The first research requirement could be fulfilled only by designing a device that would feature two surfaces that would move parallel to each other so as simple shear flow would be applied to the protein mixture. The moving surfaces would have to feature some sort of corrugation pattern that would allow for increased contact between the surface and the protein mixture. The device had to feature variable moving surface speeds since this would allow for testing structure formation at various process conditions.

- **Uniform heating**

The second requirement could be fulfilled by utilizing various heating sources such as, electric, oil or steam heating. The temperature had to be accurately controlled and measured and the top temperature was set to 200 ºC. Additionally, temperature should be accurately controlled to allow for fast heating and cooling. Temperature uniformity over the device surfaces had to be ensured so as potential heat gradients would be avoided.

- **Easy process handling**

The third requirement could be fulfilled by assuring easy and flexible daily operation. This could be achieved by allowing easy loading and off-loading the protein mixture together with ease in operation and cleaning. Accurate and holistic overview of all system operations (temperature, pressure, auxiliary equipment status, etc.) would allow safe operation and product optimization.

- **Scalable (up or down) production**

The fourth requirement could be fulfilled by following a design concept that allowed for easy scale up or scale down depending on the need for operation at small or large scales. Preferably, the device should feature the possibility to be easily converted for operation at different capacities. Additionally, the conceptual process should allow for continuous operation if desired.

With these requirements in mind and by evaluating several conceptual designs we have arrived to the concentric annulus principle, the Couette Cell. The Couette Cell fulfils all the aforementioned requirements since we can apply simple shear flow and ensure uniform heating at the cylindrical surfaces. Most importantly as shown in this research work the Couette Cell concept allows for scalable operation (lab-scaled and up-scaled Couette Cells) (Krintiras et al., 2016; Krintiras et al., 2015).

4.2   The up-scaled Couette Cell

From previous studies and experimental work as has been reviewed in (Krintiras et al., 2015), a new food grade up-scaled Couette Cell was designed. It treats around 7 kg per batch, more than 45 times the lab-scaled Couette Cell volume. This up-scaling is seen as the last step before the industrial production of fibrous meat replacers, opening the possibilities of a promising new market. The up-scaled Couette Cell has been engineered entirely following FDA approval rules.

The up-scaled Couette Cell (Figure 4.1) is composed by two concentric cylinders: the housing/lid assembly and the drum. The formation of fibres in the material, situated in between the two cylinders, is achieved by rotating the drum while keeping the housing fixed. This induces a shear stress in the material that performs the material structure transformation. The rotation of the drum is driven by a rheodrive unit in combination with the up-scaled Couette Cell shaft. Also a constant heat flux is applied with three steam heating jackets, situated in the housing/lid assembly and the drum. The up-scaled Couette Cell has been designed to work with pressures up to 15 bar, with a safety limit to 20 bar. The heating jackets are supplied with steam delivered from a central location and the maximum pressure available was 8 bar. During the experimental parametric study (Krintiras et al., 2016) the temperature chosen during operation was fixed to 120 °C.

Once an experiment is finished, the material can be removed from the device by taking out the outer cylinder assembly lid off. This allows an easy access to half of the product volume. If there are any difficulties during the product recovery, the housing can be moved on

a set of rails, allowing total access to the material. Figure 4.2 shows the up-scaled Couette Cell set-up with the lid and housing in the open position.
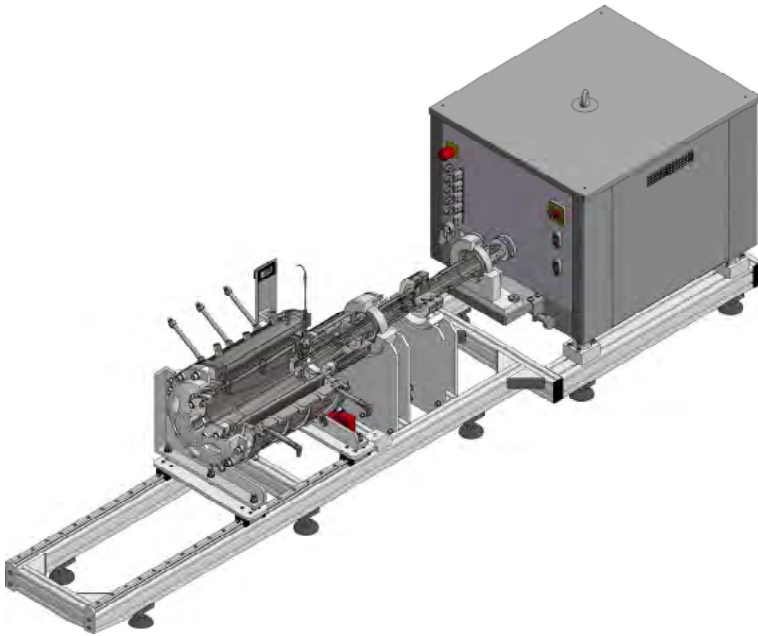
Figure 4.1: Overview of the up-scaled Couette Cell.

Figure 4.2: Picture of the real up-scaled Couette Cell.

4.3   Overall design

As explained in the introduction, the up-scaled Couette Cell (Figure 4.3) is based on the concentric cylinders principle. The protein mixture is textured by means of inducing simple shear by rotating the drum (inner cylinder) while keeping the housing and lid assembly (outer cylinder) steady. The area between the two cylinders is called the "*shearing zone*".
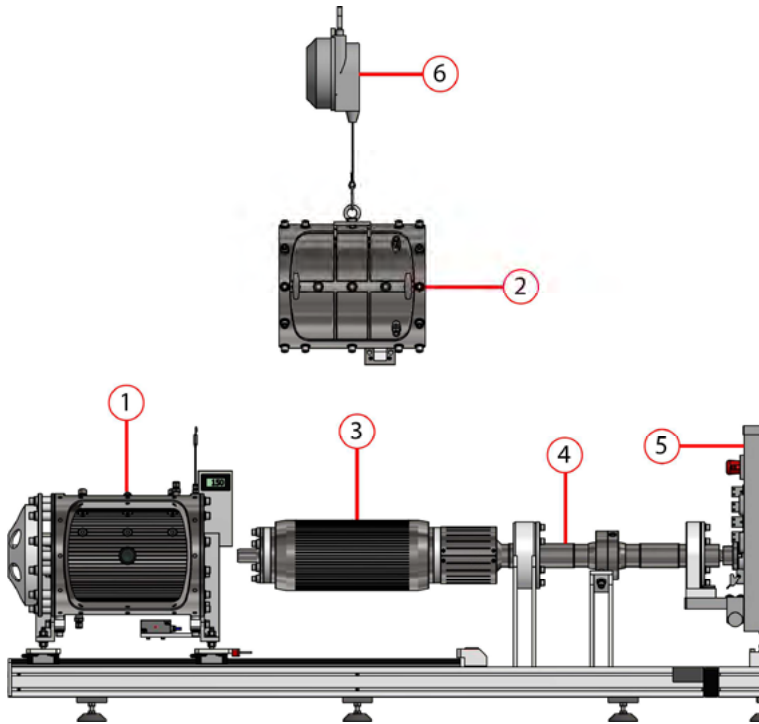
Figure 4.3: General overview of the up-scaled Couette Cell. 1.Housing, 2.Lid, 3.Drum, 4.Shaft, 5.Rheodrive unit, 6.Spring balancer

The three main parts that comprise the up-scaled Couette Cell (drum, housing/lid assembly, which are points 1, 2 and 3 in Figure 4.3) can be uniformly heated by means of steam and cooled by means of water. These parts can be seen in detail in Figure 4.4, where the heating jacket area (blue) and the product area – *shearing zone* (yellow) are represented in the device. Surface corrugations are present on both cylinders to increase the contact surface and reduce the wall slip effect.

Drum rotation is induced through a shaft (point 4 in Figure 4.3) being connected to a rheodrive unit (Haake Polylab QC, Thermo Fisher Scientific, Karlsruhe, Germany) (point 5 in Figure 4.3). The drum is fixed in the axial position, while the housing can be moved on rails

primarily for cleaning and occasionally for product removal. The use of flexible steam lines allows this displacement without having to detach any pipe lines (see Figure 4.2). The removable lid, which is hoisted via the spring balancer (point 6 in Figure 4.3), grants direct access to the product at any time. The protein mixture can be filled through three filling holes present on the lid.
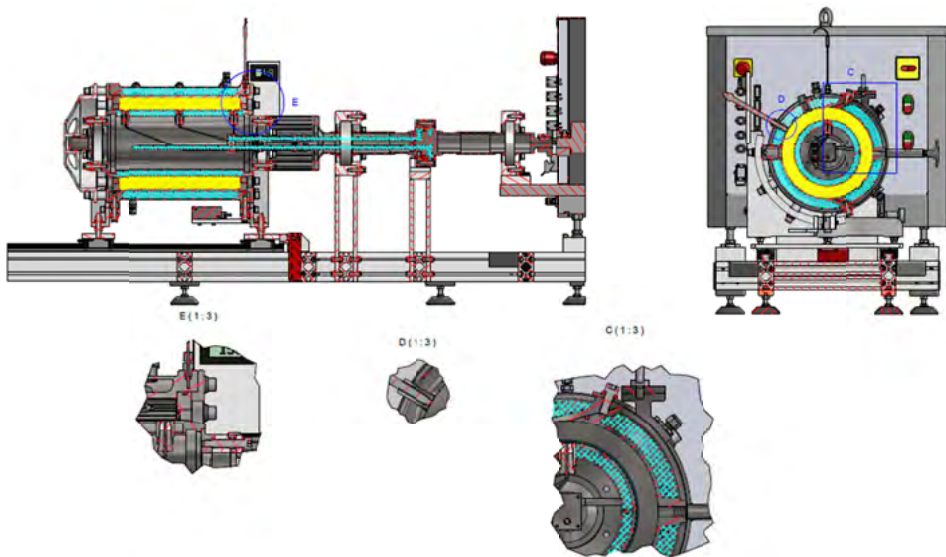
Figure 4.4: General overview of the up-scaled Couette Cell. Blue area: zones with steam flow. Yellow area: shearing zone where processing of the mixture takes place.

The entire experimentation procedure is automated by combination of the National Instruments (NI) (National Instruments, Austin, United States) controlling infrastructure and the rheodrive unit. The product temperature and drum rotational speed, as well as other operational steps, are automatically regulated. In the following sections, a detailed description of all parts is presented.

4.4   Housing

The housing (Figure 4.5) is part of the outer cylinder assembly of the up-scaled Couette Cell together with the lid. It was milled from a single piece of SS316L. Its length is 390 mm and it has an inner diameter of 250 mm. The inner surface has 1 mm deep corrugations to maximize the contact surface and decrease the wall slip effect.
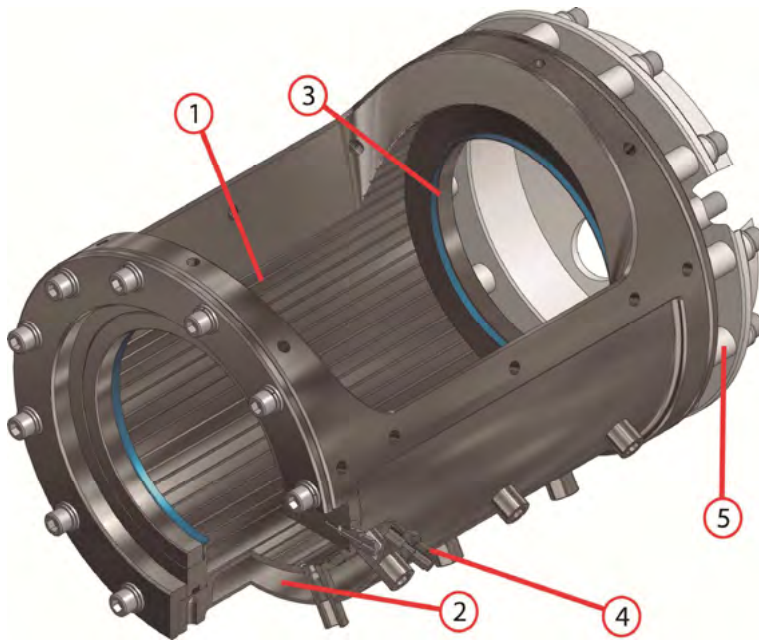
Figure 4.5: Housing of the up-scaled Couette Cell. 1. Corrugations, 2. Heating jacket, 3. Sealing block, 4. Steam outlet, 5. Ceramic thermal insulator

Since heat is needed for plant protein texturization, the housing is fitted with a heating jacket (point 2 in Figure 4.5). This, combined with the lid and drum heating jackets, allows for coverage of the material as seen in Figure 4.4. As can be seen in Figure 4.6, the steam inlet of the heating jacket is located on the top right side of the housing. The steam and condensate outlet is located on the bottom left corner of the housing. Steam circulates through the heating jacket flowing axially until it reaches the steam outlet. As the housing has an empty zone for lid placement, it forms a 220º angle between the inlet and the outlet position without covering the whole jacket radially. This space grants access to half of the product at any time.

In order for successful texturization to take place, it is important to ensure that the mixture is contained in the *shearing zone* during operation. To this end, a series of o-rings, leap seals and ring seals are used. The axial ends of the housing (left and right) are sealed using a pressure sensitive seal (PS) (point 3 in Figure 4.5). The seal (190 mm diameter) comprises four components of two different materials namely, an outer ring and a clamp ring of stainless steel, which form the rigid part of the seal. In the space between the metallic parts, two Gylon blue seals can be found. It is important to monitor the temperature in the seal area during operation. For this purpose, a k-type thermocouple (point 5 in Figure 4.6) has been placed next to it.
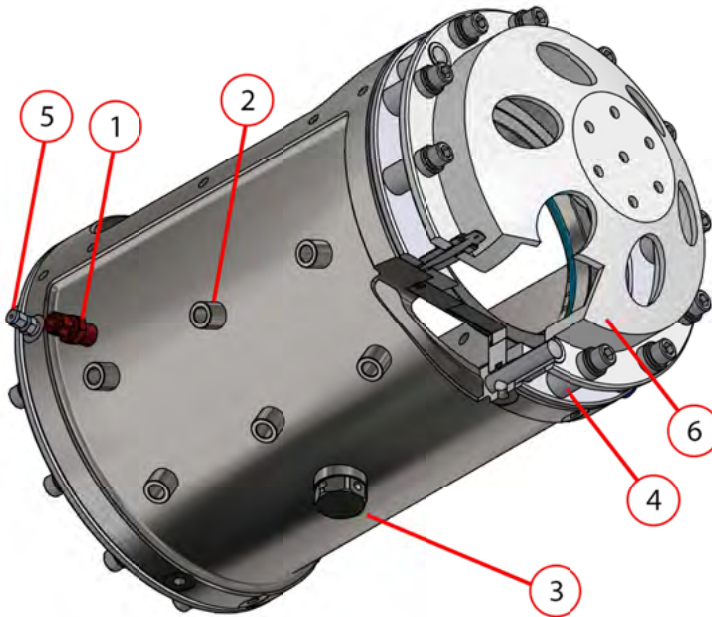
Figure 4.6: Back of the up-scaled Couette Cell housing. 1.Steam inlet 2.Sensors ports 3.Rupture disk 4.Ceramic thermal insulators 5. Seal block thermocouple 6. White cove plate

The thermal insulation of the housing is achieved by using ceramic thermal insulators (point 5 in Figure 4.5). These are used between the housing jacket and the housing white cover plate (point 6 in Figure 4.6), avoiding metal heat conduction to this part and the surroundings. The housing white cover plate is an aluminium piece where the bearing of the drum is located, keeping the up-scaled Couette Cell aligned. Aside from the ceramic thermal insulators, this part has 6 openings to accelerate cooling down of the device and to keeping the drum bearing at a moderate temperature.

Measuring, monitoring and controlling the temperature of the device during operation are crucial. To this end, the housing bears 6 sensor ports, in two separate rows as shown in Figure 4.6 (point 2). This way, the mixture is covered axially for any necessary measurements, each connection with a distance of 125 mm in between. The middle sensor ports are placed in the middle of the *shearing zone*. The three bottom ports are intended for temperature measurement, monitoring and control by means of k-type thermocouples (Figure 4.6). As explained in section 4.8, temperature control is achieved by regulation of the amount of steam entering the heating jackets (housing, lid and drum).

The middle port in the top row of sensor ports is used to measure and monitor the pressure inside the up-scaled Couette Cell. A melt pressure sensor (Dynisco, PT410, Franklin,

United States) is used for this purpose. The two remaining ports are locked with blind plugs and can be used in the future as extra sensors or for injection of ingredients (proteins, water, salt, colour additives, favour additives, fats, etc.).

As a safety measure, a rupture disk is fitted to the up-scaled Couette Cell housing (point 3 in Figure 4.6). This ensures that in the event of the device exceeding the pressure of 15 bar at 200 ºC, the content will be safely discharged. The rupture disk is situated in the centre of the axial line and has a diameter of 25.4 mm (DN25).

4.5   Lid

Part of the outer cylinder assembly in the Couette Cell is a removable lid (Figure 4.7). It allows for easy access to half of the product volume in case the product sticks to the walls or in case an inspection is desired without separating the inner/outer cylinders. A hook (point 1 in Figure 4.8) is placed in the top-centre part of the lid to assist the lifting of the lid when necessary. In order for safe operation, a magnetic safety plug (point 3 in Figure 4.8) is used. If this plug is not connected (closed lid), it is impossible to start an experiment.
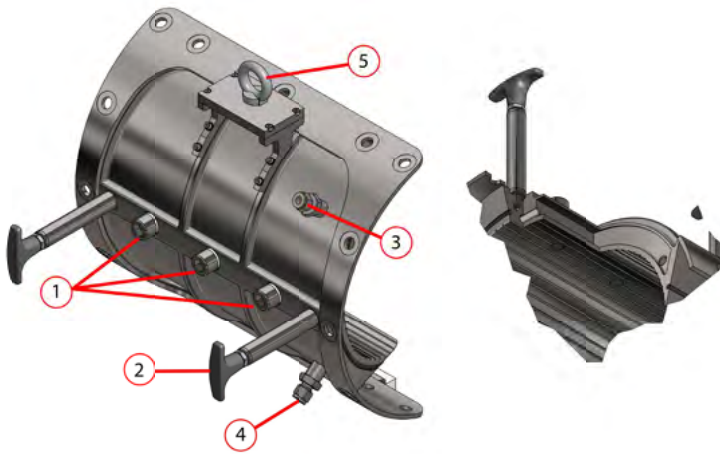
Figure 4.7: Lid of the up-scaled Couette Cell. 1. Feeding ports 2. Handle 3. Steam inlet 4. Steam outlet 5. Hook

The lid is also milled out of a single SS316L piece and has the same corrugations as on the housing's surface (point 4 in Figure 4.8). The shape of the lid corresponds to the remaining gap on the housing (half of the outer cylinder surface), see Figure 4.5. The lid's dimensions are approximately 338 mm by 291 mm and it features rounded corners. In order to ensure the lid's integrity during high temperature/pressure operation, two ribs are added crossing radially to its

surface. An o-ring (point 2 in Figure 4.8) is fitted to seal the system and keep the material inside the *shearing zone*. To attach the lid firmly and safely to the housing, the lid is surrounded by a plate with 16 holes used to bolt it.

Figure 4.8: Back of the up-scaled Couette Cell's lid. 1. Hook 2. O-ring seal 3. Magnetic safety plug 4. Corrugations

Similarly to the housing, the lid is fitted with a heating jacket. The jacket covers the entire material surface to provide uniform heating. The steam inlet and outlet is positioned on the top-right and top-bottom of the lid, respectively (points 3 and 4 in Figure 4.7). Steam can flow across the lid through orifices strategically placed on the ribs. In the detail view section of Figure 4.7, one of the holes can be seen.

One of the main features of the lid is the possibility of choosing between three mixture-feeding ports (point 1 in Figure 4.7). All of them are aligned at the centre of the lid with a total distance of 180 mm between them. As reported in (Krintiras et al., 2015), the mixture flows through the *shearing zone* until it engulfs the whole area during filling. This is possible by using one or all of the ports as feeding inlet(s). In the initial experiments conducted with the up-scaled Couette Cell, only one of the feeding ports was used. The central port remained closed and the third port was opened and used as outlet to the air contained in the device and the material. The filling was performed with a custom-made valve constructed by Teesing B.V. (Rijswijk, The Netherlands). This valve has a pin, which can stop the feeding without losing

material and pressure. After the first experimentation stages, the three ports can be used simultaneously. This provides faster filling and the option to introduce additional ingredients.

4.6   Drum

The inner cylinder, or drum, of the up-scaled Couette Cell is rotating during operation, resulting to simple shear flow within the *shearing zone*. It is fitted with a heating jacket and three thermocouples that are positioned across the axis covering the whole area (point 3 in Figure 4.9).
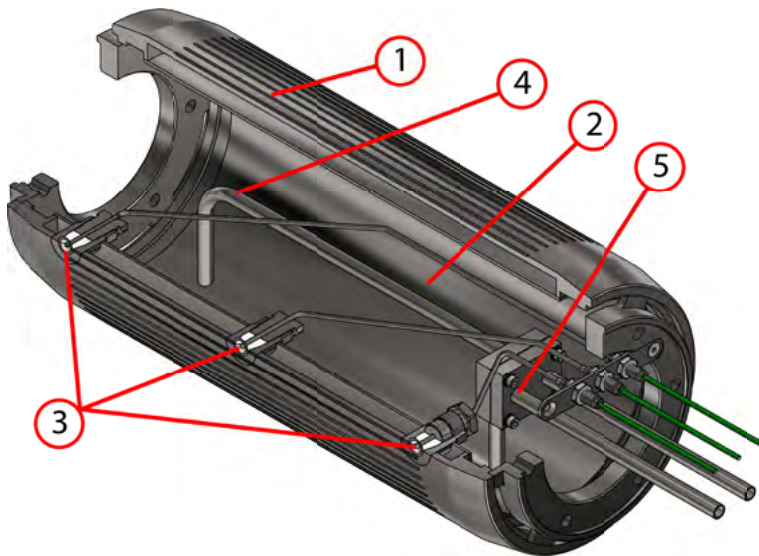
Figure 4.9: Drum of the up-scaled Couette Cell. 1. Corrugations, 2. Heating jacket 3. Thermocouples, 4. Steam inlet, 5. Steam outlet

The dimensions of the drum are 410 mm length and a diameter of 190 mm. It is milled from a single SS316L piece. On its surface, corrugations are milled similarly to the outer cylinder assembly (point 1 in Figure 4.9). The inlet and outlet of the heating jacket are on the shaft connection side and do not interfere with the surface (Figure 4.9).

The heating jacket of the drum allows for a more uniform heating of the mixture during processing since this was found to be crucial in the lab-scaled Couette-Cell. The steam inlet of the drum-heating jacket comes from the shaft and continues into the far end of the cylinder (point 4 in Figure 4.9). Then, the steam fills the heating jacket and leaves again through the shaft (point 5 in Figure 4.9).

Ceramic thermal insulators are present in the axial ends of the drum. These are used to confine the heat and protect sensible elements, such as the bearings and other auxiliaries of the up-scaled Couette Cell. This reduces the amount of energy required and the risk of an injury for the operator.

The drum has three j-type melt temperature thermocouples distributed axially over 300 mm (point 3, Figure 4.9). This allows for measurement of the temperature in the inner surface of the material. The thermocouples are connected to the control system with a slip ring, as explained in subsection 4.6.

4.7   Shaft

The shaft (Figure 4.10) has two primary functions: rotating the drum and supplying steam to the drum heat jacket. It has a total length of 796.3 mm and is composed of six SS316 parts that are welded together. These are the shaft reducer, two shaft thin wall tubes, the shaft feed-through part, the shaft slide over and the shaft drum connector.
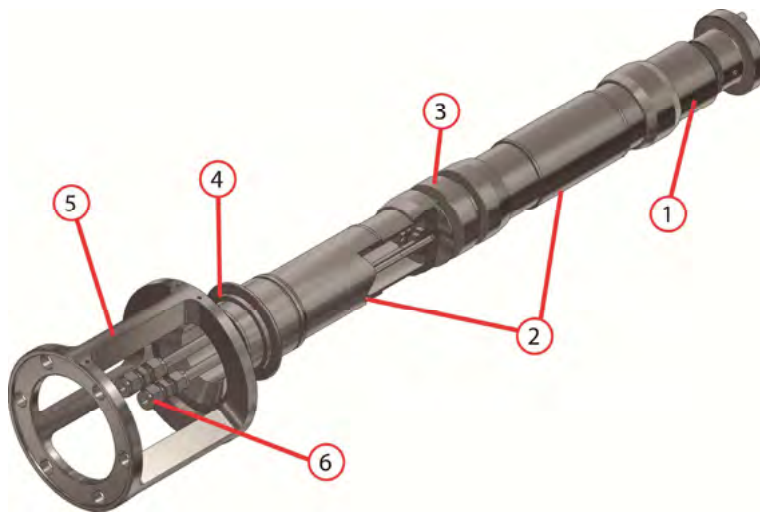
Figure 4.10: Shaft of the up-scaled Couette Cell. 1. Reducer, 2. Thin wall tubes, 3. Feed-through, 4. Slide over, 5. Drum connector, 6. Steam lines

The shaft reducer's (point 1 in Figure 4.10) purpose is to connect the device with the rotating motor. Its main characteristic is the change of diameter from the rheodrive unit connection diameter to the shaft diameter and it is connected to the shaft thin wall tube. The shaft thin wall tube (point 2 in Figure 4.10) is a piece of the shaft used only to extend its length and

connect to the next functional piece. The shaft feed-through part (point 3 in Figure 4.10) is a high temperature zone, as it is located where the drum steam connections are attached. These consist of two 10 mm connections, for the inlet and outlet of the steam. Starting from this point, the steam flows through the streamline running through the downstream parts of the shaft. The leap-seal blocks located in this part are described in section 4.6.1. Next to the shaft feed-through, another shaft thin wall tube is attached. It is similar to the previously described shaft thin wall tube. The shaft slide over (point 4 in Figure 4.10) connects the second shaft thin wall with the drum connector. It is composed of a cylinder with a ring on its connection with the shaft thin wall tube, which acts as a stopper for the bearing block. It is also in this part where a slip-ring is located (JINPAT, model LPT096, Shenzhen, China). This ring allows the connection of the rotating sensors situated inside the drum (Figure 4.9) with the rest of stationary connections. The shaft drum connector (point 5 in Figure 4.10) is the joining part between the up-scaled Couette Cell drum and the shaft.

4.7.1   Bearing & seal blocks

The shaft and drum of the up-scaled Couette Cell are rotating during the whole operation. In order to prevent mechanical problems and stresses, it is highly important to have all the different pieces aligned perfectly. It is also important to avoid a moment of force in the shaft produced by its length and the weight of the drum.

In order to preserve this alignment and reduce the moment of force magnitude, two aluminium-bearing blocks were installed along the shaft. They are composed by two hold-plates (point 1 in Figure 4.11) and a ring that covers a bearing (point 2 in Figure 4.11). The second support-bearing block can be found right after the connection with the rheodrive unit. This support has an upper ring that covers the bearing. To facilitate the assembly and disassembly of the shaft, both bearing blocks were modified. The block's upper part is cut and held with a screw, allowing easy access to the bearing and the shaft.

The seal block is located after the drum, between the two bearing blocks. Its support has the same dimensions as the first bearing block support. Two seals (point 3 in Figure 4.11) are found on the support. These are used to connect the steam inlet and outlet (point 4 in Figure 4.11) to the shaft. As the shaft rotates, a rotary joint of 70 mm diameter is used.
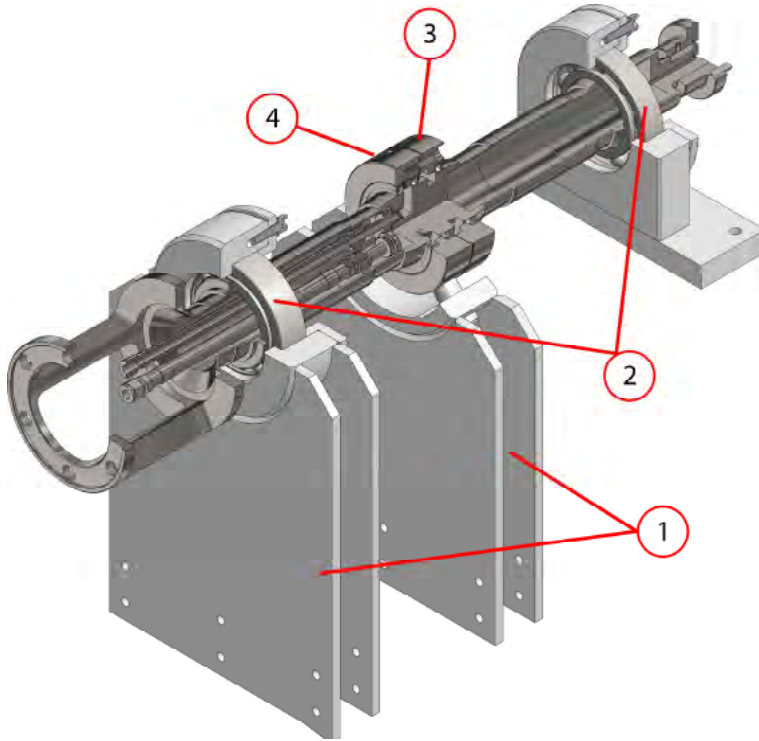
Figure 4.11: Bearing and seal blocks attached to the shaft. 1. Supports, 2. Bearings, 3. Seals, 4. Steam connection

4.8   Polylab QS – Rheodrive unit

The Polylab QS rheodrive unit is an all-in-one device that allows the control of extruders at the same time that it acts as their motor. Control is performed with its own software, Polylab OS. For our application and setups, the Polylab QS has limited performance and utilization; it essentially performs as a torque measuring motor. In the lab-scaled Couette Cell, this unit was used to rotate and control the inner cylinder speed and monitor temperature.

In the up-scaled Couette Cell, this unit will be used as a driver and logger of the system's RPM. Additionally, it will also be used to log the Couette Cell's pressure during operation. Due to these limitations, an alternative control system is used (explained in section 4.8).

4.9   Control

Proper control of the rotational speed and the material temperature is needed to realize homogeneous and reproducible experiments and ensure safe operation of the unit. In this section, the control unit is described, analysing the control loops required and the hardware used for this configuration.

4.9.1   Control hardware

The hardware used to control the up-scaled Couette Cell can be divided in two groups: the operational elements, like the valves and their actuators and the electrical elements, which include wiring, the control computer or other items. The first operational elements are the automatic valves (Samson, Pneumatic control valve 3351, Frankfurt, Germany). These are digital valves (open-closed) that allow for the desired stream (either steam, air or water) to flow into the system, one at a time. Their position in the system can be seen when looking for AV-101 to AV-106 in the attached P&ID (Figure 4.13).

In the steam line, an additional analogical valve can be found (Samson, Pneumatic control valve 3241-7, Frankfurt, Germany). It is used to regulate the temperature of the mixture in the *shearing zone* by varying the steam flow to the heat jackets. It corresponds to the valve CV-101 in the P&ID.

The electronic components used are entirely composed of NI products (National Instruments, Austin, United States). The most important one is the real time controller (National Instruments cRIO-9074), which establishes the communication between the sensors, the valves and the operator. In order to connect the different valves to the control system, an analogue input module (NI 9203, 8-ch AI module) and an output module (NI 9265, 4-ch AO module) were used, as well as digital input (NI 9421, 8-ch DI module) and output modules (NI 9472, Sourcing DO module).

Figure 4.12 shows a picture of the described elements as they are positioned in the up-scaled Couette Cell set-up.

Figure 4.12: Picture of the control hardware used in the up-scaled Couette Cell.

4.9.2   Control logic

Operational control of the up-scaled Couette Cell is performed using the LabVIEW (National Instruments, Austin, United States) program in combination with the Polylab OS. Before coding the required software, the behaviour of each element of the system at each operational stage was considered. By combining all these events, a series of control logic schemes were designed. Figure 4.14 shows the control logic diagram of all the described stages.

4.9.2.1   Flow regulation

The up-scaled Couette Cell has the possibility of employing three different streams through the heating jacket system: air, water or steam. When a feed is selected, this goes through a manifold, which splits the flow into three sub-streams that fill the drum, housing and lid heat jackets.

In order to ensure that the device is correctly sealed, the operator should use the air circuit to test the connections for possible leakages. For this purpose, a control logic scheme was designed. In particular, a system of six automatic valves is used. The first protection layer

is prepared such that no more than one inlet valve can be opened at the same time. The second layer is used when changing between different inlets, applying a time delay after any inlet valve is closed. Additionally, during the whole operation, the real position of the valves is monitored by its autonomous digital input. This avoids dangerous operation in case of a control failure. A final backup protection layer is introduced by "hardwiring" the system's electrical connections, such that it becomes impossible to open two valves simultaneously.

The normal operating procedure consists of three stages: the first one is the safety check and cleaning; the second one is the normal operation; and the third one is the device cooling. At the start of each stage, all valves are closed except the drain. This is considered the idle state.

4.9.2.2   Safety test and cleaning

The safety test and cleaning control logic defines the first steps realized before every experiment. A timer is used to flush air in and out of all the heat jackets to clean possible rests of condensation or dust. After this, the air outlet is closed and the device is pressurized up to 4 bars, closing also the air inlet once the pressure is reached. Then a pressure test is realized. The pressure test is done by using an analogical pressure sensor connected to one of the manifold streams. During a certain period of time, the system pressure is measured and compared with its first value. If it does not decrease more than a certain margin, the test is considered to be passed. If this is not the case, the test fails, driving the system to a waiting stage which is manually overridden to perform again the pressure test. If the pressure test has a positive result, then the air outlet is open for a couple of seconds and the idle state is activated again.

4.9.2.3   Heating and experimentation

Once the safety test and cleaning stage has been performed, it is possible to start the heating and experiment stage. This stage contains the temperature control of the system during the preheating, device filling and operation. Starting in the idle state, the drain is closed and the steam in and out valves are opened, allowing the steam to flow through all the heating jackets. Then the temperature control program is started (explained in the following subsection), maintaining the system temperature at a certain set-point until the user considers the experiment finished and manually stops the control. Then the idle state is resumed.

4.9.2.4   Temperature control

In order to perform successful experiments, continuous temperature regulation is required. To this end, a feedback control system is used. A set point is fixed for the material temperature, which is monitored by external thermocouples. With the difference between the measured and the set point, a controller regulates the opening of the steam control valve. If a higher temperature is needed, the controller will open the valve until the set point is reached and then it slowly reduces the opening.

The control logic is implemented by a standard PID controller. As the process conditions were unknown before the first operation, the different term values were found by posterior tuning operation. The Ziegler-Nichols method was considered to systematically explore the optimum proportional, integral and derivative gains.

4.9.2.5   Cooling

The cooling stage is the last stage during an experiment. It guarantees a safe cool down of the system so that the user can extract the material without any risk. From the idle state, the system drain is closed and the first cooling down stage is started. This is done by flushing air into the heating jackets until a certain temperature threshold is reached. Then the air system is closed and the second cooling down stage commences, using water as a coolant. When the second threshold has been achieved, the water circuit is closed and air is reopened for a couple of seconds to drain the device, before going back to the idle state. It was initially considered to use only water in order to perform the unit cool down. However, gradual cooling was preferred in order to avoid sudden temperature changes that would result in material stresses.

4.9.2.6   Logging

A last additional stage can be found in the control program. As in an experimental set-up, the acquisition of data of different parameters during experimentation is very important, as different process conditions can modify the final product characteristics and quality. For this reason, temperature logging is enabled to compare different experiments. This logging stage allows the user to record temperature values throughout the experimentation process comprising the previously described stages.

4.10   Conclusions and future improvements

During this research we have effectively developed an up-scaled prototype based on the Couette Cell concept. We have successfully verified that the application of simple shear and heat in a protein mixture can lead to fibrous meat-like structured products meant as meat replacers. Moreover, we have not found any limitations to further up-scale this process or switch to a continuous process. It is worth mentioning that there is room for future improvements in the following areas:

- **Process heating**

The up-scaled Couette Cell features heating jackets in the Drum, Housing and Lid sections where steam has been used as a heating medium. During the experimental work and at certain temperatures especially bellow 120 ºC we noticed the formation of excess condensate which would limit heat transfer. This was primarily due to the design of the heating jackets lacking proper drainage in some areas. These limitations could not be foreseen during the design stage since oil was considered the main heating medium initially. Therefore, redesigning or modifying the heating jackets appropriately is advised.

- **Process control**

The up-scaled Couette Cell's temperature is controlled by regulating the steam flow via a single control valve. Steam is then directed in a manifold and split in three streams in order to heat the three heating jackets (Housing, Drum and Lid). This was once more a design choice related to the early design phase where oil was believed to be the heating medium. It is now clear that the overall process control (temperature) can be drastically improved while the overall inventory can be reduced by using three separate control valves for each heating jacket. Implementing this is straight forward and would only require minor modifications and changes in the control logic.

- **Cleaning**

As explained in this chapter the up-scaled Couette Cell has been designed following FDA approval rules, however, cleaning and specifically a Clean In Place (CIP) cycle was not considered. After each experiment the device and the surface with immediate contact with food were thoroughly cleaned. This task required extensive manual labour which in an industrial environment would be highly avoided. Therefore, a possible solution would be an integrated CIP cycle while the Couette Cell is modified for industrial usage. This would require redesigning of the workspace and position of the Couette Cell, while steam could be used for the cleaning step.

- **Automation and process integration**

The up-scaled Couette Cell process can be further improved by introducing automation and process integration when introduced in the industrial environment. Tasks such as feeding, cleaning, open/closing of the lid and the process control can be automated while the overall process can be integrated with other steps such as protein mixture preparation, product handling, packaging and freezing.

References

Krintiras, G.A., Gadea Diaz, J., van der Goot, A.J., Stankiewicz, A.I., Stefanidis, G.D., (2016). On the use of the Couette Cell technology for large scale production of textured soy-based meat replacers. Journal of Food Engineering 169, 205-213.

Krintiras, G.A., Göbel, J., van der Goot, A.J., Stefanidis, G.D., (2015). Production of structured soy-based meat analogues using simple shear and heat in a Couette Cell. Journal of Food Engineering 160(0), 34-41.

4
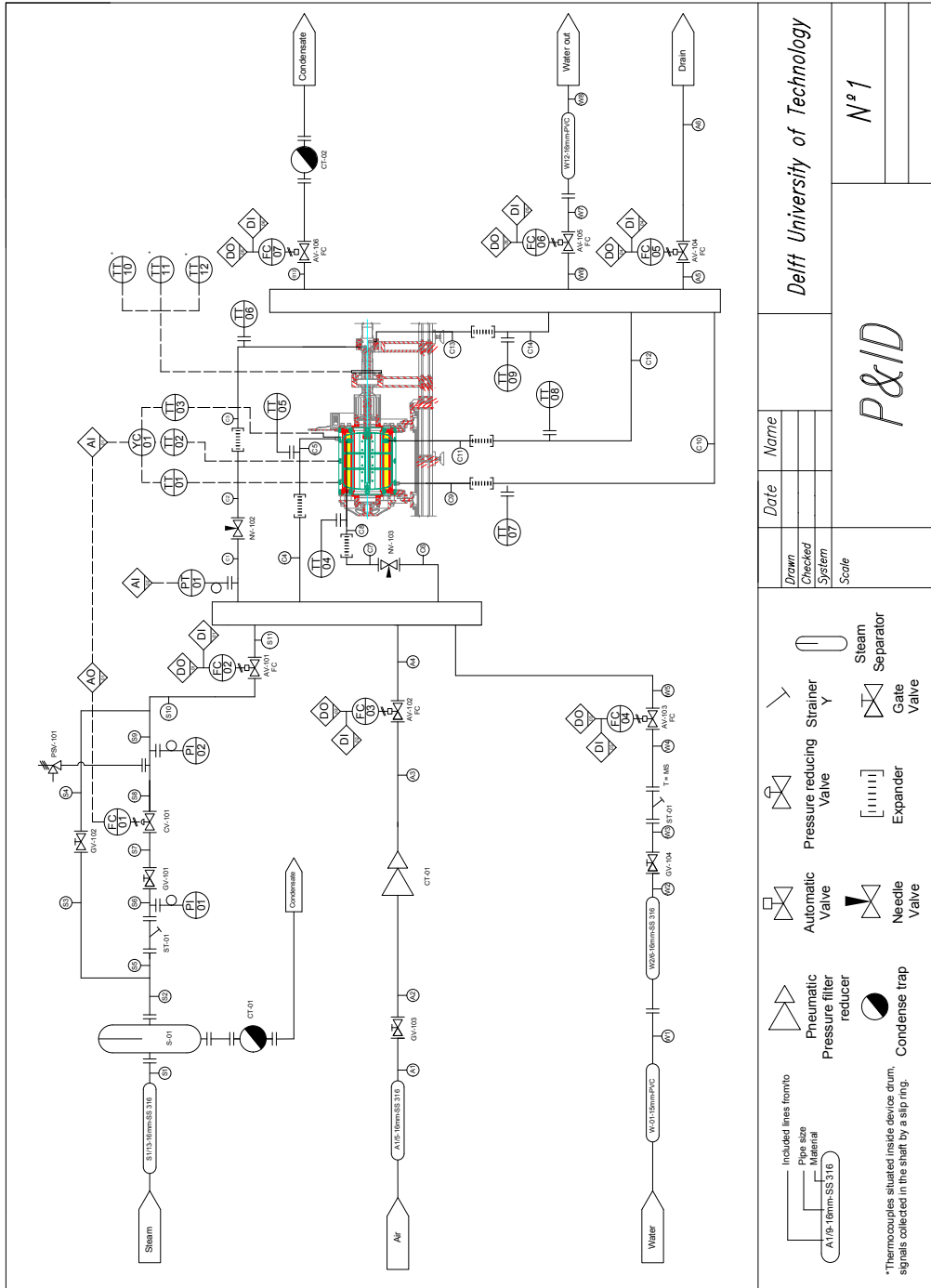
Figure 4.13: P&ID scheme of the up-scaled Couette Cell
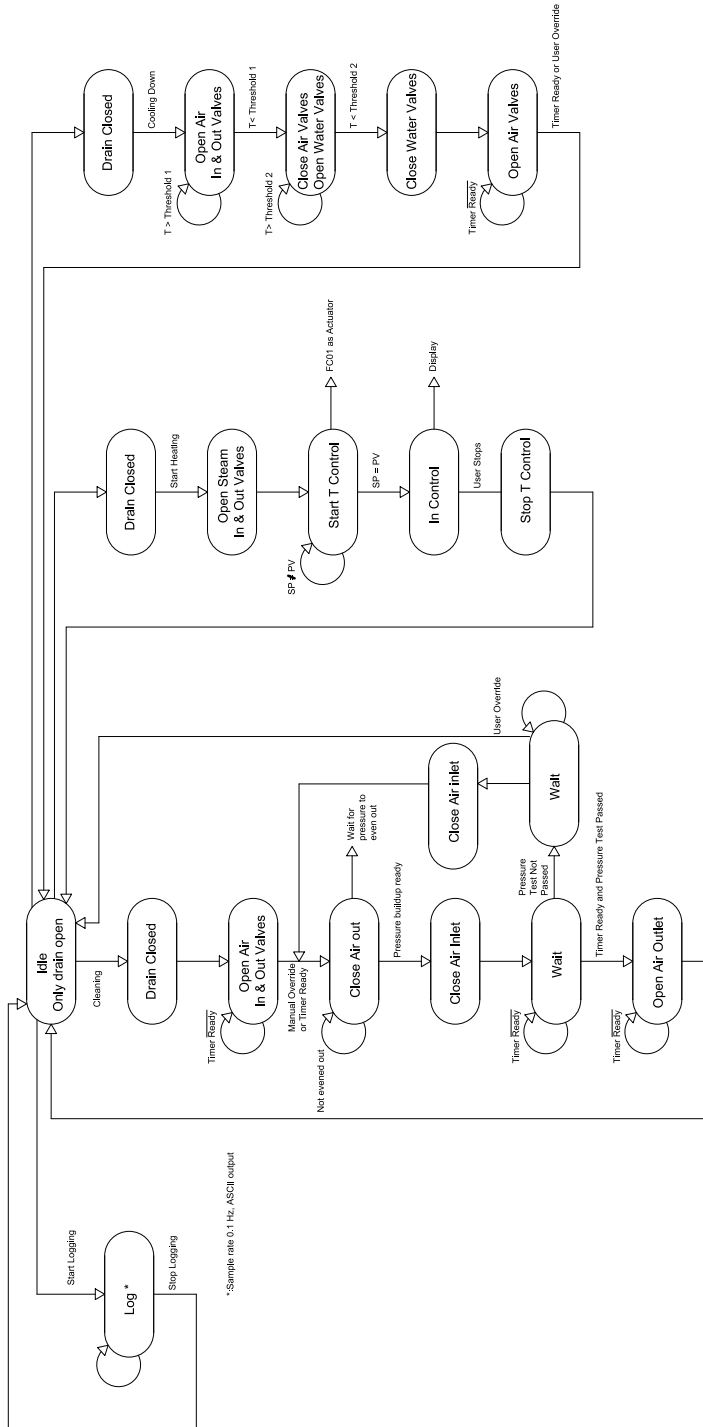
Figure 4.14: Control logic scheme of the up-scaled Couette Cell
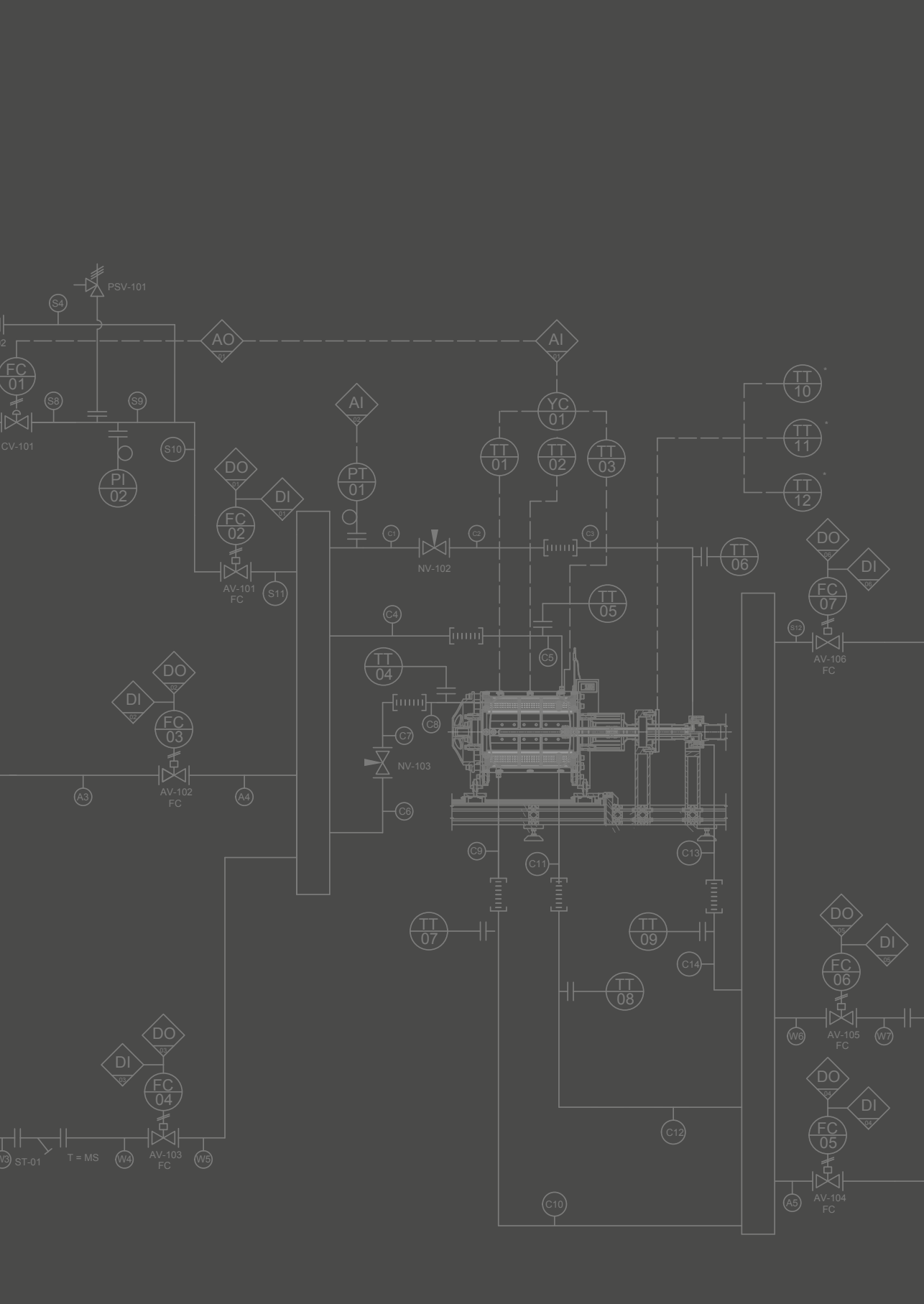
Chapter **5**

ON THE USE OF THE COUETTE CELL TECHNOLOGY FOR LARGE SCALE PRODUCTION OF TEXTURED SOY-BASED MEAT REPLACERS

Condensate

CT-02

W12-16mm-PVC   Water out

W8

Drain

A6

Abstract

We have demonstrated that application of simple shear flow and heat in a Couette Cell is a scalable process concept that can induce fibrous structural patterns to a granular mixture of plant proteins at mild process conditions. In particular, a Couette Cell device with 7-litre capacity was employed for the production of structured soy-based meat replacers. A reduced factorial experimental design was used to find the optimum process conditions between two relevant process parameters (process time and rotation rate), while the process temperature remained constant at 120 °C. Fibre-structured products with high anisotropy indices were produced. Fibrousness is favoured at 30 ± 5 min and 25 ± 5 RPM. The up-scaled Couette Cell can be operated in higher industrial values and yield 30 mm thick meat replacers, which emulate meat. Besides, the study did not reveal any barriers for further upscaling of this concept. The flexibility in design allows production of meat alternative products with sizes that are currently not available, but could have advantages when aiming at replacement of complete muscular parts of animals, for instance, chicken breast or beef meat.

5.1   Introduction

Plant protein-based products (i.e. meat replacers) form a more sustainable source for food compared to meat. As an example, the average water footprint for beef on world scale is 4235 L/60 g protein (Aldaya et al., 2012). This value is 6.6 times higher than the corresponding one for production of soy bean proteins (Hoekstra and International Institute for Infrastructural Hydraulic and Environmental Engineering (IHE), 2003). On another example, contamination of water with NO_3- due to poultry production is 21.9 mg/L; this value could be reduced to 6.2 mg/L if poultry production were to be substituted by a soybean production area (Hooda et al., 2000). Additionally, meat production is responsible for 18% of the annual global greenhouse gas emissions (Steinfield et al., 2006), higher than transportation emissions (13%) (Pachauri, 2008).

Consumers are interested in plant-based products that can replicate meat in terms of mouthfeel, texture, taste, colour and smell. In a recent survey however, consumers stated that these aspects were not at all recognized in current meat replacers (Hoek et al., 2011). Lack of fibrousness makes those products less appealing to the general public (Hoek et al., 2013). Even when in many cases the substitutes are healthier, this is still not enough to convince the consumers (Hoek et al., 2004). Currently, however, there is a clear growth in the meat alternatives market and higher consumer acceptance. Besides, there is a need for novel technologies, such as cultured meat (Post, 2012). The Couette Cell is a technology that might help expand the market even further.

Texturization processes currently available, such as extrusion, spinning and simple shear flow, can provide highly structured meat replacers. Presently, extrusion is the most widely applied technology for the production of meat replacers. A protein based mixture is subjected to intensive heating and mixing in the barrel screw region. Structure formation occurs only at the die region where the melted mixture is cooled and sheared (Riaz, 2000). During extrusion, the plant protein based mixtures are subjected to high temperatures, pressure and shear that can greatly influence the structural and chemical properties of the product (Ilo and Berghofer, 2003). Recent work in the field of extrusion cooking has been focusing on increased moisture content and various protein sources (Liu and Hsieh, 2008; Osen et al., 2014).

In previous experimental projects, structured samples of a plant protein mixture (Soy Protein Isolate (SPI) and vital Wheat Gluten (WG)), were obtained using the concept of shear-induced structuring through simultaneous application of simple shear and heat (Grabowska et al., 2014; Krintiras et al., 2014; Krintiras et al., 2015). These experiments were performed either in a cone-cone device, called Shear Cell (SC), or in a lab-scaled Couette Cell (CC). With both devices, it was possible to obtain highly anisotropic fibrous samples at mild process conditions. After having obtained these promising results, the study has focused on process upscaling using the CC principle. The CC principle was chosen because it is amenable to up-scaling and

5

can possibly be operated in a continuous mode in the future. Besides, we can obtain products with constant thickness. The SC seems better suitable for lab-scale operation due to its geometry (cone-cone), ease of filling and manual operation.

Previous studies with the lab-scaled CC (Krintiras et al., 2015) showed that by means of simple shear flow and heat, SPI-gluten mixtures could be texturized. Depending on the process conditions, variable structures were obtained and were classified as homogeneous, layered and fibrous. These experiments were performed to study the influence of temperature, rotational speed and time. The optimum process conditions (process time, rotational speed and temperature) for enhanced fibre structure formation were 15 min, 30 RPM and 95 °C, respectively. Additionally, fibrous samples had consistently higher AI_σ values than the layered and homogeneous samples.

In this work, an up-scaled Couette Cell has been developed and tested. It was designed for a capacity of 7 L, which is 50 times higher than that of the lab-scale Couette Cell (Krintiras et al., 2015). The aim of the paper is therefore to demonstrate the possibility to upscale the concept of shear-induced structuring to make anisotropic structures. This concept allows for new opportunities, such as flexibility in product shape, via increased thickness. Product thickness in extrusion processes is typically limited to 5-10 mm (Thiébaud et al., 1996), whereas in the up-scaled CC, a product of 30 mm is obtained. A mixture of SPI and gluten was processed at 120 °C with variable process time and rotational speed, based on a reduced factorial experimental design, in order to obtain the optimum process conditions for structuring samples at large scale. The products were examined by means of scanning electron microscopy (SEM) and texture analysis. Texture analysis was performed to determine the global (whole sample) and local (across the thickness of the sample) Anisotropy Indices (AI) in order for quantitative characterization of the samples' fibrousness.

5.2 Materials and Methods

5.2.1 Materials

For the mixture used in this study, Soy Protein Isolate (SPI) (SUPRO EX37 HG IP, Solae, USA) and Vital Wheat Gluten (WG) (VITEN, Roquette, France) were used. The protein content of SPI was 90%, while gluten had a protein content of 81% based on a nitrogen-to-protein conversion factor of 6.25. These values were quantified using the Dumas method with a NA 2100 Nitrogen and Protein Analyser (ThermoQuest-CE Instruments, Rodeno, Italy). In addition, sodium chloride, referred to as salt hereafter, and demineralized water (demi-water) were used.

5.2.2   Experimental set-up – Couette Cell

The up-scaled CC is based on the same principle as the lab-scaled CC (Krintiras et al., 2014; Krintiras et al., 2015; Peighambardoust et al., 2007), being the concentric cylinder rheometer concept. The up-scaled CC is shown in Figure 5.1 and 5.2 and is composed of four main parts: the outer cylinder assembly, which consists of the housing and lid, the inner cylinder and the shaft. The inner cylinder can rotate via the shaft, while the outer cylinder remains stationary. The outer cylinder (housing) can be axially displaced and its removable lid grants access to half of the material. The material can be extracted from the device by slow rotation of the inner cylinder. The inner cylinder is connected by a shaft to a rheodrive unit (Haake PolyLab QC, Thermo Fisher Scientific, Karlsruhe, Germany). The main purpose of this unit is to control the angular velocity of the rotating inner cylinder. It is also used to record the pressure in the up-scaled CC, the torque response and the specific mechanical energy (SME). The sample material is placed in the space between the two cylinders; this space is called *shearing zone* and has a volume of ~ 7 litres. The distance between the two cylinders is 30 mm. The device can be filled through a hole located in the middle of the lid. During the experiments, three temperature sensors (K-type) were fitted in the housing, along the axial direction, to monitor temperature. Additionally, the housing is fitted with a pressure sensor and an air outlet port, which is used during the filling procedure only.
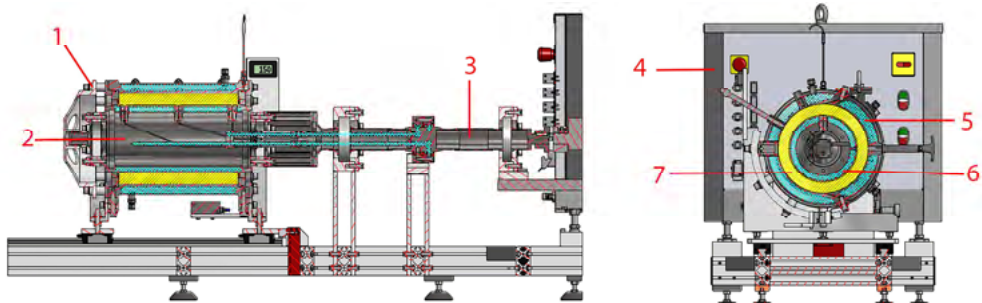
Figure 5.1: Axial (left) and radial (right) cross sections of the Couette Cell. 1. Outer cylinder (radius R_o = 0.125 m); 2. Inner cylinder (radius R_i = 0.095 m); 3. Shaft; 4. Rheodrive unit; 5. Housing heating jacket; 6. Inner cylinder heating jacket; 7. Shearing zone (length L = 0.332 m).

Both the inner and outer cylinders are heated by means of steam and cooled by means of air and/or water. The housing, lid and inner cylinder have their own separate heating jackets. A manifold is employed for this purpose to equally split the supply to the three heating jackets. The steam for heating up the device is at a constant pressure of 7 bar and is supplied by an industrial boiler unit. A flow regulation valve is used to control the temperature of the system. A controller (NI cRIO-9074, National Instruments, Austin, United States) is used to control all the valves and monitor and regulate temperature. Custom-made software programme

(LabView, National Instruments, Austin, United States) is used to operate the device and vary the operating conditions.

Figure 5.2: Actual picture of the Up-Scaled Couette Cell. 1. Housing; 2. Lid; 3. Inner cylinder; 4. Shaft; 5. Rheodrive unit.

5.2.3   Shear rate and velocity profile estimation

Couette Cells with inner to outer cylinder radius ratio, $b = R_i / R_o > 0.97$, are described as "narrow-gap" cells (Chhabra and Richardson, 1999). The up-scaled Couette Cell, used in this study, has $b = 0.76$ and is called a "wide-gap" concentric-cylinder cell. This means that the shear stress will be dependent on the viscosity of the mixture. By means of a dynamic oscillatory test, the rheological properties of the SPI – gluten mixture has been characterized and can be described as a power-law fluid.

Dynamic oscillatory tests were carried out on a TA Instruments AR-G2 rheometer (TA Instruments, Delaware, USA) for the rheological study of the SPI – gluten mixture. For these tests, a plate-plate configuration was employed. The top rotating plate was oscillated from 0.1-100 rad/s and the material response was recorded. As a result of these tests, a consistency index K [Pa·s^n] of 16603 and a flow behaviour index n of 0.13 were measured. These values indicate that the nature of the mixture is shear thinning.

If the torque or the rotational speed is known, the shear rate and velocity profile in the CC can be calculated for given boundary conditions and fluid properties. The following boundary conditions are applied to the up-scaled CC: $v_{\theta_o} = 0, r = R_o$ and $v_{\theta_i} = \Omega R_i, r = R_i$, where Ω [rad/s] is the angular velocity, v_θ [m/s] is the azimuthal velocity of the rotating cylinder, and generally $R_i \le r \le R_o$.

Since only the inner cylinder is rotating, the shear stress can be defined as (Macosko, 1994):

$$\tau = \frac{T_i}{2\pi R_i^2 H} \tag{5.1}$$

where τ [Pa] is the shear stress; T [Nm] is the torque applied to the inner cylinder and H [m] is the height of the CC cylinders.

Since the mixture in this study is a Power-Law fluid, the shear stress is related to the viscosity and can be given by the following power-law model equation

$$\tau = K\left(r\frac{d\left(v_\theta / r\right)}{dr}\right)^n = K\dot{\gamma}^n \tag{5.2}$$

where $\dot{\gamma}$ [s^{-1}] is the shear rate; K [Pa·s^n] is the consistency index and n is the flow behaviour index. From Equations 5.1 and 5.2, the shear rate can be calculated as (Rao, 2007)

$$\dot{\gamma} = \left(\frac{T}{2\pi KH}\right)^{(1/n)} \cdot \frac{1}{r^{(2/n)}} \tag{5.3}$$

Integration of Equation 5.3 and application of the $v_{\theta_o} = 0, r = R_o$ boundary conditions yields Equation 5.4 for the velocity profile

$$v_\theta = \frac{rn}{2}\left(\frac{T_i}{2\pi KH}\right)^{(1/n)}\left(\frac{1}{R_o^{(2/n)}} - \frac{1}{r^{(2/n)}}\right) \tag{5.4}$$

Application of the $v_{\theta_i} = \Omega R_i, r = R_i$ boundary conditions to Equation 5.4 yields

$$\frac{2\Omega}{n\left[\dfrac{1}{R_o^{(2/n)}} - \dfrac{1}{R_i^{(2/n)}}\right]} = \left(\frac{T}{2\pi KH}\right)^{(1/n)} \tag{5.5}$$

Substitution of the left hand side of Equation 5.5 into Equation 5.3 yields a relation between the rotational speed and the shear rate profile

$$\dot{\gamma} = \frac{2\Omega}{n\left[\dfrac{1}{R_o^{(2/n)}} - \dfrac{1}{R_i^{(2/n)}}\right]} \frac{1}{r^{(2/n)}} \tag{5.6}$$

Substitution of the left hand side of Equation 5.5 into Equation 5.4 yields the following relation for the velocity profile

$$v_\theta = \frac{\Omega r}{\left[\dfrac{1}{R_o^{(2/n)}} - \dfrac{1}{R_i^{(2/n)}}\right]}\left(\frac{1}{R_o^{(2/n)}} - \frac{1}{r^{(2/n)}}\right) \tag{5.7}$$

Equations 5.6 and 5.7 can accurately predict the shear rate and velocity profiles, respectively, across the "*shearing zone*" for the Couette Cell as well as across the gap of "wide-gap" concentric cylinder devices. Equations 5.6 and 5.7 were used in this study to select the optimum inner/outer cylinders ratio and size that would determine the process conditions that allow for anisotropic structure formation. In addition, the shear rate and velocity profiles across the *shearing zone*, as calculated based on Equations 5.6 and 5.7 can help explain the structural patterns obtained from the experiments (see figure 5.3 (right)).

5.2.4   Sample preparation and filling procedure

During the mixture preparation step, 7.5 kg of SPI-gluten mixture was prepared likewise as in previous experiments with the lab-scaled Couette Cell (Krintiras et al., 2015). The mixture was prepared with 30% w/w SPI – gluten with ratio of 3.3:1. The rest of the mixture is demi-water (69%) and salt (1%). First, 5175 g of demi-water and 75 g of salt were manually mixed in a bucket. The solution was then added and mixed for 10 minutes with 1725 g of SPI in a Z-blade mixer (Winkworth Machinery Ltd., Basingstoke, UK). The mixture was left inside the mixer with its lid closed for 30 min in order to pre-humidify. Following this step, 525 g of gluten were added in the SPI-demi-water-salt mixture and the content was mixed for 15 minutes. The SPI - gluten - demi-water - salt mixture, further referred to as mixture, was then ready to be processed.

The protein mixture consists of deformable granules. An in-house developed feeder was employed to insert the mixture into the device. It uses a pneumatic piston to press the material through a silicon tube connected to the up-scaled Couette Cell's custom-made feeding valve (Teesing BV., Rijswijk, the Netherlands), which is composed of a ball valve and a pin assembly.

After tightly packing the mixture in the *shearing zone* so as no cavities are present, the ball valve and the pin of the feeding valve were closed. The housing air-outlet port was closed as soon as the measured pressure in the *shearing zone* was lower than 1 bar. Then the experiment was commenced.

At the end of each experiment, the steam heating of the jackets was switched to air/water for the cooling stage of the process. In order to extract the material, the lid was then removed. This could only be done when pressure reached values lower than 0.7 bar. The sample was taken out by cutting it axially at the lower part and by slowly rotating the inner cylinder. The samples were stored in a seal bag and placed inside a freezer at -20 °C.

5.2.5   Process conditions and mathematical regression

A reduced factorial experimental design was used to identify the optimum process conditions for the production of anisotropic meat replacers (Ferreira et al., 2007; Li et al., 2013). Two independent variables were used in this study namely, processing time (min) and rotational speed (RPM) of the inner cylinder. Temperature was fixed at 120 °C. Preliminary experiments revealed that temperatures <120 °C could not be consistently achieved due to excessive steam condensate accumulation in the heating jackets, while processing at temperatures >120 °C would result in severely burned and deformed samples when processed for 15-45 minutes in total. The processing temperature in the up-scaled CC is higher compared to the processing temperature in the lab-scaled CC, since higher temperatures are needed due to the increased material thickness. The process conditions selected for this study are shown in Table 5.1. This configuration was employed to avoid operation at extreme values of time and RPM at the same time, since preliminary experiments yielded undesired samples. Sample integrity and presence of anisotropic structures were the main criteria to define the maximum and minimum values of time and RPM. An extra experimental point (30 min, 20 RPM) was added to increase the accuracy in the area believed to host the optimum process conditions.

Table 5.1: Actual and coded values of the independent variables in the reduced factorial experimental design with the average experimental values for tensile stress Anisotropic Index (AI$_\sigma$). Average SME values for each test performed.

Test	Time [min]	Rotational Speed [RPM]	X_1	X_2	Average AI_σ	Average SME [kJ/kg]
1	15	30	-1	0	1.18	11.3
2	30	10	0	-1	0.79	8.6
3	30	20	0	-0.5	1.67	18.5
4	30	30	0	0	1.70	32.6
5	30	50	0	1	1.05	63.1
6	45	30	1	0	0.81	59.9

The AI_σ values obtained in the texture analysis were used to study the influence of time and RPM on the product structure. A second-order polynomial with interaction model (Equation 5.8) was used to fit the experimental values of AI_σ.

$$Y = \beta_0 + \sum_{(i=1)}^{2} \beta_i X_i + \sum_{(i=1)}^{2} \beta_{ii} X_i + \beta_{12} X_1 X_2 \qquad (5.8)$$

where β_0, β_i, β_{ii}, and β_{12} are the equation regression coefficients; X_i and X_j are the independent variables and Y is the dependent variable. The software STATISTICA 12 (Statsoft Inc., Tulsa, U.S.A.) was used to fit the model to the experimental points; perform the statistical analysis and draw the surface plots. It was also used to compute the optimum conditions of the model. Later on, an experiment was performed at these conditions in order to compare and verify the model.

5.2.6   Texture Analysis

The selection of the optimum process conditions requires a method, which allows for quantitative comparison of different product samples. The mechanical properties of each product sample may vary depending on the structures present in the bulk. In particular, samples with fibrous structures will show significant differences in tensile stress values between specimens obtained parallel and perpendicular to the formed fibres. For this reason, the tensile stress Anisotropy Index (AI_σ) was devised to reveal the physical presence of anisotropic structures in the samples and their degree of fibrousness (Krintiras et al., 2014). Additionally, the tensile strain Anisotropy Index (AI_ε) can quantify the textural and sensorial characteristics of the meat replacer.

The maximum values for tensile stress and strain were determined for each specimen. The maximum tensile strain was determined at the point of maximum tensile stress. The maximum tensile stress and strain per direction were averaged and the relevant Anisotropy Indices (AI) were calculated through Equations 5.9 and 5.10, respectively.

$$AI_\sigma = \frac{\sigma_\parallel}{\sigma_\perp} \qquad (5.9)$$

where, AI_σ[-] is the stress anisotropy index; $\sigma_\parallel$ [Pa] is the normal stress for specimens cut parallel to the fibres and $\sigma_\perp$ [Pa] is the normal stress for specimens cut perpendicular to the fibres

$$AI_\varepsilon = \frac{\varepsilon_\parallel}{\varepsilon_\perp}$$
(5.10)

where, AI_ε[-] is the strain anisotropy index, $\varepsilon_\parallel$ [mm/mm] is the normal strain for specimens cut parallel to the fibres and $\varepsilon_\perp$ [mm/mm] is the normal strain for specimens cut perpendicular to the fibres.

Three specimens were cut for each sample created, both parallel and perpendicular to the formed fibres, resulting in a total of 108 tested specimens. The specimens were cut in a rectangular shape with a thickness of 30 mm. The cross-sectional area relevant for calculating the normal stress was manually measured each time. The tensile tests were performed on a Zwick Roell Z005 (Zwick Roell AG., Ulm, Germany). The tensile tests were performed with a constant deformation rate of 0.5 mm s^{-1}. Two plain clamps with rough surfaces were employed to fixate the specimens in the tester. Additionally, for the study of the local thickness characteristics of the sample, roller clamps fitted with sandpaper were employed to fixate the specimens. In this case, smaller strips of 5 x 5 mm were cut from the bottom, centre and top of the total sample thickness (30 mm) in order to examine the local structure formation.

5.2.7   Scanning Electron Microscopy

The microstructures of the samples were investigated with SEM (S-4800, Hitachi, Tokyo, Japan). The SEM at hand is a cold field emission scanning electron microscope, which features a maximum resolution of 1.0 nm at 15 kV. Inspection of the samples is possible with acceleration voltages of 0.5 - 30 kV without beam deceleration. The SEM bears a beam deceleration feature that can be used to inspect sensitive or charging samples. For these inspections, a low voltage of 2 kV was utilized. The microscope allowed for specimen imaging without gold or other coating. In SEM, the samples, in specimens of 5 x 5 x 5 mm, were cut parallel to the fibres at room temperature. The specimens were dried for 24 hours in an oven set at 60 °C to reduce the moisture content. Both the parallel and perpendicular surfaces to the fibres were inspected by SEM.

5.3   Results and discussion

In this study, the SPI-gluten mixture was treated by means of simple shear flow and heat at variable process conditions. After each experiment, visual inspection of the product was performed. Figure 5.3 (left) shows a typical sample obtained at 120 °C, 20 RPM and 30

minutes; it exhibits fibrous formations over the whole bulk of the sample when bending it by hand to the point that it starts tearing in half. Figure 5.3 (right) shows the cross-section of the same sample where fibre formation is also evident. Structure formation follows the flow direction from the inner rotating cylinder to the outer one, which is stationary. Figure 5.3 (right), shows what is expected to be the structure formation mechanism for highly viscous systems, namely phase separation between SPI and gluten to form individual fibre structures (Krintiras et al., 2015). Specifically, (Manski et al., 2007), showed that highly viscous systems can favour structure formation when simple shear flow is applied. It can be seen in Figure 5.3 (right) that long fibres are distributed over the bulk of the sample. The pale yellow coloured fibres are believed to be gluten fibres. It can also be seen that the shear rate profile, as calculated by Equation 5.6, across the *shearing zone* (sample thickness) matches the structural profile of the samples produced at 30 RPM rotational speed applied to the inner cylinder. The match between the shear rate and structural profiles has been reproducible for all the samples in this study except for those treated at 50 RPM and 45 min, respectively.

Figure 5.3: Left: Typical fibre structured sample obtained at 120 ºC, 20 RPM and 30 minutes. Right: Sample thickness (30 mm). Notice the structure formation following the flow direction and the similar pattern of the shear rate profile across the thickness as calculated by Equation 5.6.

Figure 5.4 shows a typical slab of the structured meat replacer. The striped and other patterns visible on the surface are due to the presence of corrugations at the inner and outer cylinder to help increase the surface contact and friction between wall and mixture. From such a slab, we cut the specimens needed for texture analysis and SEM inspections. To the best of our knowledge, this is the first time that fibrous meat replacers are produced in such characteristic dimensions as the slab depicted in Figure 5.4 and with a thickness of 30 mm as shown in Figure 5.3 (right). This characteristic thickness can help produce meat replacers that resemble complete muscular parts of animals, for instance, chicken breast or meat. Typical dimensions of a chicken breast are 10-15 cm long, 5-8 cm wide and 3-5 cm thick.

Figure 5.4: Typical product slab obtained at 120 °C, 20 RPM and 30 minutes (Length = 596 mm, Height = 332 mm).

After each experiment, we would obtain, through the rheodrive unit, the measurement and recording of the specific mechanical energy (SME), which in our case is the response from the mixture, the seals and bearings in the up-scaled CC. The SME at the optimum process conditions for 120 °C, 30 min and 20 RPM was in average 18.5 kJ/kg and for 120 °C, 30 min and 30 RPM was in average 32.6 kJ/kg. The SME values reported from extrusion cooking vary between about 200 to 1200 kJ/kg depending on the mixture composition, the extruder set-up and the die shape (Fang et al., 2014; Jin et al., 1994; Lue et al., 1994; Osen et al., 2014). The SME values obtained while operating the up-scaled CC do not include the additional energy spent for the mixing step during the mixture preparation.

5.3.1   Texture Analysis

Figure 5.5 shows the tensile stress/strain and AI values obtained for samples treated at a constant process temperature of 120 °C and process time of 30 min at varying rotational speed. The tensile stress and strain values are shown for both perpendicular and parallel directions to the movement of the inner cylinder. Figure 5.5 (left) shows that in the event of 10 and 50 RPM, the AI_σ values are 0.79 and 1.05 respectively; AI_σ values ~1 are typical for homogeneously or layered textured samples. During visual inspection, it was found that samples treated at 10 RPM were not sufficiently structured (homogeneous samples), whereas at 50 RPM the samples were damaged and deformed. On the other hand, samples processed at 20 and 30 RPM yielded high AI_σ values, 1.67 and 1.7, respectively, with an individual sample yielding an AI_σ value of 3.6. Figure 5.5 (right) shows the AI_ε values for the same samples; the main observation is that the samples treated at 30 RPM are rigid compared to the more elastic samples obtained at 20 RPM. It is remarked that Figure 5.5 reveals a local area of optimum process conditions; specifically, samples treated between 20-30 RPM will yield highly fibrous samples.
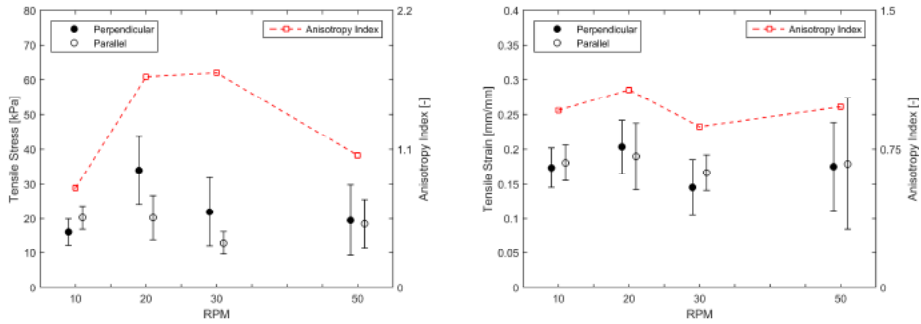
Figure 5.5: Tensile stress (left) and strain (right), with standard deviation error bars, in the direction parallel and perpendicular to the formed fibres (direction of rotation) vs. rotation rate (RPM). The line connecting the Anisotropy Index points is only to guide the eye. Process temperature = 120 ºC and Process time = 30 minutes.

Figure 5.6 shows the tensile stress, strain and AI values for samples processed at a constant process temperature of 120 °C and rotational speed of 30 RPM at varying processing times. In Figure 5.6 (left), it can be seen that samples processed at 15 and 45 minutes yielded AI_σ values of 1.18 and 0.81, respectively. At 15 min the samples did not exhibit any visual fibrous structures. Due to the increased thickness (30 mm) of the sample, thermal treatment for 15 min is not sufficient. On the other hand, samples treated for 45 minutes showed burned, deformed and plasticized areas due to excessive heating. The optimum process time that resulted in fibrous structured samples was 30 min, as can be seen in Figure 5.6 (left). Figure 5.6 (right) shows that samples treated at 15 and 45 minutes were more rigid and stiff compared to the more elastic ones produced at 30 minutes.

Figure 5.6: Tensile stress (left) and strain (right), with standard deviation error bars, in the direction parallel and perpendicular to the formed fibres (direction of rotation) vs. process time (min). The line connecting the Anisotropy Index points is only to guide the eye. Process temperature = 120 °C and Rotation rate = 30 RPM.

In the course of this study, additional analysis was performed to explore the local structure formation across the samples within their 30 mm thickness. Specimens were collected from the

same samples as in the above described texture analysis. Figure 5.7 presents a comparison between samples created at 120 °C, 30 min and varying RPM, for specimens collected from the bottom (close to the inner cylinder), centre and top (close to the outer cylinder) of these samples (see Figure 5.3, right). The AI_σ values for all cases suggest that the specimens obtained from samples processed at 20 RPM would yield the most anisotropic structures locally.

Bottom   *Centre*   *Top*
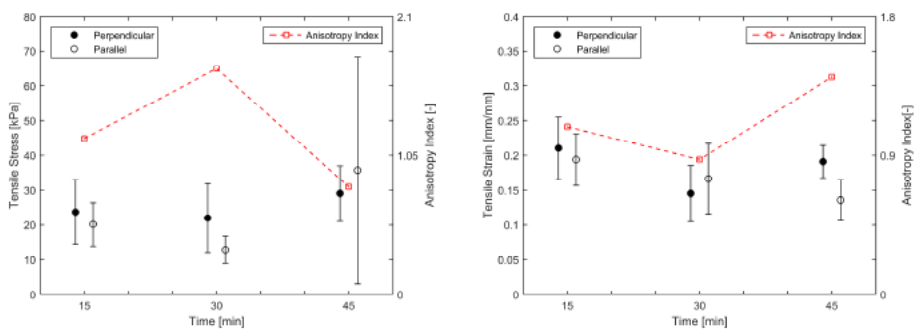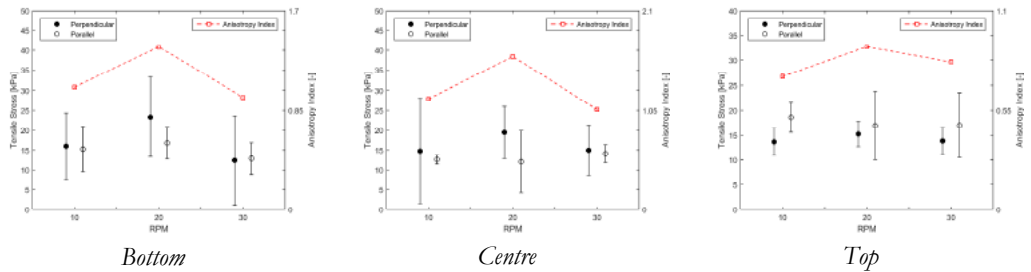
Figure 5.7: Tensile stress, with standard deviation error bars, in the direction parallel and perpendicular to the formed fibres (direction of rotation) vs. rotational speed (RPM). For specimens obtained from the bottom, centre and top of the 30 mm thick samples. The line connecting the Anisotropy Index points is only to guide the eye. Process temperature = 120 °C and process time = 30 min.

Figure 5.8 shows the difference between the bottom, centre and top part of the samples processed at 120 °C, 30 min and 20 RPM. These samples were picked and further analysed due to the pronounced fibrous structures and the high AI_σ values as shown in Figure 5.7. No significant difference between the three positions was observed. It is therefore stated that the samples showed uniform strength over the sample thickness (Figure 5.8). It is remarked that the global AI_σ of a sample would then depend on the interconnection of layers and fibres, being similar at a local scale for all conditions. The averaged values of AI_σ suggest that the middle part of the samples is the one with the highest density of fibres. This is also supported by Figure 5.3 (right), where the top and bottom parts of the sample have slightly different textures than that in the centre. However, for both Figures 5.9 and 5.10, due to the high deviation in the tensile stress values, and based on a t-test performed, the textural differences at local scale were not significant.
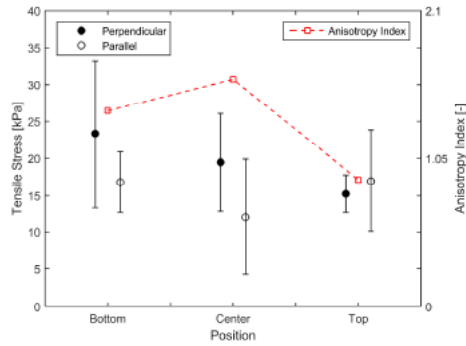
Figure 5.8: Tensile stress, with standard deviation error bars, in the direction parallel and perpendicular to the formed fibres (direction of rotation) vs. specimen position for a sample processed at 120 °C, 30 min and 20 RPM. The line connecting the Anisotropy Index points is only to guide the eye.

5.3.2   SEM analysis

SEM imaging allowed for identification of structure formation within the bulk of the treated samples. Figure 5.9 (left) depicts a sample treated at 120 °C, 30 min and 20 RPM. Fibre structures of variable sizes are visible; micro-fibres of 1 – 5 µm in diameter bundle up to form fibres of 100 - 400 µm in diameter. The fibres are aligned along the flow direction, which is in accordance with Figure 5.3. In Figure 5.9 (right), the tips of fibres from the same specimen are shown and the characteristic round cavities scattered in the domain might have contained air or water in its initial state. A closer look at the bottom left in Figure 5.9 (right) reveals the presence of a single gluten fibre with its characteristic needle-like structure (Abang Zaidel et al., 2008; Krintiras et al., 2014; Krintiras et al., 2015).
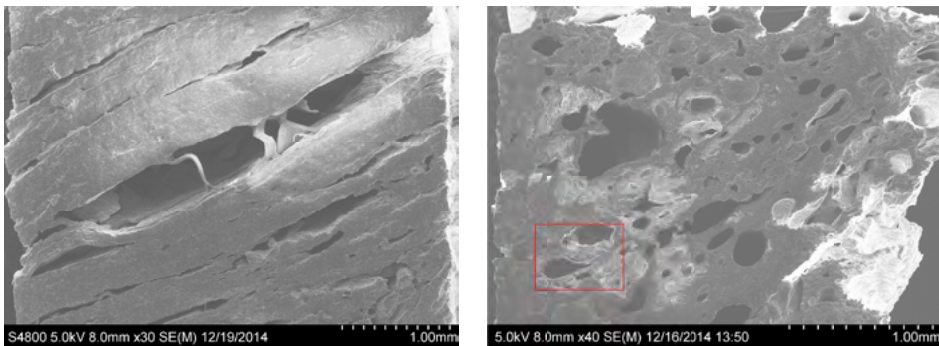

Figure 5.9: SEM images of a fibrous sample at different view planes; left: the displayed surface is of the fibre structures; right: the displayed surface is of the tips of fibres. Process conditions: Temperature = 120 °C; Rotation rate = 20 RPM; Process time = 30 minutes.

5.3.3 Model fitting and statistical analysis

The obtained AI_σ values from the first part of the texture analysis (see Figures 5.5 and 5.6) were fitted in a quadratic model. The experiments performed at the edges (15, 45 min and 10, 50 RPM) of the experimental design (see table 5.1) yielded the lowest AI_σ values. Additionally, the highest averaged AI_σ was found when processing for 30 min and 30 RPM, in the middle of the experimental design. Therefore, the proposed region of study and the experimental design were acceptable for this study and their results were used to adjust the coefficients of Equation 5.8. The objective of this model was to gain deeper insight into the system behaviour and to estimate the best conditions to obtain fibrous structures. High standard deviation values for AI_σ were obtained due to the samples' and specimens' size, thickness and unpredictable values of AI_σ. That is why the predictions were used as a tool to confirm the experimental study and highlight a region of confidence in which processing will result in fibrous structures. Figure 5.10 (left) shows the surface plot obtained from the regression function (Equation 5.8) for the ranges of 10 to 50 RPM and 15 to 45 min. As seen in Figure 5.10 (right), the surface plot has a circular shape over the whole domain. In this case, the interaction term was not used. As reported in a previous study (Krintiras et al., 2015), the process time and rotational speed have similar influence.
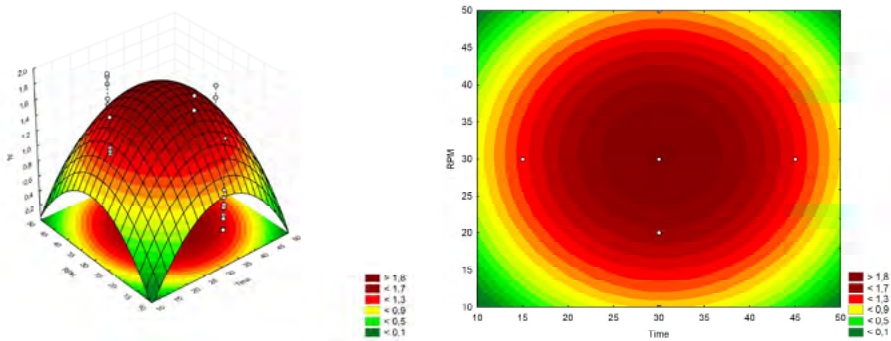
Figure 5.10: Response surface (left) and contour (right) plot of the combined effects of rotational speed and processing time on AI_σ. The values of the experimental points are shown as white dots in both pictures.

The optimum process conditions extracted from the model were 30.3 min and 31 RPM and yielded an AI_σ of 1.8, which is in agreement with the optimal experimental AI_σ of 1.7 obtained at the conditions of 30 RPM and 30 min (Table 5.1). Due to the deviance of the experimental points, the R^2 had a low value of 0.2. The statistical analysis of the regression coefficients is summarized in Table 5.2. It was found that 4 out of 6 coefficients were statistically significant, having p-values lower than 0.05. Although lower values were obtained while fitting, the visual inspection of the samples agreed with the model behaviour. A comparison between the averaged AI_σ and the predicted value by the model can also be seen in Table 5.1. Higher relevance is given to the qualitative results obtained during the inspection of the samples than

the specific quantitative AI_σ values. In order to confirm the results obtained from the model, a verification experiment was performed at the optimal process conditions predicted by the model. The average AI_σ at the optimal process conditions was lower (AI_σ of 1.4) than the predicted value (AI_σ of 1.8). However, the obtained samples showed well-defined fibrous structures all over the domain as can be seen in Figure 5.11. The results of the model, together with the verification experiment, suggest that working in a range between 25 to 35 minutes and 20 to 30 RPM will always lead to fibrous structured products.

Table 5.2: List of regression coefficients and their significances for Equation 5.8.

Coefficient	Value	Standard error	t-value	p-value
X_0	-2.33	1.23	-1.89	0.06
X_1	0.14	0.06	2.35	0.02
X_{12}	-0.002	0.001	-2.36	0.02
X_2	0.13	$8 \cdot 10^{-3}$	3.49	0.001
X_{22}	-0.002	$5 \cdot 10^{-4}$	-3.58	0.001
$X_1 \cdot X_2$	0	-	-	-

Figure 5.11: Picture showing the fibrous structures in a sample obtained during the verification experiment.

5.4   Conclusions

We have demonstrated that application of simple shear flow and heat in a Couette Cell is a scalable process concept that can induce fibrous structural patterns to a granular mixture of plant proteins at mild process conditions. In particular, after processing the protein blend at 120 ºC and variable rotational speeds and process times, a structured SPI-gluten product was formed. A reduced factorial experimental design was used to search for the optimum process conditions. It was found that the optimum area of operation is located at 30 ± 5 min process time and 25 ± 5 RPM rotational speed of the inner cylinder. In particular, samples created at 120 ºC, 30 min and 20 RPM exhibited highly fibrous structures and yielded high average AI_σ values of 1.67 with individual samples yielding values up to 3.6. The fibres formed were clearly observed both visually and with SEM imaging. In the event of a lab-scale Couette Cell with 6 times smaller gap between the two cylinders (5 mm vs. 30 mm) and 50 times lower capacity (0.14 L vs. 7 L), a product with the same fibrous structural patterns was obtained at 95 ºC, 30 RPM and 15 min. The increase in temperature and process time in the up-scaled Couette Cell, compared to the lab-scale counterpart, is necessary due to the increased product thickness. A study of the local structure formation across the thickness of the product (bottom, centre and top) was conducted and no significant differences were observed due to the high variations in the results. The energy input (SME) for the production of highly fibrous meat replacers with the up-scaled Couette Cell was ranging between 8.6-63.1 kJ/kg. The Couette Cell can be further scaled up linearly (increased length) and is amenable to continuous operation.

5

References

Abang Zaidel, D.N., Chin, N.L., Abdul Rahman, R., Karim, R., (2008). Rheological characterisation of gluten from extensibility measurement. Journal of Food Engineering 86(4), 549-556.

Aldaya, M.M., Chapagain, A.K., Hoekstra, A.Y., Mekonnen, M.M., (2012). *The water footprint assessment manual: Setting the global standard.* Routledge.

Chhabra, R.P., Richardson, J.F., (1999). *Non-Newtonian flow in the process industries : fundamentals and engineering applications.* Butterworth-Heinemann, Oxford ; Boston, MA.

Fang, Y., Zhang, B., Wei, Y., (2014). Effects of the specific mechanical energy on the physicochemical properties of texturized soy protein during high-moisture extrusion cooking. Journal of Food Engineering 121(0), 32-38.

Ferreira, S.L.C., Bruns, R.E., Ferreira, H.S., Matos, G.D., David, J.M., Brandão, G.C., da Silva, E.G.P., Portugal, L.A., dos Reis, P.S., Souza, A.S., dos Santos, W.N.L., (2007). Box-Behnken design: An alternative for the optimization of analytical methods. Analytica Chimica Acta 597(2), 179-186.

Grabowska, K.J., Tekidou, S., Boom, R.M., Goot, A.J.v.d., (2014). Shear structuring as a new method to make anisotropic structures from soy-gluten blends. Food Research International.

Hoek, A.C., Elzerman, J.E., Hageman, R., Kok, F.J., Luning, P.A., Graaf, C.d., (2013). Are meat substitutes liked better over time? A repeated in-home use test with meat substitutes or meat in meals. Food Quality and Preference 28(1), 253-263.

Hoek, A.C., Luning, P.A., Stafleu, A., de Graaf, C., (2004). Food-related lifestyle and health attitudes of Dutch vegetarians, non-vegetarian consumers of meat substitutes, and meat consumers. Appetite 42(3), 265-272.

Hoek, A.C., Luning, P.A., Weijzen, P., Engels, W., Kok, F.J., de Graaf, C., (2011). Replacement of meat by meat substitutes. A survey on person- and product-related factors in consumer acceptance. Appetite 56(3), 662 - 673.

Hoekstra, A.Y., International Institute for Infrastructural Hydraulic and Environmental Engineering (IHE), (2003). *Virtual water trade.* IHE, Delft.

Hooda, P., Edwards, A., Anderson, H., Miller, A., (2000). A review of water quality concerns in livestock farming areas. Science of the Total Environment 250(1), 143-167.

Ilo, S., Berghofer, E., (2003). Kinetics of Lysine and Other Amino Acids Loss During Extrusion Cooking of Maize Grits. Journal of Food Science 68(2), 496-502.

Jin, Z., Hsieh, F., Huff, H.E., (1994). Extrusion cooking of corn meal with soy fiber, salt, and sugar. Cereal Chemistry 71(3), 227-234.

Krintiras, G.A., Göbel, J., Bouwman, W.G., van der Goot, A.J., Stefanidis, G.D., (2014). On characterization of anisotropic plant protein structures. Food & Function 5(12), 3233-3240.

Krintiras, G.A., Göbel, J., van der Goot, A.J., Stefanidis, G.D., (2015). Production of structured soy-based meat analogues using simple shear and heat in a Couette Cell. Journal of Food Engineering 160(0), 34-41.

Li, Y.-L., Fang, Z.-X., You, J., (2013). Application of Box-Behnken Experimental Design to Optimize the Extraction of Insecticidal Cry1Ac from Soil. Journal of Agricultural and Food Chemistry 61(7), 1464-1470.

Liu, K., Hsieh, F.-H., (2008). Protein–Protein Interactions during High-Moisture Extrusion for Fibrous Meat Analogues and Comparison of Protein Solubility Methods Using Different Solvent Systems. Journal of Agricultural and Food Chemistry 56(8), 2681-2687.

Lue, S., Hsieh, F., Huff, H.E., (1994). Modeling of twin-screw extrusion cooking of corn meal and sugar beet fiber mixtures. Journal of Food Engineering 21(3), 263-289.

Macosko, C.W., (1994). *Rheology : principles, measurements, and applications*. VCH, New York.

Manski, J.M., van der Goot, A.J., Boom, R.M., (2007). Advances in structure formation of anisotropic protein-rich foods through novel processing concepts. Trends in Food Science & Technology 18(11), 546 - 557.

Osen, R., Toelstede, S., Wild, F., Eisner, P., Schweiggert-Weisz, U., (2014). High moisture extrusion cooking of pea protein isolates: Raw material characteristics, extruder responses, and texture properties. Journal of Food Engineering 127(0), 67-74.

Pachauri, R.K., (2008). Climate change 2007. Synthesis report. Contribution of Working Groups I, II and III to the fourth assessment report.

Peighambardoust, S.H., Brenk, S.v., Goot, A.J.v.d., Hamer, R.J., Boom, R.M., (2007). Dough processing in a Coutte-type device with varying eccentricity: effect on glutenin macro-polymer properties and dough microstructure. Journal of Cereal Science 45(1), 34-48.

Post, M.J., (2012). Cultured meat from stem cells: Challenges and prospects. Meat Science 92(3), 297-301.

Rao, M.A., (2007). *Rheology of fluid and semisolid foods : principles and applications* (2nd ed). Springer, New York.

5

Riaz, M.N., (2000). *Extruders in Food Applications*. Taylor & Francis.

Steinfield, H., Gerber, P., Wassenaar, T., Castel, V., Food, of the United Nations, A.O., Livestock, E., (Firm), D., De Haan, C., (2006). *Livestock's long shadow: environmental issues and options*. Food and agriculture organization of the United Nations.

Thiébaud, M., Dumay, E., Cheftel, J.C., (1996). Influence of Process Variables on the Characteristics of a High Moisture Fish Soy Protein Mix Texturized by Extrusion Cooking. LWT - Food Science and Technology 29(5–6), 526-535.

PSV-101

S4

AO

AI

FC
01

YC
01

S8   S9

CV-101

S10

PI
02

DO

DI

AI

TT
01

TT
02

TT
03

TT
10

TT
11

TT
12

DO

DI

FC
02

PT
01

TT
06

FC
07

AV-101
FC

S11

TT
05

S12

AV-106
FC

C1   C2   C3

NV-102

C4

TT
04

C5

DO

DI

FC
03

C7

C8

NV-103

DO

DI

FC
06

A3

AV-102
FC

A4

C6

C9

C11

C13

C14

DO

DI

FC
04

TT
07

TT
09

AV-105
FC

W6   W7

DO

DI

FC
05

DI

DO

FC
04

TT
08

W3   ST-01   T = MS   W4   AV-103
FC   W5

C12

AV-104
FC

A5

C10
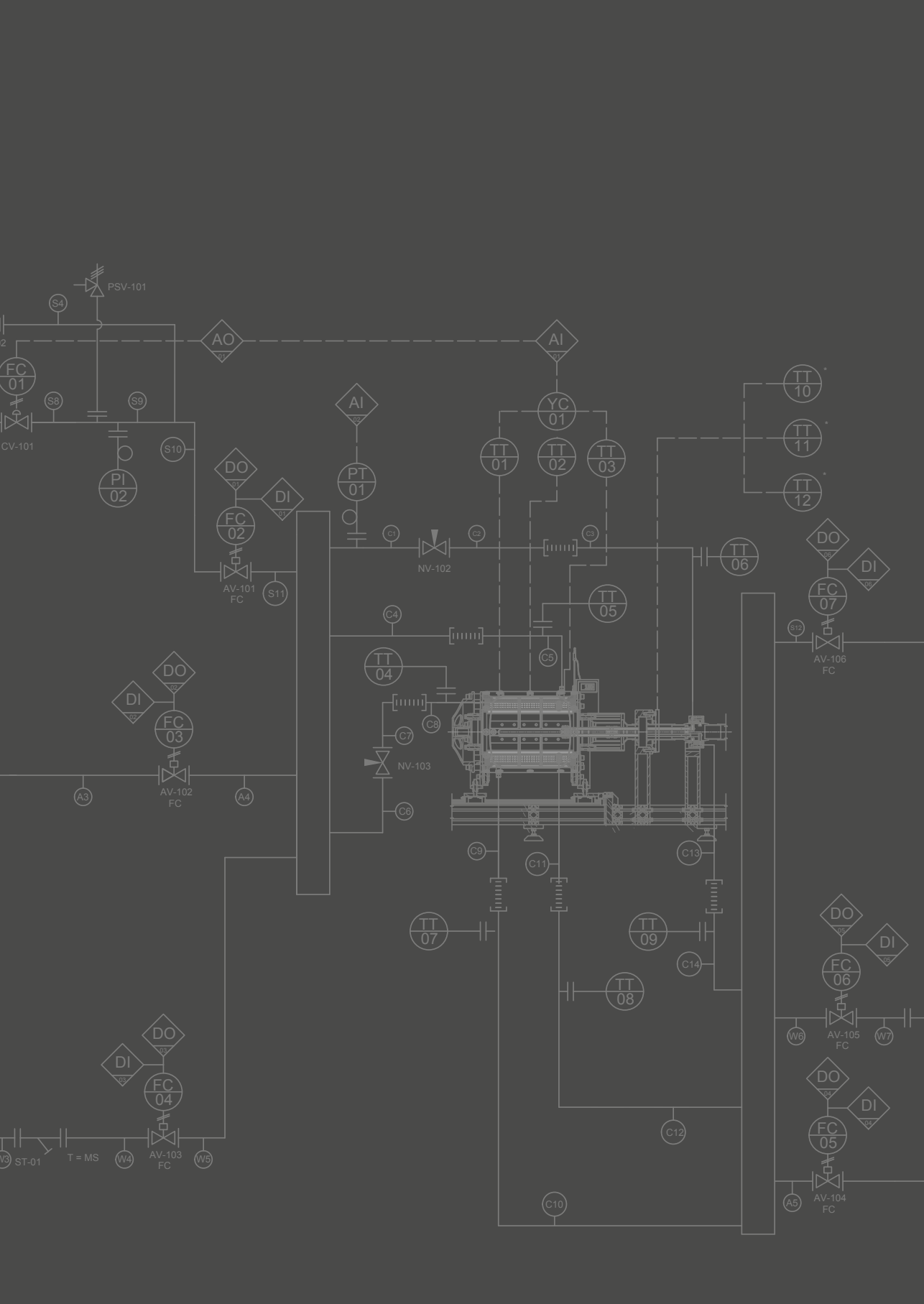
Chapter **6**

CONCLUSIONS AND RECOMMENDATIONS

CT-02

Condensate

W12-16mm-PVC

W8

Water out

A6

Drain

The main objective of this thesis is to introduce a novel scalable technology for processing plant-based mixtures to produce high quality fibrous meat substitutes. The research work resulted in a scalable and process optimized technology called the Couette Cell. This thesis also provides a new complementary characterization technique called neutron scattering and offers a holistic characterization of meat replacers with various other standard techniques. The conceived technology can be used for production of meat replacers at commercially relevant scales. The up-scaled Couette Cell can be operated for the dedicated production of meat replacers. Therefore, food industries can improve their existing product range by producing up to 30 mm thick slabs of meat replacer.

6.1   Conclusions

6.1.1   Texturization of soy-based meat replacers with the lab-scaled Couette Cell

The thesis starts with the introduction of the Couette Cell concept as a novel technique for the production of structured meat replacers. In Chapter 2, we introduce the lab-scaled Couette Cell, which is comprised of two concentric cylinders with the inner cylinder rotating while the outer remains stationary. Both cylinders are heated by means of oil. In the gap between the two cylinders, called the *shearing zone*, we tightly pack a soy-gluten blend mixture. During the thermo-mechanical treatment of the mixture, we induce simple shear flow and heat, which results in anisotropic meat-like structures. The Couette Cell concept has been verified as a successful technique for the production of texturized vegetable products. The lab-scaled Couette Cell operates in batch mode with a capacity of 0.14 L and an end-product thickness of 5 mm. The lab-scaled Couette Cell can serve as a versatile, user-friendly technique for extensive experimental studies on food materials. We operate it, particularly, for fast testing and verification of different recipes that could potentially serve as alternative meat replacers. The Couette Cell concept allows for scalable and continuous process operation.

We have successfully structured meat replacers by means of simple shear and heat under mild process conditions. A local parametric study was initiated by varying the temperature, the process time and the rotation rate of the inner cylinder of the Couette Cell. It has been found that the process time and rotation rate do not have much influence on the quality of the final product, while the process temperature should be maintained at 95 ºC $\pm$ 5 ºC. The optimum process conditions were found to be at a process temperature of 95 ºC, rotation rate of 30 RPM and process time of 15 min. At these process conditions, we produced highly fibrous samples with average stress anisotropy index (AI_σ) values of 2.3, with individual samples exhibiting values up to 3.2, which resembled meat very accurately. During this study, all samples were characterized by means of visual inspection, SEM imaging and texture analysis.

We have identified three typical structure formations, i. homogeneous, ii. fibrous and iii. layered type of structures depending on the process conditions.

6.1.2   Characterization of texturized meat replacers

By means of complementary techniques we have characterized the plant-based meat replacers produced with the lab-scaled Couette Cell. Specifically, a sample that yielded the highest anisotropic structures (fibres) was cross-examined. This sample was created while processing at 95 °C, 30 RPM and 15 min. The techniques used to characterize the product were i. Light Microscopy, ii. Scanning Electron Microscopy, iii. Texture Analysis and iv. neutron refraction with the novel spin-echo small angle neutron scattering (SESANS) technique. Light Microscopy was used to differentiate between proteins (SPI, gluten) present in the product. This was only possible by using toluidine blue stain mountant, which revealed anisotropic formations in the direction of the flow. Scanning Electron Microscopy was used to observe the morphology of the product at micro-scale and the fibre thickness was found to be ±150 µm. Texture Analysis enabled a quantitative comparison between the mechanical properties (tensile stress and strain) of raw meat (beef) and the meat replacer produced. It was found that both the product and raw meat (beef) yielded comparable tensile stress and strain anisotropy indices. Neutron refraction by SESANS was used to quantify the number of fibre layers (±36) and the thickness of fibre layers (±138 µm) in the bulk of the product, enabling us to *look inside* the material.

Overall, the findings in **Chapter 3** of this thesis suggest that all the techniques used provided insight into the structures formed at the surface and bulk of the material. No single technique can independently provide a comprehensive analysis of the product characteristics. Combining several characterization techniques allowed for better understanding of the nature of plant-based meat replacers as well as their functionality and structuring mechanisms. Hence, common techniques such as light microscopy, scanning electron microscopy and texture analysis complemented by neutron refraction (SESANS) can give the full qualitative and quantitative three-dimensional picture of the structures formed inside the material.

6.1.3   Design of the up-scaled Couette Cell

The Couette Cell concept is introduced as a novel, dedicated technique for the production of fibrous meat replacers via the application of simple shear and heat. In **Chapter 2** of this thesis, the design and principle of the lab-scaled Couette Cell was presented. The lab-scaled Couette Cell features a *shearing zone* gap size of 5 mm and a capacity of 0.14 L. Since the Couette Cell concept proved to be successful we have initiated a scaled-up version. Since this concept allows for scalable and possibly continuous processing, in **Chapter 4** of this thesis we present

the design and operating principles of the up-scaled Couette Cell. Scale-up in the radial direction is more valuable as it would result in increased product thickness. Eventually, the up-scaled Couette Cell features an increased *shearing zone* gap size of 30 mm and a capacity of about 7 L. This gap size is far bigger compared to the products offered by extrusion cooking, which are normally up to 15 mm thick. The up-scaled Couette Cell follows the same operating principle as in the case of the lab-scaled Couette Cell. The device is comprised of two concentric cylinders; an inner rotating cylinder and an outer one, which is stationary. Both cylinders are heated by means of steam. The device has been optimized for user-friendly operation and effective control. Special attention was given in the collection of process data while operating. Therefore, the device is fitted with various thermocouples and pressure sensors.

The up-scaled Couette Cell can serve as a step towards the production of meat replacers at industrially relevant scales. The Couette Cell concept can be further scaled-up in the axial direction, which is straightforward and does not require redesign of the process and equipment. This device allows for operation in continuous mode, which is highly considered for the near future.

6.1.4 Texturization of soy-based meat replacers with the up-scaled Couette Cell

In **Chapter 2**, the effect of simple shear flow and heat on a plant protein-based mixture in a lab-scaled Couette Cell was investigated. The overarching aim of this thesis was to study scale up of this process. This necessitates investigation upon the effect of rotation rate, shear forces, energy input and heating time on the flow and heating patterns developed within the material as function of the distance between the two cylinders. In **Chapter 5** of this thesis, we have demonstrated that application of simple shear flow and heat in a Couette Cell is a scalable process concept that can induce fibrous structural patterns into a granular mixture of plant proteins at mild process conditions.

In particular, we have developed the up-scaled Couette Cell as an intermediate step towards future industrial production of meat replacers. The up-scaled Couette Cell, which is described in detail in **Chapter 4** of this thesis, follows the same principle as the lab-scaled Couette Cell. In **Chapter 5**, we demonstrated the use of a reduced factorial experimental design to scan for the optimum process conditions for the production of highly fibrous meat replacers. As a result, we processed a 7 kg SPI-gluten protein blend at 120 ºC and variable rotational speeds and process times. We found an optimum operation window at ±25 min process time and ±30 RPM rotational speed of the inner cylinder. In particular, samples created at 120 ºC, 30 min and 20 RPM exhibited highly fibrous structures. The fibres formed

were clearly observed both visually and with SEM imaging. Texture analysis was employed to quantitatively measure the degree of fibrousness, at an average stress anisotropy index (AI_σ) of 1.7; in some cases, values of up to 3.6 were found. Additionally, we examined the local structure formation across the thickness of the product (bottom, centre and top) and no significant differences were observed. The novelty of the Couette Cell lies in the unique 30 mm gap size, which allows for thick meat replacers that can accurately emulate meat. The Couette Cell can be further scaled up linearly (increased length) and is amenable to continuous operation.

6.2   Recommendations

1.   We have demonstrated in this thesis that the application of simple shear flow and heat to a plant protein blend in a Couette Cell will induce structure formation. The treated samples have been characterized with several techniques including the novel SESANS method. The findings revealed that it is possible to obtain highly fibrous products. We investigated the structure formation mechanism, which is believed to be based on the presence of highly viscous materials that phase separate under simple shear flow. We also identified the effect of pre-humidification during the protein mixture preparation phase as a possible mechanism in our system. However, deeper and more detailed insight into the structure formation mechanism is needed. The SESANS method can shed light by allowing for in-situ and in-real time observations while processing. Development of a titanium or aluminium Couette Cell that can allow such observations is essential.

2.   We have successfully introduced the up-scaled Couette Cell, which could treat plant based protein mixtures and could yield highly fibrous meat replacers that can emulate real meat. Further up-scaling to industrially relevant scales is trivial by linearly increasing the length of the device. Additionally, increased capacity can be achieved by increasing the cylinder dimensions while keeping their ratio similar to the up-scaled Couette Cell. The most valuable step would be the development of a continuous process by investigating the effect of process time, which will affect the device design, dimensions, and process conditions. This task is not trivial, as it will most probably require a different design. We also recommend that sophisticated automation should be applied so as the overall process time is reduced and becomes more user-friendly, especially in an industrial production facility. With this respect, an appropriate Clean-In-Place (CIP) cycle should be incorporated in the design.

3.   The novelty in the up-scaled Couette Cell lies in the increased 30 mm gap size, which is unique for meat replacers since the current thickest meat replacers produced by extrusion cooking is 15 mm. It is therefore recommended to investigate increasing the gap size of the Couette Cell further since this will lead to meat replacers that emulate a wider range of meats,

such as beefsteak. The highest limit will primarily depend on the plant protein mixture properties (i.e. viscosity, thermal characteristics, and water content).

4.   Since the Couette Cell design does not allow for visual inspection during processing it is recommended that detailed CFD modelling be carried out to provide insight in the process itself and would assist in further development of this technology. CFD modelling with dedicated software packages is highly advised, since taking into account the non-Newtonian nature of the food mixtures is essential. Based on our initial estimations, the mixture studied in this thesis exhibits a shear thinning behaviour. It is also possible that the effect of viscous dissipation during processing has a positive effect in a Couette Cell with bigger *shearing zone* gap size; however, careful management of the local hotspot formation is crucial.

5.   In many cases during this research, we came across the challenge of using detailed and accurate properties for the protein mixture. No rheological data and mixture properties were available, such as viscosity, thermal conductivity, thermal diffusivity, heat capacity and density. Therefore, we relied on estimations of these values based on mass fraction average mixture properties. Measurement of the aforementioned properties of the plant protein mixtures is important for meaningful CFD simulations and process optimization.

6
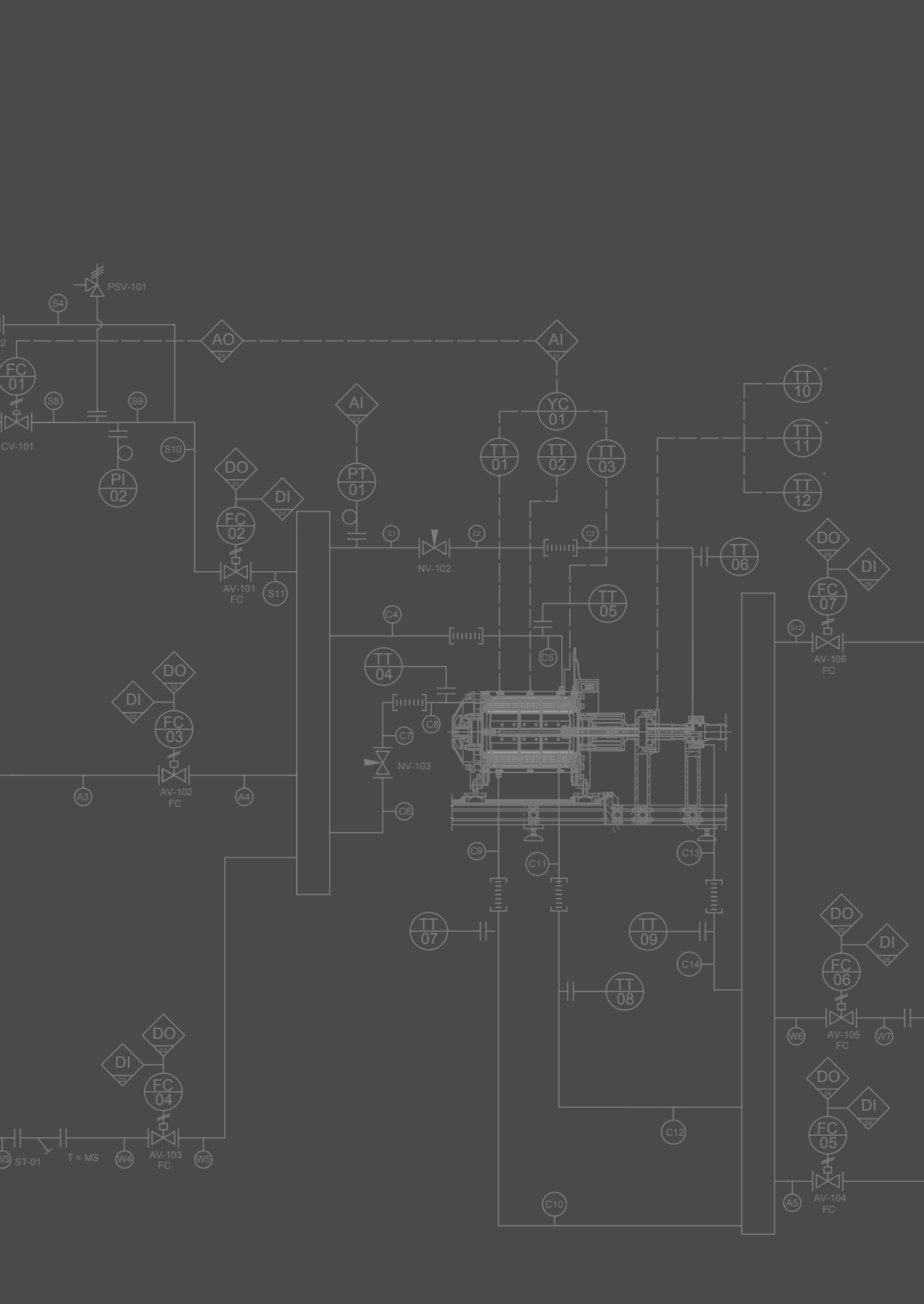
LIST OF PUBLICATIONS
CURRICULUM VITAE
ACKNOWLEDGEMENTS

Condensate

CT-02

W12-16mm-PVC   Water out

W8

Drain

A6

List of publications

Journal articles:

1. <u>Krintiras, G.A.</u>, Gobel, J., Bouwman, W.G., van der Goot, A.J., Stefanidis, G.D., 2014. *On characterization of anisotropic plant protein structures*, Food Funct., 5 (12), 3233–3240.

2. <u>Krintiras, G.A.</u>, Göbel, J., van der Goot, A.J., Stefanidis, G.D., 2015, *Production of structured soy-based meat analogues using simple shear and heat in a Couette Cell*, J. Food Eng., 160, 34-41.

3. <u>Krintiras, G.A.</u>, Diaz, J.G., van der Goot, A.J., Stankiewicz, A.I., Stefanidis, G.D., 2016. *On the use of the Couette Cell technology for large scale production of textured soy-based meat replacers*, J. Food Eng., 169, 205-213.

4. Reus, M.A., <u>Krintiras, G.A.</u>, Stefanidis, G.D., ter Horst, J.H., van der Heijden, A., 2016. *Immobilization and controlled release of gluten in food-grade hydrogels*, submitted.

5. <u>Krintiras, G.A.</u>, Bislip, D.A., Kemna, D., Lambers, L.H.R., van Nunen, D., de Roo, R., Verlinden, J., 2016. *3D food printing – Development of a 3D meat printer*, submitted.

Conference Proceedings

Selected oral presentations:

1. <u>Krintiras, G.A.</u>, Stankiewicz, A.I., Stefanidis, G.D., 2013. *Intensified protein structuring - Production of fibrous meat analogs using a Couette Cell.*, 9th European Congress of Chemical Engineering. The Hague, The Netherlands, 21-25 April, 2013.

2. <u>Krintiras, G.A.</u>, van der Goot, A.J., Stankiewicz, A.I., Stefanidis, G.D., 2014, *Intensified protein structuring - Production of fibrous meat analogs using a Couette Cell.*, 3rd International ISEKI Food Conference. Athens, Greece, 21-23 May, 2014.

3. <u>Krintiras, G.A.,</u> van der Goot, A.J., Stefanidis, G.D., 2014, *Intensified protein structuring of plant protein based mixture for the production of meat replacers using a Couette Cell.,* Netherlands Process Technology Symposium (NPS-14). Utrecht, The Netherlands, 3-5 November, 2014.

Selected poster presentations:

1. <u>Krintiras, G.A.,</u> Stankiewicz, A.I, Stefanidis, G.D., 2012, *Intensified protein structuring for more sustainable food: development of a continuous process.,* 6th International Symposium on Food Rheology and Structure (ISFRS 2012). Zürich, Switzerland, 10-13 April, 2012.

2. <u>Krintiras, G.A.,</u> Stankiewicz, A.I, Stefanidis, G.D., 2012, *Intensified protein structuring for more sustainable food: development of a continuous process.,* 20th International Congress of Chemical and Process Engineering (CHISA 2012). Prague, Czech Republic, 25-29 August, 2012, Abstract No. 493.

3. <u>Krintiras, G.A.,</u> Stankiewicz, A.I, Stefanidis, G.D., 2012, *Intensified protein structuring for more sustainable food: development of a continuous process.,* Netherlands Process Technology Symposium (NPS-11). Papendal, The Netherlands, 24-26 October, 2011.

Curriculum vitae

George Krintiras was born in Athens, Greece on 6th September 1985. He attended secondary and higher school at Volos, Greece. He received his Bachelor of Engineering degree in Mechanical Engineering from the University of Southern Denmark (SDU), Denmark in 2005. For his B.Eng. thesis he worked on CFD modelling of the aerodynamic drag on a student formula racing car. At the same time he worked for a year as a Junior Mechanical Engineer at Odense Steel Shipyard (OSS) in Denmark in the department of heavy constructions and maintenance.

He completed his Master of Science from Delft University of Technology (TU Delft), the Netherlands in 2011, specializing in Sustainable Energy Technology (SET). For his M.Sc. thesis he worked on CFD modelling of gas diffusion limitations in fuel cell (SOFC) anodes. During his studies he founded and chaired the student association for SET master students. Additionally, he worked for a year as a Junior Energy Consulting Engineer at Deerns Consulting Engineers in the Netherlands in the department of energy and building physics.

He joined Delft University of Technology (TU Delft) as Ph.D. candidate in September 2010 in the Department of Process and Energy (P&E) under the supervision of Prof. A.I. Stankiewicz and Prof. G.D. Stefanidis. His Ph.D. topic dealt with the development of a scalable process for the production of fibrous meat replacers. He introduced and developed a pilot-scale process for the production meat replacers that emulate beef meat. At the same time he was exposed to advanced research tools like light microscopy, SEM, TEM, texture analysis, encapsulation and neutron refraction (SESANS). These techniques helped him during his scientific research and led to a publication devoted to the use and significance of these techniques for a food technologist. During his Ph.D. he worked for half a year for the Vegetarian Butcher (De Vegetarische Slager) in Utrecht, the Netherlands to further develop and promote the Couette Cell for industrial production of meat replacers. His latest interests and research activities were focused on the development of 3D food printers for home cooking and for industrial production. This work led to the development of the first 3D "meat" printer for the production of vegetable-based chicken breast.

At present he is working at FeyeCon D&I in Weesp, the Netherlands, as a Project Leader Food Process Technology.

Acknowledgements

Looking back at the start of my Ph.D. journey, I remember all the friends, colleagues and family that have been by my side and who have helped and supported me though this endeavour. Words are not enough to describe how thankful I am, but nevertheless I do not want to miss the opportunity to express my appreciation for their contributions.

With a deep sense of gratitude, I would first like to thank my promotor, Professor Andrzej Stankiewicz, who has been a constant figure for stability and inspiration during my work. Andrzej, I want to thank you for the wonderful trip to Poland, your home country, to celebrate your 60th birthday. I am still fascinated by the Wieliczka Salt Mine, the polish hospitality and the endless dinners. Everyone should try, at least once, a zapiekanka. It was a pleasure to be there with you and your family during this special day. I feel more special since I was the one to deliver a speech for your "Real life defence" that day.

I am equally grateful and to my co-promotor and now promotor, Professor Georgios Stefanidis, the dominant force behind this dissertation. Giorgo, σε ευχαριστώ, thank you for your endless hours spent guiding, assisting and helping me, while additionally, proofreading my publications. You stand by me during challenging moments in the past years and you never placed barriers to my scientific explorations. I wish you the best for your academic carrier at KU Leuven.

I would also like to thank the recently appointed Professor Atze Jan van der Goot from Wageningen University, our project leader, for his help, ideas and collaboration during my Ph.D. research. Dear Atze Jan, I thank you for your support and swift replies and corrections to my papers. I admire you remarkable passion for food technology and structuring but also your support for my ideas, especially for the Couette Cell. I hope my research and skills expanded your horizons and I hope for a bright future for the Couette Cell.

I am thankful to Dr. Wim Bouwman and Chris Duif from the Reactor Institute of Delft (RID), for their crucial help and support with my work on neutron refraction. Our collaboration is a bright example on how TU Delft can bring together expertise in different fields. Working with the SESANS technique was one of the most exciting parts of my Ph.D. and I am really proud for the experience obtained during our work together.

Many thanks to the brilliant students that worked with me in the past years, Jesse Gobel, Niels van Dijk and Javier Gadea Diaz. You have all been incredible and your motivation for research has always inspired me to go further. I enjoyed every moment spend working with you and I hope you learned from me as much as I learned from you.

I want to thank my dear fellow Ph.D. researchers in this project Jacqueline Berghout, Kasia Grabowska and Pascalle Pelgrom for their collaboration and great work. Thank you to Birgit and Jarno from Wageningen University. Thank you to Barentz B.V. for the protein supplies, a very special thank you to Erwin and Simone from Teesing B.V. for your great engineering skills and enthusiasm while working with me. The development of the feeding system for the Couette Cell was a real breakthrough. The research was financially supported by the Institute for Sustainable Process Technology (ISPT) and the Peas Foundation. Thank you to De Vegetarische Slager (The Vegetarian Butcher) for your help, ideas and especially your passion for a more sustainable and animal free consuming world.

A big thank you to the DEMO staff for helping me design, construct and assemble the up-scaled Couette Cell. Specifically, Martijn Karsten, Jeroen Koning, Jos van Meurs and Rein van den Oever you guys can not imagine how thankful I am for your support. Each and everyone of you are part of the Couette Cell development. Big thanks to Patrick van Holst and Harry Jansen from PME group for your help with texture analysis; you have assisted an important part of my work. Thank you also to Leslie van Leeuwen and Helma Duijndam-Nieuwpoort our wonderful and always smiling secretaries for helping me each time I reach out to you.

I thank all the present and past members and colleagues of the Intensified Reaction and Separation Systems group. Anamaria Soare, Christian Brunchi, Marloes Reus (thank you for the summary translation to Dutch), Rohit Kacker, Javier Fernandez de la Fuente and Daniel Irimia you guys made my Ph.D. life more fun during the past years. Also thank you Ernesto Altman, Tomasz Durka, Magda Komorowska, Samir Kulkarni, Somanth Kadam, Lalit Gagurde, Wei-Wei Li, Norbert Radasci, Fatemeh Anisi, and Maryam Khodadadian. I wish best of luck to the ones still pursuing their Ph.D.. I hope that you keep alive the great tradition of presenting the "real defence" to graduating Ph.D. students.

I thank all the present and past members and colleagues of the Process & Energy department. George Tsalidis, Gerasimos Sarras, Kostas Anastasakis, Onursal Yakaboylu, Manuela Di Marcello, Nafiseh Taleban Fard, Yash Joshi, Aditya Thallam Thattai, Hassan Nemati and Alessandro Cavalli. My warm thanks to all of you for all the lunch brakes, our wonderful dinners, our long "pointless" and many times philosophical discussions and most of all for bearing me all these years! My best wishes to the ones that are about to finish with their Ph.D. research.

Thank you to my good friends and colleagues around TU Delft the great times we spend together, Antonio Jarquin Laguna, Bernat Goni Ros (our tip to Rhodes was unforgettable) and Ilias Tapeinos I wish you guys good luck with your Ph.D. and Diomidis Katzourakis for allowing me to be your paranymph.

I would never forget all of the beautiful moments I shared with my Greek friends from all these years living in Delft. My former roommates Kostas P., Orestis, Panos and Thanasis you offered great relaxing times when returning home. I specifically remember our epic parties and even more epic BBQ's. Aristidis, Christos, Eirini, Emma, Kostas G., Maria, Nantia, Petros, Sotiris O. and Soritis K. thank you for being there for me for the past eight years at Delft. I enjoyed and still enjoy your company and I find myself lucky to have friends like you in my life from my journey to the Netherlands. Big thanks to my home town friends for being there all my life. Thank you Christos, Giannis, Kostas, Konstantinos, Vasilis N., Vasilis M., Xanthos and Oh YES, Michalis I am finally done with it.

My acknowledgements would be incomplete without thanking a few very special people in my life. I would like to thank my parents Andreas and Nerantzia you have both been a continuous source of support, encouragement and unconditional love for me. You both struggled hard to raise me and my sister; this thesis is maybe just a small proof of what your efforts have resulted. I would have never been here without you; I owe you everything! To my sister Aspasia; Aspasoni mou, you have been really supportive especially during the last stages of my Ph.D. you are an amazing English teacher and I thank you very much for the proofreading and your corrections. I could have not wished for a more wonderful sister than you!

Finally, I would like to acknowledge a very important person in my life – my partner Anna-Maria. She has been a constant source of strength and inspiration. Thank you for your support and for your remarkable advice during moments of stress. I do hope I can make you as happy as you make me all the time.

The support of all these wonderful people made it possible for me to see this research through to the end!

Steam

S1/13-16mm-SS 316

S-01

ST-01

CT-01

Air

A1/5-16mm-SS 316

GV-103

Water

W-01-15mm-PVC

W2/6-16mm-SS

TUDelft Delft University of Technology